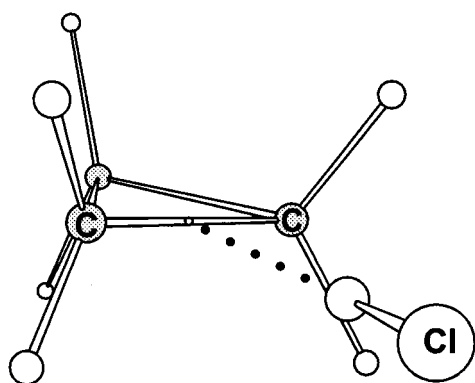
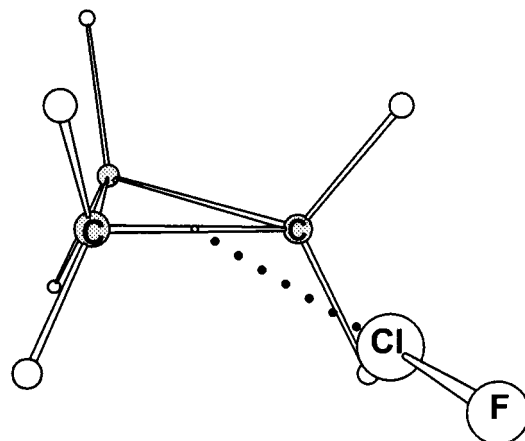


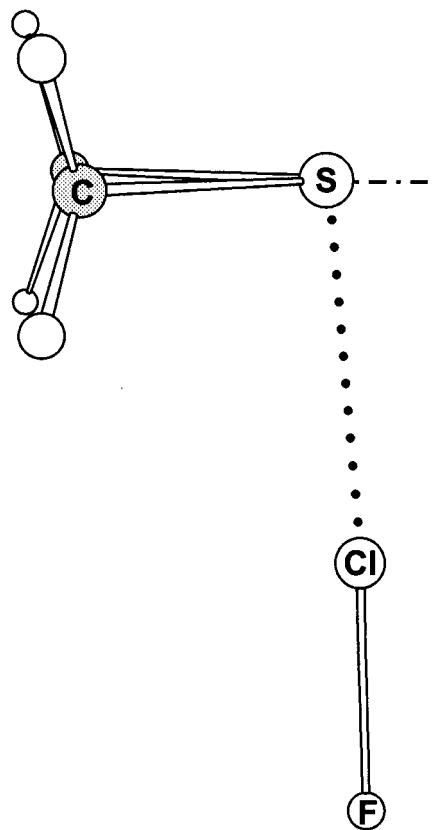
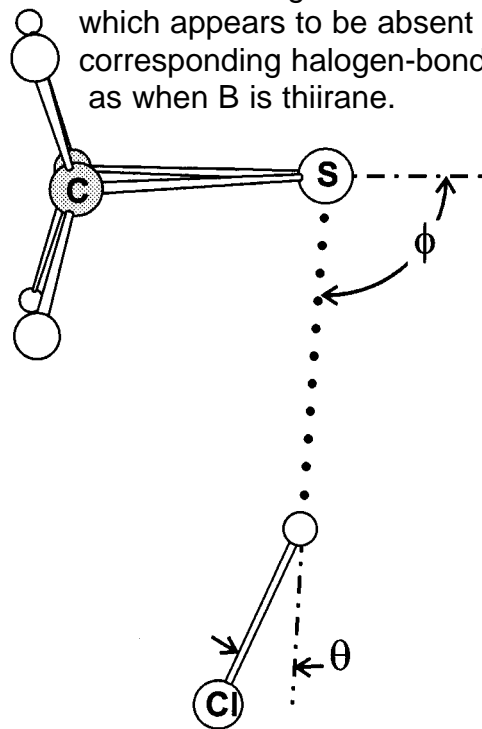
Pseudo- π model
of cyclopropane



The hydrogen bond resembles the “halogen” bond so that complexes $B\cdots\text{HCl}$ and $B\cdots\text{ClF}$ are isostructural, as when B is cyclopropane.



When symmetry allows, the hydrogen bond can show a significant nonlinearity, which appears to be absent in the corresponding halogen-bonded system, as when B is thiirane.



Prereactive Complexes of Dihalogens XY with Lewis Bases B in the Gas Phase: A Systematic Case for the Halogen Analogue $B \cdots XY$ of the Hydrogen Bond $B \cdots HX$

Anthony C. Legon*

Reactions between dihalogen molecules XY and simple Lewis bases B are of fundamental interest in organic and inorganic chemistry and, consequently, have featured prominently in the history of these subjects. When XY is F_2 or ClF, such reactions can be especially violent. Accordingly, it is a challenge for the chemist to isolate and characterize in detail the species produced in the initial, prereactive encounter of B/XY pairs in a potentially reactive mixture. Moreover, prereactive complexes of this type impact on our understanding of the mechanisms of the reactions, for they have been invoked as intermediates. Mulliken postulated that two types of complexes

exist: those of the outer type $B \cdots XY$ (weak, no significant charge transfer) and those of the inner type $[BX]^+ \cdots Y^-$ (strong, substantial charge transfer). Here we demonstrate how prereactive adducts of both the Mulliken outer and inner types can be isolated in the gas phase by using supersonic coexpansion of the components, and then characterized precisely by observation of their rotational spectra. Generalizations about the properties of $B \cdots XY$, obtained by investigating carefully tailored series in which B and XY are systematically varied, can be understood on the basis of a simple electrostatic model of the XY interaction. Among the properties of importance

are the extent of electric charge redistribution in XY, the radial and angular geometries, and the strength of the intermolecular binding. A close parallelism of the properties of $B \cdots XY$ and the corresponding $B \cdots HX$ suggests the existence of a halogen bond analogue of the hydrogen bond. The main difference between halogen and hydrogen bonds lies in the propensity for significant nonlinearity in the latter that is absent in the former.

Keywords: gas-phase chemistry • halogens • hydrogen bonds • intermediates • prereactive complexes

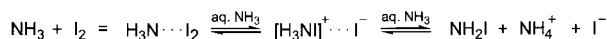
1. Introduction

This year marks an important anniversary in the history of molecular interactions. Fifty years ago, Benesi and Hildebrand^[1] published their landmark paper describing the UV/Vis spectrum of molecular iodine dissolved in liquid benzene. “Charge-transfer” complexes, subsequently renamed electron donor–acceptor complexes by Mulliken, have been a matter of serious interest in chemistry ever since. In the decade or so after the Benesi–Hildebrand paper, much experimental work followed, notable among which were some important X-ray diffraction studies of complexes of Lewis bases and dihalogen molecules in the solid state by Hassel and co-workers.^[2] In the same period, Mulliken developed a detailed theory of such

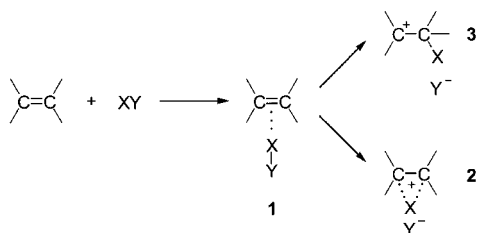
interactions.^[3] An important thread running through Mulliken’s work is the classification of complexes according to whether the intermolecular interaction $B \cdots XY$ is weak and there is little charge transfer between the components (outer complexes in Mulliken’s notation) or whether there is extensive charge redistribution to give $[BX]^+ \cdots Y^-$ (an inner complex). In this review B is used as the symbol for a generalized Lewis base and XY for a generalized dihalogen molecule, either homonuclear (F_2 , Cl_2 , Br_2) or heteronuclear (ClF, BrCl). An inner complex is written $[BX]^+ \cdots Y^-$ without any prejudice as to whether complete transfer of X^+ to B has occurred. This notation is meant only to imply significant charge transfer.

Both outer and inner complexes have been invoked in describing the mechanisms of reactions of halogens with simple Lewis bases in solution. For example, $[H_3NX]^+ \cdots Y^-$ was invoked^[4] as an intermediate in reactions of halogens with ammonia (Scheme 1), while the halogenium ion **2** in Scheme 2 was identified in the reactions of halogens and alkenes in polar solvents and in the dark.^[5] In Schemes 1 and 2, the

[*] Prof. Dr. A. C. Legon
School of Chemistry
University of Exeter
Stocker Road, Exeter EX44QD (UK)
Fax: (+44) 1392-263434
E-mail: a.c.legon@exeter.ac.uk



Scheme 1. A mechanism proposed for the reaction of molecular iodine with aqueous ammonia solution. It involves an outer complex $\text{H}_3\text{N} \cdots \text{I}_2$ and then an inner complex $[\text{H}_3\text{NI}]^+ \cdots \text{I}^-$ as intermediates.



Scheme 2. Possible mechanisms for the reaction of halogen molecules with alkenes in polar solvents in the dark; **1** and **2** are Mulliken outer and inner complexes, respectively.

initial, presumably weak, complex $\text{B} \cdots \text{XY}$ is often referred to as a preequilibrium complex. In general, we shall use the phrase prereactive complex (or intermediate) to describe the complex formed in the initial interaction prior to chemical reaction or significant charge transfer. This article is concerned with prereactive complexes which are mainly of the outer type but occasionally of the inner type.

Theoretical approaches to $\text{B} \cdots \text{XY}$ have almost invariably involved the isolated complex, while most experimental work has been conducted in condensed phases (liquids, solutions, or the solid state). If one wishes to provide experimental evidence that makes direct contact with theory, it is clearly desirable for it to be derived from the investigation of complexes in isolation, either in inert gas matrices at low temperature or, preferably, in the gas phase at low pressure, so that molecules undergo few or no collisions. In the latter case, the observed properties are unperturbed by lattice or solvent effects and hence refer to the isolated molecule.

The objectives of the investigations described in this review are to examine experimentally how the properties of complexes $\text{B} \cdots \text{XY}$ change as first B and then XY are systematically varied, with the aim of deducing the nature of the $\text{B} \cdots \text{XY}$ interaction and its dependence on the Lewis base and the halogen involved. Inevitably, this approach requires that simple Lewis bases B are chosen, but many of them are highly reactive with respect to halogens. For example, mixtures of $\text{F}_2/$

NH_3 and of $\text{ClF}/\text{C}_2\text{H}_4$ react violently in the gas phase. Therefore, to achieve the above objectives, it is necessary to mix B and XY and allow the component molecules to interact to give $\text{B} \cdots \text{XY}$ but to preclude further progress along the reaction coordinate, that is, to isolate the prereactive complex.

There are two ways of isolating prereactive complexes. The first involves the use of low-temperature inert gas matrices, as exemplified by the work of Pimentel et al.,^[6] Ault et al.,^[7] Andrews et al.,^[8] Barnes et al.,^[9] and others. These authors used mainly IR spectroscopy to probe the matrix-isolated complexes. There have been several reviews of this important general method.^[10–13]

The second method for forming and isolating prereactive complexes is more recent^[14] but in many ways similar. It involves the rapid mixing and supersonic coexpansion of the components from the gas phase at moderate pressure into a vacuum. This approach allows prereactive complexes to be investigated by means of their rotational spectra in the collisionless phase of expansion and therefore in the absence of interaction with any other molecule. It thus brings to bear on the species so isolated all the precision and detailed knowledge that are typical of rotational spectroscopy. The results obtained in this way are the subject of discussion here.

We shall first consider how to characterize complexes $\text{B} \cdots \text{XY}$ by rotational spectroscopy, assuming they can be produced and isolated before chemical reaction. This involves a brief description of FT microwave spectroscopy and a survey of the spectroscopic constants that can be extracted from analysis of the rotational spectra. A delineation of those relevant molecular properties of the complex that can be derived from the spectroscopic constants follows. These are radial and angular geometries, the strength of the intermolecular binding, and the extent of electric charge redistribution accompanying complex formation.

The main body of the review is concerned with an examination of the properties of isolated complexes $\text{B} \cdots \text{XY}$ and how they change as B and XY are varied. From this systematic investigation of the properties, generalizations about $\text{B} \cdots \text{XY}$ complexes are deduced and the nature of the $\text{B} \cdots \text{XY}$ interaction inferred. An important part of the process are comparisons of the properties of $\text{B} \cdots \text{XY}$ complexes with those of their hydrogen-bonded analogues $\text{B} \cdots \text{HX}$ (X = halogen). The work on hydrogen-bonded complexes has been reviewed elsewhere.^[15]



Tony Legon was born in Suffolk, England but was educated in London: at the Coopers' Company School in Bow and later in the Chemistry Department at University College London (UCL). He conducted his doctoral research at UCL under the supervision of Jim Millen, with whom he subsequently had a long and happy collaboration. Following a period as Turner and Newall Fellow in the University of London, he became Lecturer and then Reader in Chemistry at UCL. He spent 1980 working at the University of Illinois with the late W. H. Flygare. In 1984 he moved to the Chair of Physical Chemistry at the University of Exeter where he has remained, apart from a year (1989/90) as Thomas Graham Professor of Chemistry at UCL. His main research interests are in understanding gas-phase interactions of molecules through the rotational spectra of hydrogen-bonded and charge-transfer complexes. This work was recognized by the award of the Tilden Lectureship and Medal of the Royal Society of Chemistry (RSC) in 1989, an EPSRC Senior Fellowship in 1997, and the Spectroscopy Award of the RSC in 1998.

2. Prereactive Complexes $B \cdots XY$: Formation, Isolation, and Characterization

This section consists of two parts. First, the means of detecting and characterizing the species $B \cdots XY$ by their rotational spectra will be described, under the assumption that the complexes can somehow be formed and isolated before chemical reaction between the components B and XY. In the second part, the means by which prereactive complexes can be formed and isolated prior to chemical reaction are discussed.

2.1. How to Detect and Characterize Prereactive Complexes

Rotational spectroscopy is a powerful method of measuring the precise properties of molecules in effective isolation in the gas phase. The rotational spectra of complexes with a reasonably strong intermolecular bond have been observed in equilibrium gas mixtures of the two components at low temperature by using Stark modulation microwave spectroscopy.^[16] For more weakly bound complexes, techniques that involve supersonic jets or beams must be employed, namely, molecular beam electric resonance spectroscopy (MBERS, pioneered by Klemperer et al.)^[17] and pulsed-nozzle, Fourier-transform microwave spectroscopy (developed by Flygare et al.).^[18] In each technique, a supersonic jet or beam of gas mixture—formed by premixing the components and then strongly diluting them with, for example, argon—is expanded from a reservoir held at a relatively high pressure through a small circular nozzle into a vacuum. The gas emerging from the nozzle is rich in weakly bound complexes which achieve collisionless expansion on a short time scale (ca. 10 μ s), after which they are frozen in their lowest rotational and vibrational energy states until the gas hits a wall of the vessel, for example. While in the state of collisionless expansion, the complexes can be interrogated by microwave radiation and their rotational spectra recorded. The results presented here were obtained, for the most part, by pulsed-nozzle, FT microwave spectroscopy. Good descriptions of the MBERS technique and its achievements are given in refs. [19] and [20], respectively.

Figure 1 shows a schematic diagram of the spectrometer.^[21] In the first of a sequence of carefully timed events, a short pulse of a mixture of the appropriate components is expanded with the aid of a solenoid valve from a pressure of a few bar into the evacuated chamber of the spectrometer. This chamber contains a pair of nearly confocal, concave aluminum mirrors that constitute a microwave (mw) Fabry–Pérot (FP) cavity. When the gas pulse has reached the center of the FP cavity, a 1- μ s pulse of monochromatic radiation of frequency ν , to which the cavity is tuned, is allowed to enter the cavity, where it forms a standing wave pattern. Molecules in the gas pulse that have a rotational transition within the bandwidth of the FP cavity (ca. 0.5 MHz) are rotationally polarized by the radiation. The half-life for spontaneous coherent emission from the polarized gas at frequency ν_m is on

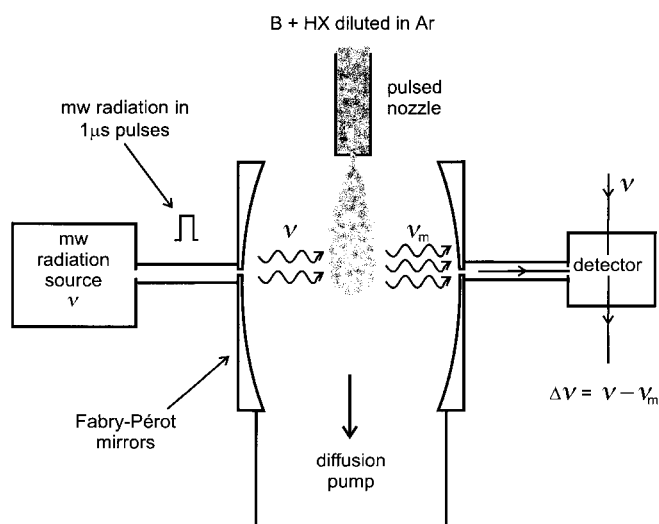


Figure 1. Schematic diagram showing the essential components of a pulsed-nozzle, FT microwave spectrometer. The nozzle is of the conventional type, suitable only for observing rotational spectra of complexes $B \cdots HX$ that can be formed from premixed components B and HX.

the order of 100 μ s, while the polarizing pulse has a half-life of only about 0.1 μ s. Consequently, by delaying detection for a few microseconds, the free-induction decay at the rotational transition frequency ν_m can be detected in the effective absence of the initial microwave pulse. The emission at ν_m is processed by mixing it down in two stages (although only one is shown in Figure 1), as a signal proportional to the strength of the oscillating electric field of frequency $|\nu - \nu_m|$, which normally lies in the range 0–500 kHz. Fourier transformation then gives the intensity versus frequency spectrum in the range ± 500 kHz centered on ν . The experiment is an exact analogue of FT NMR spectroscopy, except that the molecules undergo an electric polarization in the former, instead of the magnetic polarization of the latter.

By analysis of rotational spectra observed in this way, a variety of spectroscopic constants that contain much information about the complexes can be determined. Those of most direct interest to the present discussion are listed in Table 1. Rotational constants are inversely proportional to principal moments of inertia, which are in turn simple functions of the distribution of the mass of the complex in space. Accordingly, these quantities can be used to determine the separation of the two subunits B and XY and their relative orientation in space, that is, the radial and angular geometries of the complex.

The centrifugal distortion constant D_J (linear or symmetric-top molecules) or Δ_J (asymmetric-rotor molecules) is simply related to the intermolecular stretching force constant k_o for the approximation of rigid, unperturbed subunits B and XY with the neglect of terms higher than quadratic in the intermolecular potential energy function.^[22] Since k_o is the restoring force per unit infinitesimal extension of the weak bond, it provides one measure of strength of the interaction (the other is the dissociation energy).

The final spectroscopic constants of particular interest here are the halogen nuclear quadrupole coupling constants $\chi_{a\beta}(X)$ and $\chi_{a\beta}(Y)$, where α and β are to be permuted over the

Table 1. Spectroscopic constants from rotational spectroscopy and the molecular properties to which they lead.

Spectroscopic constant	Molecular property	Comment
Nature of the spectrum	Symmetry	Spectral pattern is different for linear, symmetric-top, and asymmetric-top molecules. Observation of a particular pattern often allows molecular symmetry to be established.
Rotational constants, A_0, B_0, C_0	Radial and angular geometry	$B_0 = h/8\pi^2 I_b$, where $I_b = \sum m_i(a_i^2 + c_i^2)$ is a principal moment of inertia. I_b depends on the relative positions (i.e., principal axis coordinates a_i, c_i) of atoms.
Centrifugal distortion constant, D_J or Δ_J	Intermolecular stretching force constant k_σ of a weakly bound complex	For weakly bound complexes $B \cdots XY$, the components B and XY can in good approximation be assumed rigid. Then, if higher than quadratic force constants can be neglected, D_J is proportional to k_σ^{-1} .
Nuclear quadrupole coupling constants $\chi_{a\beta}(X) = -(eQ_X/h)\partial^2 V_X/\partial\alpha\partial\beta$	Electric field gradient at a nucleus X having a nonzero electric quadrupole moment Q_X	Depends on the detailed electric charge distribution within the molecule. If a molecule XY is subsumed into a complex, $\partial^2 V/\partial\alpha\partial\beta$ at X and Y change. The $\chi(X)$ and $\chi(Y)$ can be used as a probe of the change.

principal inertial axis directions a, b , and c . The importance of these quantities lies in the definition of the nuclear quadrupole coupling tensor $\chi_{a\beta}(X) = -(eQ_X/h)\partial^2 V_X/\partial\alpha\partial\beta$, where Q_X is the conventional electric quadrupole moment of nucleus X and $-\partial^2 V/\partial\alpha\partial\beta$ is the electric field gradient (EFG) tensor at nucleus X. Further details of the nuclear quadrupole interaction are given in Section 3.1. For present purposes, the fact that $\chi_{a\beta}(X)$ is proportional to the electric field gradient at nucleus X means that changes in $\chi_{a\beta}(X)$ and $\chi_{a\beta}(Y)$ on formation of $B \cdots XY$ provide a quantitative measurement of the changes in the EFGs at X and Y, and hence in the electric charge distribution of XY. In addition, when the complete tensor $\chi_{a\beta}(X)$ or $\chi_{a\beta}(Y)$ is available, it provides important information about the orientation of the XY subunit with respect to the principal inertial axis system a, b, c and hence about the angular geometry of $B \cdots XY$.^[23]

2.2. How to Form and Isolate Prereactive Complexes

Section 2.1 outlines how to determine certain properties of a complex $B \cdots XY$ from spectroscopic constants obtained by analysis of its rotational spectrum, as observed in a supersonically expanded jet by pulsed-nozzle FT microwave spectroscopy. Normally, the mixture of the two components of interest, diluted in argon, would be held in a stagnation tank at a total pressure of about 3 bar prior to its expansion in short pulses (produced by a solenoid valve) into the vacuum chamber. For most of the complexes of interest here this approach could not be used because the two components B and XY would undergo chemical reaction. This is a particular problem with, for example, mixtures B/XY in which B is ammonia, ethene, or ethyne and XY is F_2 , ClF, or Cl_2 , for which the reaction can be rapid. Clearly, to observe the prereactive complexes $B \cdots XY$, a device is required which achieves a time between mixing of the components and the collisionless phase of the supersonic expansion short enough to preclude chemical reaction.

Such a device is the fast-mixing nozzle^[14] shown schematically in Figure 2. It consists essentially of a pair of concentric, nearly coterminal tubes of circular cross-section and is attached to the outlet of a solenoid valve. One of the reactive components flows (usually undiluted) continuously through the central glass capillary (0.3 mm internal diameter) into the evacuated chamber of the spectrometer. The other compo-

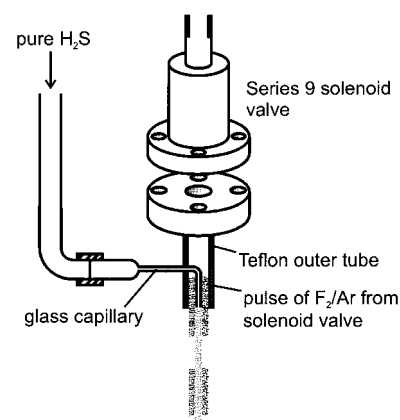


Figure 2. Schematic diagram of a fast-mixing nozzle. The component gases illustrated are those required to detect the rotational spectrum of $H_2S \cdots F_2$, a transition of which is shown in Figure 3. The glass capillary used in this experiment had an internal diameter of 0.3 mm.

nent diluted in, say, argon, is sent in short pulses from a stagnation pressure of about 3 bar down the outer tube. The gas pulses are produced by the solenoid valve. The two components meet only in the approximately cylindrical interface between the concentric gas streams as they emerge in simultaneous expansion from the tubes. Moreover, they encounter each other while moving at high speed away from surfaces, so the possibility of surface-initiated radical reactions is reduced. We shall see that complexes formed at the interface of the gas flows achieve states of low internal energy and collisionless expansion on the order of 10 μ s. Thereafter, there is no possibility of unimolecular, bimolecular, or surface-initiated reaction until the gas flow hits a wall of the vacuum chamber. The complexes are effectively frozen as prereactive intermediates for about 300 μ s, during which their rotational spectrum can be recorded by the method outlined in Section 2.1.

Figure 3 shows a rotational transition of $H_2S \cdots F_2$ recorded by using the fast-mixing nozzle in an FT microwave spectrometer. The effectiveness of the device becomes clear when it is recalled that ignition is observed in H_2S/F_2 mixtures at room temperature at pressures as low as 10^{-6} bar.^[24] The reasons for its success may be sought in the properties of the supersonic expansion which can be discussed conveniently in terms of the ratio X/d , where X is the distance traveled by the gas downstream from the circular nozzle exit of diameter d .

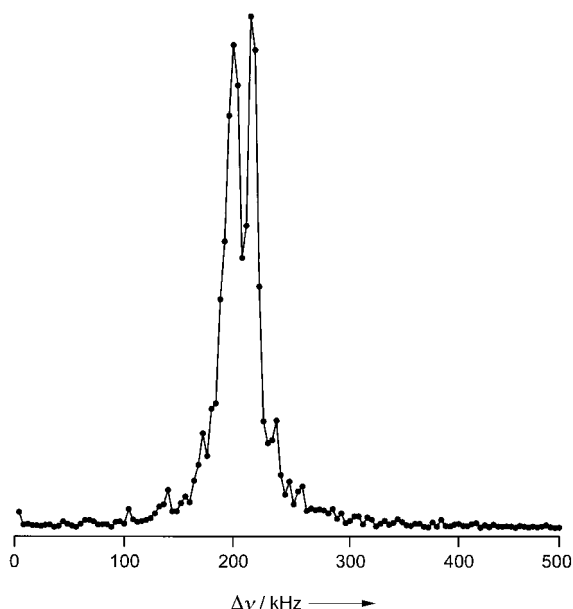


Figure 3. A frequency domain recording of the $3_{03}-2_{02}$ transition in the ground state of $\text{H}_2\text{S}\cdots\text{HF}$. Frequencies are offset from 10384.1660 MHz at a rate of 3.90625 kHz per point. Solid dots have been joined by straight lines. The transition is centered at 10383.9668 MHz. The doublet structure arises from F,F spin–spin splitting. See reference [64] for further details.

Gas dynamics calculations^[25] show that for an axisymmetric expansion of room-temperature argon from a pressure of a few bar through a circular nozzle with $d=0.3$ mm, the gas flow reaches its terminal speed of $5 \times 10^4 \text{ cm s}^{-1}$ after a few nozzle diameters of travel downstream from the exit, and the temperature drops to around 1 K by about $X/d=10$ or soon after. The number of three-body collisions Z_3 for each molecule diminishes very rapidly, so that the formation of complexes, which requires three-body collisions, is effectively over within a few nozzle diameters. Two-body collisions cease after the gas has traveled about ten nozzle diameters, that is, after about 10 μs . Clearly, if the complexes formed in the first few microseconds survive until then, there is no mechanism by which they can undergo reaction and they are effectively frozen. Hence, the rapid expansion in the absence of surfaces, coupled with the dilution of one component in argon, appears to be responsible for the efficacy of the fast-mixing nozzle.

3. Systematic Variation of B and XY: The Nature of the $\text{B}\cdots\text{XY}$ Interaction

This part of the review is concerned with examining how the properties of $\text{B}\cdots\text{XY}$ (see Section 2.1 and Table 1) change as B and XY are systematically varied and the conclusions about the nature of the $\text{B}\cdots\text{XY}$ interaction that can be thereby deduced. The first question to be addressed is whether the observed complexes belong to the weak, outer type or to the strong, inner type in the classification of Mulliken.^[3] The most important criterion is the extent of electric charge redistribution that accompanies formation of $\text{B}\cdots\text{XY}$, since it will be minor for an outer complex $\text{B}\cdots\text{XY}$ but major for an inner complex $[\text{BX}]^+\cdots\text{Y}^-$. A less direct criterion is the binding

strength, as measured by k_a . Once it has been established that certain $\text{B}\cdots\text{XY}$ species belong to the outer type, it will be profitable to consider their angular and radial geometries.

3.1. Electric Charge Redistribution in XY on Formation of $\text{B}\cdots\text{XY}$

A powerful probe of electric charge redistribution is provided by the nuclear quadrupole coupling constants, particularly those associated with the XY subunit, since they lead to the electric field gradients at the nuclei (Section 2.1). This information is most straightforwardly interpreted in terms of changes in the electronic distribution when XY is a homonuclear dihalogen, such as Cl_2 or Br_2 . Less directly obtainable, but equally valuable, information about electronic structure results when XY is a heteronuclear dihalogen such as BrCl or ClF . The absence of a nuclear electric quadrupole moment for ^{19}F means that a similar probe of the modified charge distribution of F_2 when subsumed into $\text{B}\cdots\text{F}_2$ is not available. However, indirect evidence of a negligible modification in most $\text{B}\cdots\text{F}_2$ will be adduced below.

3.1.1. Nuclear Quadrupole Coupling as a Probe of Electric Charge Redistribution in a Homonuclear Dihalogen X_2 in $\text{B}\cdots\text{X}_2$

Apart from ^{19}F , halogen nuclei have an electric quadrupole moment \mathbf{Q}_x and an intrinsic (or spin) momentum \mathbf{I}_x . The nuclear spin vector \mathbf{I}_x can couple in only a limited number of discrete orientations to the rotational angular momentum vector \mathbf{J} of the framework of a molecule carrying the atom X. This corresponds to different orientations of \mathbf{Q}_x with respect to the electric field gradient ∇E_x at X and therefore to a set of different potential energies of interaction. The result is a hyperfine splitting of rotational energy levels and transitions. Analysis of this hyperfine structure gives nuclear quadrupole coupling constants $\chi_{\alpha\beta}(\text{X}) = -(eQ_x/h)\partial^2 V_x/\partial\alpha\partial\beta$, where α and β are to be permuted over the principal inertial axes a , b , and c . Only zero-point values of the $\chi_{\alpha\beta}(\text{X})$ are measured.

The analysis that follows^[26–28] applies to complexes $\text{B}\cdots\text{X}_2$ of axial symmetry (C_{3v} or higher) or of C_{2v} symmetry in which the X_2 internuclear axis z coincides in the equilibrium conformation with the C_2 axis and with the a axis. The equilibrium nuclear quadrupole coupling constants along z (or a) are denoted $\chi_{zz}^e(\text{X}_i)$ and $\chi_{zz}^e(\text{X}_o)$, where the subscripts i and o refer to the inner and outer X nuclei in $\text{B}\cdots\text{X}_2$ and it is assumed implicitly that both atoms X belong to the same nuclide.

Although there is only one coupling constant $\chi_0(\text{X})$ for free X_2 , the formation of $\text{B}\cdots\text{X}_2$ leads to a divergence of the zero-point values $\chi_{zz}^e(\text{X}_i)$ and $\chi_{zz}^e(\text{X}_o)$, as the former increases and the latter decreases in magnitude. This is a result mainly of the polarization of the electric charge distribution of X_2 by the molecule B. Ab initio calculations have shown^[29] that when $\text{N}_2\cdots\text{HX}$ is formed, the effect of HX on the equilibrium ^{14}N nuclear quadrupole coupling constants leads to the relation $\chi_{zz}^e(^{14}\text{N}_i) + \chi_{zz}^e(^{14}\text{N}_o) \approx 2\chi_0(^{14}\text{N})$ for all but very small intermolecular separations. Similarly, $\chi_{zz}^e(\text{X}_i)$ of $\text{B}\cdots\text{X}_2$ increases in

magnitude while $\chi_{zz}^e(X_o)$ suffers a nearly equal decrease,^[30] leading to $\chi_{zz}^e(X_i) + \chi_{zz}^e(X_o) \approx 2\chi_0(X)$. This means that the quotient f defined in Equation (1) can be written as Equation (2) to a high degree of approximation, where $\Delta\chi_{zz}^e(X) =$

$$f = \{\chi_{zz}^e(X_i) - \chi_{zz}^e(X_o)\} / \{\chi_{zz}^e(X_i) + \chi_{zz}^e(X_o)\} \quad (1)$$

$$f = \Delta\chi_{zz}^e(X_i) / 2\chi_0(X) \quad (2)$$

$\chi_{zz}^e(X_i) - \chi_{zz}^e(X_o)$. In view of the definition of nuclear quadrupole coupling constants, it follows that f is related to the EFG at the two nuclei X_i and X_o by Equation (3), where F_0 is the

$$f = \Delta F_{zz} / 2F_0 \quad (3)$$

electric field gradient along z at X in free X_2 and ΔF_{zz} is the difference in EFG between the nuclei X_i and X_o in $B \cdots X_2$.

The Townes–Dailey model^[31] provides a conveniently simple approximate method of estimating the EFG at nuclei in terms of the contributions of p, d, ... valence electrons. It predicts that when a fraction δ of a $3p_z$ electron is transferred from Cl_i to Cl_o in Cl_2 to give $Cl_i^+ \cdots Cl_o^-$, the difference $\Delta F_{zz} = F_{zz}^i - F_{zz}^o = 2\delta F_0$. Then Equation (3) becomes Equation (4).

$$f = \delta \quad (4)$$

Hence, the quotient defined in Equation (1) is, in the approximation of the Townes–Dailey model, the fraction δ of an electronic charge transferred from X_i to X_o when $B \cdots X_2$ is formed. This analysis ignores intermolecular charge transfer, but in view of the small values of δ thus found this neglect seems reasonable.

The fact that zero-point quantities $\chi_{zz}(X_i)$ and $\chi_{zz}(X_o)$ are observed rather than their equilibrium counterparts is not a problem. For an axially symmetric complex $B \cdots X_2$, zero-point averaging can be taken into account in good approximation by Equation (5) with an analogous equation in X_o ,

$$\chi_{zz}(X_i) \approx \frac{1}{2}\chi_{zz}^e(X_i)(3\cos^2\phi - 1) \quad (5)$$

where ϕ is the instantaneous angle between the X_2 axis and its equilibrium direction z . Equation (5) is an exact equality if the EFGs at X_i and X_o are independent of the motion of B and if intermolecular stretching is ignored. It then follows that Equation (2) also holds when zero-point coupling constants are used instead of equilibrium values.

Figure 4 plots values of δ for a series of complexes $B \cdots Cl_2$ ^[27, 28, 32–38] and $B \cdots Br_2$ ^[39, 40] against k_o , which is a measure of the strength of the interaction. Two features of Figure 4 are noteworthy. First, apart from the $H_3N \cdots Br_2$ complex, the values of δ are all on the order of a few hundredths of an electronic charge. Second, the δ values all lie on the same straight line. Evidently, these complexes are Mulliken complexes of the outer type, with very small electric charge redistribution on complex formation. The values of δ are in accord with those from ab initio calculations. For example, values of $\delta = -0.015$ and 0.018 were obtained for ethene $\cdots Cl_2$ ^[41] for the changes in electronic population at Cl_i and Cl_o , respectively. A Sternheimer-like response property $g_{zz,z}$ was

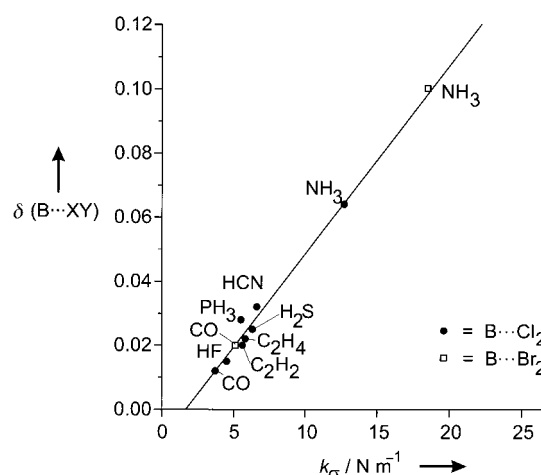


Figure 4. Systematic variation of the fraction of an electronic charge δ transferred from X_i to X_o on formation of $B \cdots X_2$ ($X = Cl$ and Br). The intermolecular stretching force constant k_o is used to order the $B \cdots X_2$ according to the strength of the interaction.

deduced for free Cl_2 from the observed variation of δ with B .^[30] A similar approach was applied to the δ value of $H_3N \cdots Br_2$.^[42]

3.1.2. Nuclear Quadrupole Coupling as a Probe of Electric Charge Redistribution in a Heteronuclear Dihalogen XY in $B \cdots XY$

The foregoing treatment needs some modification when XY is a heteronuclear dihalogen such as $BrCl$. According to the Townes–Dailey model, if the formation of $B \cdots XY$ in its equilibrium conformation leads to transfer of a fraction δ of an electronic charge from X to Y , the equilibrium coupling constants $\chi_{zz}^e(X)$ and $\chi_{zz}^e(Y)$ (z is the XY internuclear axis) are related to those of the free XY molecule $\chi_0(X)$ and $\chi_0(Y)$ by Equations (6) and (7) where $\chi_A(X)$ and $\chi_A(Y)$ are the nuclear

$$\chi_{zz}^e(X) = \chi_0(X) + \delta\chi_A(X) \quad (6)$$

$$\chi_{zz}^e(Y) = \chi_0(Y) - \delta\chi_A(Y) \quad (7)$$

quadrupole coupling constants of the halogen atoms X and Y , respectively. Values of $\chi_A(X)$ and $\chi_A(Y)$ are well established.^[43]

With the same approximation that holds in Equation (5), the zero-point values $\chi_{zz}(X)$ and $\chi_{zz}(Y)$ are related to the equilibrium quantities by Equations (8) and (9). Given $\chi_A(X)$, $\chi_A(Y)$, $\chi_0(X)$, and $\chi_0(Y)$, solutions of Equations (8) and (9) with the experimental values of $\chi_{zz}(X)$ and $\chi_{zz}(Y)$ provide δ and $\phi_{av} = \cos^{-1}(\cos^2\phi)^{1/2}$.

$$\chi_{zz}(X) = \frac{1}{2}[\chi_0(X) + \delta\chi_A(X)](3\cos^2\phi - 1) \quad (8)$$

$$\chi_{zz}(Y) = \frac{1}{2}[\chi_0(Y) - \delta\chi_A(Y)](3\cos^2\phi - 1) \quad (9)$$

Values of δ so obtained for the series of complexes $B \cdots BrCl$ ^[44–50] are plotted in Figure 5 against k_o as a measure of the intermolecular binding strength. Note that δ is again an approximately linear function of k_o and is small ($\delta \leq 0.06$) except for the fairly strong complex $H_3N \cdots BrCl$ ($\delta = 0.11$).^[50] We therefore conclude that electric charge redistribution within $BrCl$ on formation of $B \cdots BrCl$ is small. In fact, comparison of Figures 4 and 5 indicates that, for a given B , the

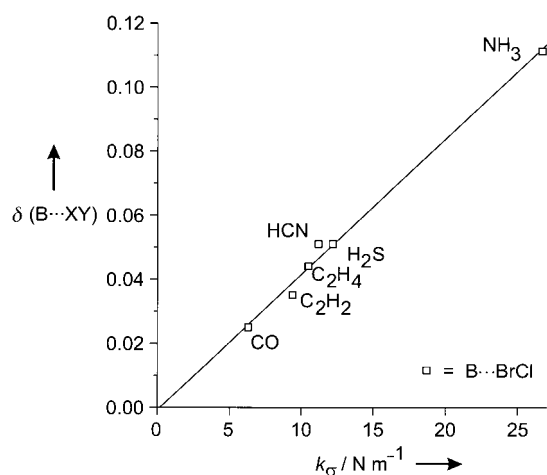


Figure 5. Systematic variation of the fraction of an electronic charge δ transferred from Br to Cl on formation of $B \cdots BrCl$. The intermolecular stretching force constant k_σ is used to order the $B \cdots XY$ according to the strength of the interaction.

value of δ for $B \cdots BrCl$ is approximately twice that of $B \cdots Cl_2$. It is of interest that $k_\sigma(B \cdots BrCl) \approx 2k_\sigma(B \cdots Cl_2)$ for a given B also (see Section 3.2).

Application of a similar approach to complexes $B \cdots ClF$ encounters the problem that F does not possess a nuclear electric quadrupole moment, and hence only Equation (8) is available for $X = Cl$. To deconvolute δ and ϕ_{av} , some assumption is then necessary. One approach is to make sensible assumptions about ϕ_{av} , which are discussed in detail elsewhere.^[51] The result is that, for the $B \cdots ClF$ in which B is N_2 ,^[52] CO ,^[53] C_2H_2 ,^[54] C_2H_4 ,^[55] HCN ,^[56] H_2S ,^[57] or H_2O ,^[58] δ lies in the range 0.00 to 0.040. $H_3N \cdots ClF$ ^[59] is excluded from the list of $B \cdots ClF$ complexes discussed because there is evidence from the value of $\chi_{zz}(Cl)$ for a contribution of a few percent of the ionic structure $[H_3NCl]^+ \cdots F^-$ to a valence bond description of the molecule (see Section 4.2).

3.1.3. Are $B \cdots XY$ Complexes Considered Here of the Mulliken Outer or Inner Type?

The discussion of Sections 3.1.1 and 3.1.2 is based on a simple interpretation of the changes in the XY nuclear quadrupole coupling constants when $B \cdots XY$ is formed. Some general conclusions about the nature of the intermolecular interaction are possible by consideration of the fractional electronic charge transferred from X to Y so determined.

First, with the exceptions of $H_3N \cdots BrCl$ ^[50] and $H_3N \cdots ClF$,^[59] which are both fairly strongly bound according to the k_σ criterion (see Section 3.2), δ is only a few hundredths of an electronic charge. Evidently, the XY molecule suffers only a minor electronic perturbation. Accordingly, we describe all the complexes $B \cdots ClF$, $B \cdots BrCl$, $B \cdots Cl_2$ so far mentioned as belonging to the weak, outer type defined by Mulliken.^[3] This is the reason why intermolecular charge transfer was ignored in the analysis of XY nuclear quadrupole coupling constants in Section 3.1.1.

Second, we note that for a given B the values of δ are in the order $B \cdots BrCl > B \cdots Br_2 > B \cdots Cl_2 > B \cdots ClF$. For example, when B is CO the values of δ are 0.025,^[45] 0.020,^[40] 0.012,^[28]

and 0.013,^[51] respectively. This order is that which might be expected in terms of the axial dipole polarizabilities of the interhalogen/halogen molecules, which follow the same pattern.^[60]

We shall show in Section 4 that it is possible to observe complexes that do show significant charge transfer between the Lewis base and Lewis acid.

3.2. Systematic Behavior among Intermolecular Stretching Force Constants k_σ of $B \cdots XY$

Intermolecular stretching force constants k_σ have been determined from centrifugal distortion constants D_J or Δ_J for a sufficient number of halogen or interhalogen complexes with Lewis bases B to establish whether there is any systematic behavior of k_σ when B or XY is systematically varied. Such behavior has already been identified^[61, 62] in the series of complexes $B \cdots HX$ ($X = F, Cl, Br$).

Table 2 displays the values of k_σ for some $B \cdots XY$ complexes with axial or C_{2v} symmetry ($H_2S \cdots XY$ complexes are an exception, but they differ inertially so little from axial

Table 2. Values of the intermolecular stretching force constant k_σ [$N m^{-1}$] for complexes $B \cdots XY$.^[a]

B	XY				
	F ₂	Cl ₂	Br ₂	BrCl	ClF
CO	– (1.3)	3.7 ^[32] (3.6)	5.1 ^[40] (6.3)	6.3 ^[45] (6.3)	7.0 ^[53] (6.9)
C ₂ H ₂	– (2.0)	5.6 ^[36] (5.4)	– (7.8)	9.4 ^[47] (9.5)	10.0 ^[54] (10.3)
C ₂ H ₄	– (2.2)	5.9 ^[27] (6.0)	– (8.7)	10.5 ^[46] (10.6)	11.0 ^[55] (11.5)
HCN	2.6 ^[63] (2.3)	6.6 ^[37] (6.2)	– (9.1)	11.1 ^[49] (11.0)	12.3 ^[56] (12.0)
H ₂ S	2.4 ^[64] (2.6)	6.3 ^[35] (6.9)	– (10.0)	12.2 ^[48] (11.0)	13.3 ^[57] (13.2)
NH ₃	4.7 ^[65] (4.7)	12.7 ^[38] (12.6)	18.5 ^[39] (18.3)	26.7 ^[50] (22.3)	34.3 ^[59] (24.3)

[a] Values in parentheses are calculated from the N_B and E_{XY} values of Table 5 by using Equation (10). See text for discussion of the discrepancy of observed and calculated k_σ for $H_3N \cdots ClF$.

symmetry that they can be considered here with negligible error). Several conclusions are immediately evident from Table 2. First, for a given XY, the order of k_σ is $OC < HCCH \approx H_2CCH_2 < HCN \lesssim H_2S < NH_3$. This order also holds for $B \cdots F_2$ with $B = HCN$,^[63] H_2S ,^[64] or NH_3 ,^[65] for these complexes the interaction is extremely weak. Second, for a given B, the order of k_σ is $F_2 < Cl_2 < BrCl < ClF$. Both sets of observations are consistent with the deductions about δ in Section 3.1 and with the conclusion that the interaction is, for the most part, of the weak electrostatic type.

It is of interest to compare the behavior of the k_σ in the $B \cdots XY$ series with those in the related hydrogen-bonded series $B \cdots HX$. Values for the latter^[66] are listed in Table 3. In general the $B \cdots HX$ interactions are of the weak electrostatic type,^[67, 68] and the k_σ values of a large number of complexes can be reproduced by the empirical Equation (10)^[61, 62] where

$$k_\sigma = c N_B E_{HX} \quad (10)$$

N_B and E_{HX} are gas-phase nucleophilicities and electrophilicities assigned to the individual molecules B and HX, respectively, and c is a constant. Values of N_B and E_{HX} for a range of B and HX are given in Table 4 and, with the value

$c = 0.25 \text{ N m}^{-1}$, reproduce the observed k_{σ} of the $\text{B} \cdots \text{HX}$ in Table 3 very well. Questions that immediately suggest themselves are: Can the k_{σ} of the $\text{B} \cdots \text{XY}$ series be reproduced by an equation such as Equation (10) and, if so, are the

Table 3. Values of the intermolecular stretching force constant k_{σ} [N m^{-1}] for a selection of hydrogen-bonded complexes $\text{B} \cdots \text{HX}$.^[a]

B	HX		
	HF	HCl	HBr
CO	8.5 (8.5)	3.9 (4.2)	3.0 (3.6)
C_2H_2	– (12.8)	6.4 (6.4)	– (5.4)
C_2H_4	– (11.8)	5.9 (5.9)	5.2 ^[118] (4.9)
H_2S	12.0 (12.0)	6.8 (6.0)	5.9 (5.0)
HCN	18.2 (18.2)	9.1 (9.1)	7.3 (7.7)
NH_3	32.8 (30.0) ^[b]	17.6 (14.9) ^[76]	13.4 (12.5) ^[77]

[a] Experimental values are from references [61] or [62], unless otherwise noted. Values in parenthesis were calculated by using the appropriate N_{B} and E_{XY} values from Table 4 and the analogue of Equation (10). [b] Calculated by using the value of D_{H} communicated to the author by P. R. R. Langridge-Smith and B. J. Howard, in the appropriate expression from reference [22].

Table 4. Values of nucleophilicities N_{B} of Lewis bases B and electrophilicities E_{HX} of HX, as determined from k_{σ} values of $\text{B} \cdots \text{HX}$.

nucleophilicities ^[a]						
B	CO	C_2H_2	C_2H_4	H_2S	HCN	NH_3
N_{B}	3.4	5.1	4.7	4.8	7.3	11.9
electrophilicities ^[b]						
HX	HF	HCl	HBr			
E_{HX}	10.0	5.0	4.2			

[a] Values of N_{B} were obtained from the k_{σ} values of a wide range of $\text{B} \cdots \text{HX}$ in references [61] and [62], except for N_{NH_3} , which was estimated by using only the k_{σ} for $\text{H}_3\text{N} \cdots \text{HCN}$ and $\text{H}_3\text{N} \cdots \text{HCCH}$. [b] Values of E_{HX} from references [61] and [62].

nucleophilicities of B with respect to the XY identical with those obtained from the k_{σ} of the $\text{B} \cdots \text{HX}$ series.

We begin by assuming that c in Equation (10) has the same value for both the $\text{B} \cdots \text{HX}$ and $\text{B} \cdots \text{XY}$ series. We choose arbitrarily that $E_{\text{BrCl}} = 9.0$ and then use k_{σ} for the $\text{B} \cdots \text{BrCl}$ series^[45–49] in Equation (10) to obtain the N_{B} values for CO, C_2H_2 , C_2H_4 , HCN, and H_2S shown in Table 5. We do not use the $\text{H}_3\text{N} \cdots \text{BrCl}$ value^[50] to obtain N_{NH_3} because the approx-

Table 5. Values of nucleophilicities N_{B} of Lewis bases B and electrophilicities E_{XY} of dihalogen molecules XY calculated from k_{σ} values of $\text{B} \cdots \text{XY}$.^[a]

nucleophilicities						
B	CO	C_2H_2	C_2H_4	H_2S	HCN	NH_3
N_{B}	2.8	4.2	4.7	5.4	4.9	9.9
electrophilicities						
XY	F_2	Cl_2	Br_2	BrCl	ClF	
E_{XY}	1.9	5.1	7.4	9.0	9.8	

[a] Values of N_{B} and E_{XY} were obtained from the k_{σ} values of a wide range of $\text{B} \cdots \text{XY}$, as described in detail in the text.

imation of weak interaction probably does not hold in this complex, which has $k_{\sigma} = 26.7(3) \text{ N m}^{-1}$. Instead, we employ $k_{\sigma} = 12.7 \text{ N m}^{-1}$ of $\text{H}_3\text{N} \cdots \text{Cl}_2$ ^[38] with $E_{\text{Cl}_2} = 5.1$ (see below) to obtain $N_{\text{NH}_3} = 9.9$ from Equation (10). The choices of $E_{\text{F}_2} = 1.9$, $E_{\text{Cl}_2} = 5.1$, $E_{\text{Br}_2} = 7.4$, $E_{\text{BrCl}} = 9.0$, and $E_{\text{ClF}} = 9.8$ together

with the N_{B} values of Table 5 then reproduce the observed k_{σ} values (see Table 3) reasonably well; exceptions are for $\text{H}_3\text{N} \cdots \text{BrCl}$ and $\text{H}_3\text{N} \cdots \text{ClF}$, which have observed k_{σ} values considerably larger than those predicted on the basis of the E_{XY} and N_{B} values of Table 5 by using Equation (10). These larger values are thought to arise from a nonnegligible charge transfer, as represented by a small contribution of the ionic structure $[\text{H}_3\text{N}^+ \cdots \text{Y}^-]$ to the valence bond description of these complexes.^[59] In the case of $\text{H}_3\text{N} \cdots \text{ClF}$, evidence in favor of this conclusion can also be adduced from the Cl nuclear quadrupole coupling constant. (See Section 4 for further discussion.)

Table 4 contains the N_{B} values determined for the $\text{B} \cdots \text{HX}$ series, while Table 5 lists those derived from $\text{B} \cdots \text{XY}$ in the manner described above. The magnitude of N_{B} for the two classes of complex is similar for a given B, except for the case of HCN, which appears to exhibit a much greater nucleophilicity with respect to hydrogen halides than it does with respect to diatomic halogen or interhalogen molecules. The E_{XY} values of Table 5 should be compared with the set of E_{HX} derived previously from k_{σ} of $\text{B} \cdots \text{HX}$ complexes (Table 4). The order $E_{\text{F}_2} < E_{\text{Cl}_2} < E_{\text{Br}_2} < E_{\text{BrCl}} < E_{\text{ClF}}$ is reasonable in view of the order of the electric quadrupole moments^[69, 70] of $2.76 \times 10^{-40} \text{ C m}^2$, $10.79(54) \times 10^{-40} \text{ C m}^2$, and $17.52 \times 10^{-40} \text{ C m}^2$ for F_2 , Cl_2 , and Br_2 , respectively, and the fact that BrCl and ClF have small electric dipole moments of similar magnitude.^[71, 72]

3.3. Systematic Behavior among Angular Geometries of $\text{B} \cdots \text{XY}$

3.3.1. Introduction

The analysis of the halogen nuclear quadrupole coupling constants of $\text{B} \cdots \text{XY}$ (Section 3.1) established that most complexes involve only a minor perturbation of the electric charge distribution of the halogen. Similarly, the intermolecular stretching force constants k_{σ} , considered in Section 3.2, are usually small and indicate that the intermolecular binding is weak. The systematic behavior of the k_{σ} as B and XY are varied is similar to that observed previously for a large number of hydrogen-bonded complexes $\text{B} \cdots \text{HX}$, the properties of which can be understood on the basis of a simple electrostatic model. It seems likely that the properties of the series $\text{B} \cdots \text{XY}$ may also be accounted for by such a model. In this section we consider angular geometries of $\text{B} \cdots \text{XY}$ determined from the rotational spectra under the assumption of unperturbed monomer geometries. This assumption is reasonable in view of the conclusions about electric charge redistribution and the strength of the interaction given above. Moreover, ab initio calculations on some $\text{B} \cdots \text{XY}$ confirm that this assumption is unlikely to lead to serious errors.^[41, 73, 74]

The angular geometries of the $\text{B} \cdots \text{HX}$ were rationalized some time ago by using a set of empirical rules^[67, 75] that are electrostatic in origin. These rules may be stated in three parts: The angular geometry of a hydrogen-bonded complex $\text{B} \cdots \text{HX}$ can be predicted by assuming that, in the equilibrium arrangement, the axis of the HX molecule lies 1) along the axis of a nonbonding electron pair (n-pair) of the electron-

donor atom of B, with $H^{\delta+}$ closer to the n-pair than $X^{\delta-}$, or 2) if B carries no n-pairs, along the local symmetry axis of a π or pseudo- π orbital, whereby $H^{\delta+}$ interacts with the π density. 3) If B carries both n- and π pairs, rule (1) defines the angular geometry.

3.3.2. n-Type Complexes of Simple Lewis Bases ($B = CO, HCN, NH_3, H_2O, H_2S, HF$)

In this section we shall examine whether these rules apply to $B \cdots XY$ complexes and, if so, how accurate is the parallelism between the $B \cdots XY$ and $B \cdots HX$ angular geometries. We shall use mostly $B \cdots HCl$ as the example of the latter because this is the series within $B \cdots HX$ that is most extensively investigated.

We consider first those complexes $B \cdots XY$ for which the symmetry of B is such that the assumption of linearity of the systems $Z \cdots X-Y$ and $Z \cdots H-Cl$ (Z is the electron-donor atom/center in B), implicit in the rules as stated in Section 3.3.1, will hold. We shall then consider examples where the hydrogen and halogen bonds can be nonlinear.

The complexes $H_3N \cdots F_2$,^[65] $H_3N \cdots Cl_2$,^[38] $H_3N \cdots Br_2$,^[39] $H_3N \cdots BrCl$,^[50] and $H_3N \cdots ClF$ ^[59] all have C_{3v} geometry of the type shown in Figure 6. Hence they are consistent with rule (1), when it is restated to take into account that the electrophilic region of the halogen ($\delta+$ in $\delta^+X^{\delta-}X^{\delta+}$ or $\delta^+X-Y^{\delta-}$) interacts with the n-pair on N so that XY lies along

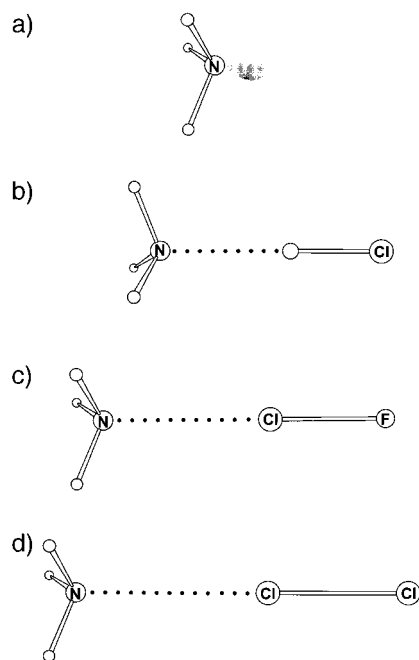


Figure 6. a) Nonbonding pair electron density model of NH_3 and the observed C_{3v} geometries of b) $H_3N \cdots HCl$, c) $H_3N \cdots ClF$, and d) $H_3N \cdots Cl_2$. All diagrams in this review are drawn to scale. Hydrogen atoms are shown as small open circles and are unlabeled. All other atoms are labeled. The orbitals of nonbonding electron pairs are drawn in the exaggerated “rabbit’s ear” form that is conventional in chemistry; they are not to be taken literally. Component geometries are assumed to be unperturbed by complex formation. Distances $r(Z \cdots X)$ for all complexes $B \cdots XY$ and $B \cdots HX$ considered here, where Z is the acceptor atom or center in B, can be found in Tables 7–10.

the C_3 axis. Similar geometries have been observed for $H_3N \cdots HX$ complexes ($X = Cl$,^[76] Br ,^[77] I ^[78]) as shown in Figure 6 for $H_3N \cdots HCl$. A similar interpretation applies to the C_{3v} complex $H_3P \cdots Cl_2$,^[34] which is isostructural with $H_3P \cdots HX$ ($X = F$,^[79] Cl ,^[80] Br ,^[81] I ^[82]).

The complexes $OC \cdots Cl_2$,^[32] $OC \cdots Br_2$,^[40] $OC \cdots BrCl$,^[45] and $OC \cdots ClF$ ^[53] all have linear arrangements in which the n-pair on C is the center of interaction with the $\delta+$ region of the halogen or interhalogen molecule. This arrangement is isomorphous with those observed for all $OC \cdots HX$ ($X = F$,^[83] Cl ,^[84] Br ,^[85] I ^[86]) and is that predicted by a suitably modified rule (3), since OC carries both n-pairs and π pairs, but the n-pair on C takes precedence. The complexes $HCN \cdots F_2$,^[63] $HCN \cdots Cl_2$,^[37] $HCN \cdots BrCl$,^[49] and $HCN \cdots ClF$ ^[56] also have a linear geometry, in which XY is preferentially attached to the axial nonbonding pair on N rather than to the π electrons of the $C \equiv N$ bond. Hence rule (3) is obeyed by this series also. The $HCN \cdots HX$ ^[87–90] have a similar geometry.

The symmetries of the Lewis bases B so far discussed lead to complexes in which the $Z \cdots X-Y$ and $Z \cdots H-X$ systems are linear in the equilibrium geometry, where Z is the electron-donor atom or the center of the π bond in B. The first, and simplest, examples in which the conventional nonbonding or π electron model of the Lewis base B leads to the possibility of a nonlinear $Z \cdots X-Y$ or $Z \cdots H-X$ system occur when B is H_2O or H_2S . The nonbonding electron pair model of H_2O is shown in Figure 7 and leads, according to

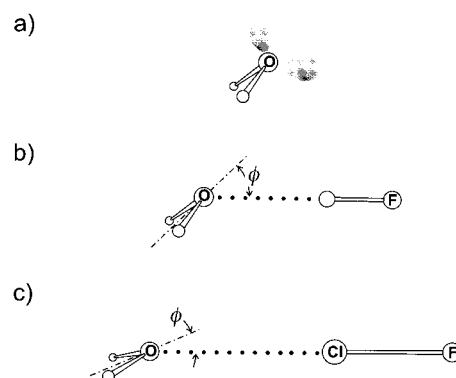


Figure 7. a) Nonbonding electron pair model of H_2O and the observed geometries (pyramidal, C_s) of b) $H_2O \cdots HF$ and c) $H_2O \cdots ClF$. The equilibrium geometry for $H_2O \cdots HF$ is shown, for which the angle $\phi = 46(5)^\circ$, as determined in reference [92]. For $H_2O \cdots ClF$, the estimated value is $\phi \approx 20^\circ$, but this is an effective value for the zero-point state (see reference [58]).

rule (1), to the prediction of a pyramidal equilibrium geometry for $H_2O \cdots ClF$ and $H_2O \cdots F_2$. In fact, the available experimental data are insufficient to determine whether the $O \cdots Cl-F$ or $O \cdots F-F$ nuclei are strictly collinear in the equilibrium arrangement and therefore collinearity was assumed. The experimental evidence was sufficient, however, to show that $H_2O \cdots ClF$ ^[58] and $H_2O \cdots F_2$ ^[91] are either effectively planar or planar in the equilibrium geometry. In this context effectively planar means that, although the equilibrium configuration at O is pyramidal, the energy

barrier at the planar conformation is low enough that the vibrational wavefunctions can be classified according to the representations of the C_{2v} point group, that is, even in the zero-point state, the molecule tunnels rapidly between the equivalent pyramidal conformers. There are some indications that $\text{H}_2\text{O} \cdots \text{ClF}$ is, like $\text{H}_2\text{O} \cdots \text{HF}$, effectively planar, so that the equilibrium geometry is pyramidal, as required by the rules and the model of Figure 7. A detailed analysis of rotational spectra in vibrationally excited states associated with the intermolecular bending modes in $\text{H}_2\text{O} \cdots \text{HF}$ showed^[92] that although the barrier to the planar form is low, it is nonzero and the equilibrium geometry is as shown in Figure 7, with the angle $\phi = 46^\circ$ between the HF axis and the C_2 axis close to half the tetrahedral angle required by rule (1). The preferred angular geometry of $\text{H}_2\text{O} \cdots \text{ClF}$ is also shown in Figure 7. It is not possible to determine whether $\text{H}_2\text{O} \cdots \text{F}_2$ is planar or effectively planar, but in view of the weakness of its binding ($k_0 = 3.63(7) \text{ N m}^{-1}$) and the fact that the barrier is below the zero-point energy level in the more strongly bound $\text{H}_2\text{O} \cdots \text{HF}$ ($k_0 = 25(2) \text{ N m}^{-1}$), it is likely to be planar for all practical purposes and is so drawn in Figure 8. Both $\text{H}_2\text{O} \cdots \text{HCl}$ ^[93] and $\text{H}_2\text{O} \cdots \text{HBr}$ ^[94] are also effectively planar. Thus, all of the $\text{H}_2\text{O} \cdots \text{HX}$ and $\text{H}_2\text{O} \cdots \text{XY}$ complexes considered here can be viewed as “floppy” with respect to intermolecular bending.



Figure 8. The observed geometry of $\text{H}_2\text{O} \cdots \text{F}_2$, which is effectively planar in the zero-point state (see reference [91]).

A nonbonding electron pair model of H_2S in which the two nonbonding pairs occupy two sp hybrid orbitals whose axes are at 180° to each other and at 90° to the plane of the H_2S nuclei (Figure 9a) is consistent with the observed geometries

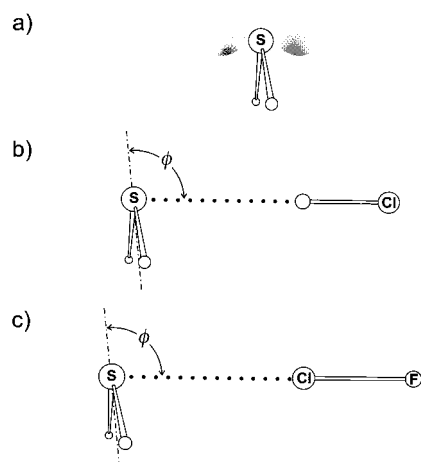


Figure 9. a) Nonbonding electron pair model of H_2S and the observed geometries of b) $\text{H}_2\text{S} \cdots \text{HCl}$ ($\phi = 93.8(5)^\circ$) and c) $\text{H}_2\text{S} \cdots \text{ClF}$ ($\phi = 95.8(5)^\circ$).

of $\text{H}_2\text{S} \cdots \text{XY}$. According to rule (1), in the equilibrium geometry of $\text{H}_2\text{S} \cdots \text{XY}$ complexes the axis of the XY molecule should lie perpendicular to the H_2S plane. In fact,

detailed interpretations of the halogen nuclear quadrupole coupling constants in $\text{H}_2\text{S} \cdots \text{Cl}_2$,^[35] $\text{H}_2\text{S} \cdots \text{BrCl}$,^[48] and $\text{H}_2\text{S} \cdots \text{ClF}$ ^[57] allow the conclusion that the $\text{S} \cdots \text{X}-\text{Y}$ nuclei in these three complexes lie within a degree or so of collinearity. The determined geometry of one such complex is shown in Figure 9c. Again it is remarkably similar to that in the series $\text{H}_2\text{S} \cdots \text{HX}$ ($\text{X} = \text{F}$,^[95] Cl ,^[96] Br ^[97]) which is exemplified by $\text{H}_2\text{S} \cdots \text{HCl}$ in Figure 9b. In none of the $\text{H}_2\text{S} \cdots \text{XY}$ or $\text{H}_2\text{S} \cdots \text{HX}$ molecules is there any evidence of other than a high potential energy barrier at the planar form, and it is concluded that, on the time scale of the microwave experiment, they are permanently pyramidal.

The situation is somewhat different for $\text{H}_2\text{S} \cdots \text{F}_2$,^[64] however. The geometry determined from zero-point rotational constants of four isotopomers is shown in Figure 10 and is

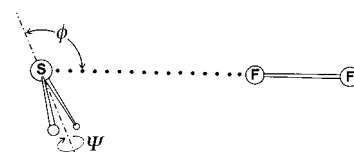


Figure 10. The observed geometry of $\text{H}_2\text{S} \cdots \text{F}_2$. The angle $\phi = 113(5)^\circ$, and the internal rotation of H_2S about its local C_2 axis (angle ψ) gives rise to a low-energy vibrational satellite in the rotational spectrum. (See text and reference [64] for discussion).

pyramidal, as for the other $\text{H}_2\text{S} \cdots \text{XY}$, with $\phi = 113(5)^\circ$. In addition, even at the low effective temperature of the supersonic expansion used for the $\text{H}_2\text{S} \cdots \text{F}_2$ complexes, a vibrational satellite is observed in the rotational spectrum. This suggests that a low potential energy barrier separates two equivalent pyramidal conformations. The barrier corresponds either to the planar C_{2v} geometry, with motion between the two equilibrium conformers like the conventional inversion of ammonia or, more likely, to the planar C_s conformation, through which the molecule passes as a result of internal rotation of the H_2S subunit about its local C_2 axis. The observation of a vibrational satellite here is consistent with the conclusion of Section 3.2 that complexes $\text{B} \cdots \text{F}_2$ are very weakly bound compared with those of the other halogens or interhalogens, at least according to the k_0 criterion. In the limit of weak binding and a long distance $r(\text{S} \cdots \text{F}_1)$, a less rigid geometry is to be expected.^[75] Nevertheless, it is significant that $\text{H}_2\text{S} \cdots \text{F}_2$ is still isostructural with the other $\text{H}_2\text{S} \cdots \text{HX}$ (see Figures 9 and 10).

In the $\text{H}_2\text{O} \cdots \text{XY}$ and $\text{H}_2\text{S} \cdots \text{XY}$ series, the electron-donor atom O or S of the Lewis base B carries two equivalent nonbonding electron pairs. There is one example of a set $\text{B} \cdots \text{XY}/\text{B} \cdots \text{HX}$ so far investigated in which B carries three equivalent nonbonding pairs in the conventional model, namely, when B is HF (Figure 11). The three complexes $\text{HF} \cdots \text{ClF}$,^[98] $\text{HF} \cdots \text{Cl}_2$,^[33] and $\text{HF} \cdots \text{HCl}$ ^[99] are again isostructural, as illustrated by the determined geometries of $\text{HF} \cdots \text{ClF}$ and $\text{HF} \cdots \text{HCl}$ drawn to scale in Figure 11. The angles ϕ are consistent with rule (1). Interestingly, the isomer $\text{HCl} \cdots \text{HF}$ has also been observed^[100] and has a right-angled geometry, as expected from rule (1) if the n-pairs on the second-row atom Cl are at 90° to each other, as is commonly assumed.

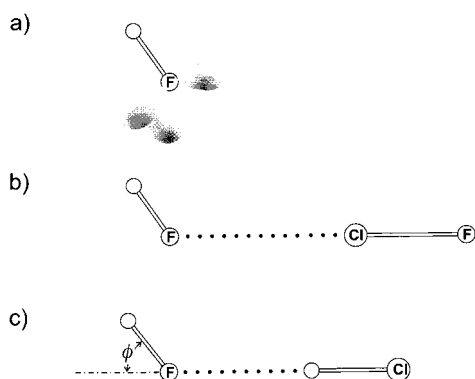


Figure 11. a) Nonbonding electron pair model of HF and the observed geometries (planar, C_s) of b) $\text{HF} \cdots \text{CIF}$ ($\phi = 55^\circ$) and c) $\text{HF} \cdots \text{HCl}$ ($\phi = 50^\circ$).

3.3.3. *n*-Type Complexes of More Complicated Lewis Bases: Deviations of $\text{Z} \cdots \text{X}-\text{Y}$ Nuclei from Collinearity

If a complex involving XY or HX with B has C_s symmetry or lower, the halogen or hydrogen bonds can be nonlinear, that is, the nuclei $\text{Z} \cdots \text{X}-\text{Y}$ or $\text{Z} \cdots \text{H}-\text{X}$ can deviate from collinearity, where Z is the electron-donor atom or center of B. This section outlines the method for measuring the angular deviation of the nuclei from collinearity and then compares the results for the two series of complexes $\text{B} \cdots \text{CIF}$ and $\text{B} \cdots \text{HCl}$, where B is an *n*-pair donor. The reasons why the method has so far been restricted largely to CIF complexes in the $\text{B} \cdots \text{XY}$ series will become apparent.

We shall focus our attention on complexes in which the Lewis base B is 2,5-dihydrofuran, formaldehyde, oxirane, or thiirane. All complexes $\text{B} \cdots \text{CIF}$ ^[101–104] and $\text{B} \cdots \text{HCl}$ ^[105–109] of these Lewis bases have C_s symmetry, and therefore the molecular symmetry plane must coincide with one of the principal inertial planes (in fact, *ab* or *ac*). Then one of the off-diagonal elements of the Cl nuclear quadrupole coupling tensor χ_{ab} or χ_{ac} will be nonzero. For such complexes it can be shown^[23, 105] that, to a good degree of approximation, the equilibrium angle α_{az} between the *a* inertial axis and the CIF or HCl axis *z* is given by Equation (11) or by the corresponding expression in which the right hand side involves χ_{ac} , χ_{aa} , and χ_{cc} .

$$\tan(2\alpha_{az}) = -2\chi_{ab}/(\chi_{aa} - \chi_{bb}) \quad (11)$$

The angle α_{az} is an important geometrical quantity because it defines the position of the CIF or HCl subunit in the equilibrium conformation of the complex and can be combined with the principal moments of inertia of appropriate isotopomers to determine precisely the relative positions and orientations of the subunits B and CIF or HCl in space. It then follows that the positions of the electron-donor atom Z and the Cl and F nuclei in, for example, $\text{B} \cdots \text{CIF}$ are precisely known and hence so is the deviation of the $\text{Z} \cdots \text{Cl}-\text{F}$ system from linearity.

Figure 12 compares the angular geometries of the two C_s planar molecules $\text{H}_2\text{CO} \cdots \text{CIF}$ ^[102] and $\text{H}_2\text{CO} \cdots \text{HCl}$ ^[106, 107] as determined by fitting their principal moments of inertia under the constraint that the geometry obtained must also repro-

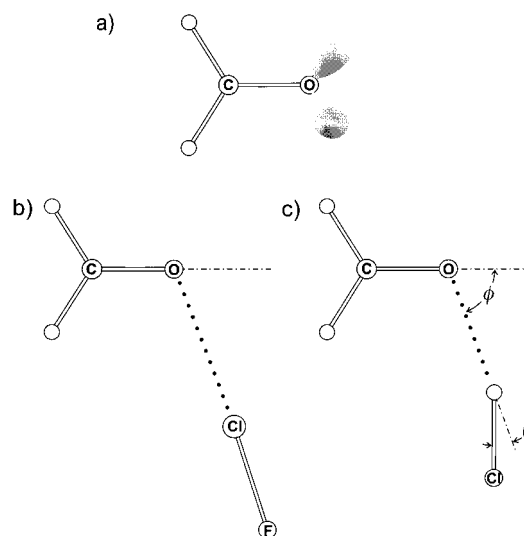


Figure 12. a) Nonbonding electron pair model of H_2CO and the observed angular geometries (C_s , planar) of b) $\text{H}_2\text{CO} \cdots \text{CIF}$ ($\phi = 69.1(7)^\circ$; $\theta = 3.2(7)^\circ$) and c) $\text{H}_2\text{CO} \cdots \text{HCl}$ ($\phi = 70.0(10)^\circ$; $\theta = 20.5(8)^\circ$). The angle θ is a measure of the angular deviation of the $\text{O} \cdots \text{Cl}-\text{F}$ or $\text{O} \cdots \text{H}-\text{Cl}$ nuclei from collinearity.

duce the angle α_{az} from Equation (11). Details of the fitting method and of the method for estimating errors are given elsewhere.^[23] The diagrams in Figure 12 are drawn to scale. The angle ϕ is nearly identical in the two complexes and is close to that expected from the rules enunciated above and the familiar *n*-pair model of formaldehyde, in which O carries nonbonding electron pairs in two sp^2 hybrid orbitals (Figure 12a). However, the angle θ , which defines the angular deviations of the nuclei in $\text{O} \cdots \text{Cl}-\text{F}$ and $\text{O} \cdots \text{H}-\text{Cl}$ from collinearity, is close to zero in $\text{H}_2\text{CO} \cdots \text{CIF}$ but is $20.5(8)^\circ$ in $\text{H}_2\text{CO} \cdots \text{HCl}$. This pattern of a highly nonlinear hydrogen bond in $\text{B} \cdots \text{HCl}$ but a nearly linear halogen bond in the corresponding $\text{B} \cdots \text{CIF}$ is common, as demonstrated below.

A Lewis base that has an oxygen atom with two nonbonding electron pairs with the tetrahedral angle between them is 2,5-dihydrofuran. The C-O-C angle in this cyclic ether is 108° ,^[110] and presumably therefore the conventional approach would require the two *n*-pairs on O to complete a nearly tetrahedral environment for the atom. The complexes of 2,5-dihydrofuran with CIF ^[101] and HCl ^[105] are of C_s symmetry and have the geometries displayed in Figure 13. The angle ϕ is again similar in both complexes and is as required if the CIF/HCl molecules lie along the axis of one of the *n*-pairs on O. As for the complexes involving H_2CO , the angular deviation $\theta = 9.5^\circ$ of the $\text{O} \cdots \text{H}-\text{Cl}$ nuclei from collinearity is significant, while that for $\text{O} \cdots \text{Cl}-\text{F}$ is negligible.

If we proceed from the cyclic ether 2,5-dihydrofuran to oxirane, the accepted view is that in closing the C-O-C angle from 108° to about 60° the angle between the *n*-pairs on O should increase. The determined geometries of the complexes of oxirane with HCl ^[108] and CIF ^[103] are drawn to scale in Figure 14. The angle ϕ is essentially identical in the two complexes and its value is indeed consistent with the rules for predicting angular geometries, as the angle between the *n*-pairs on O is increased from its value of about 110° in 2,5-

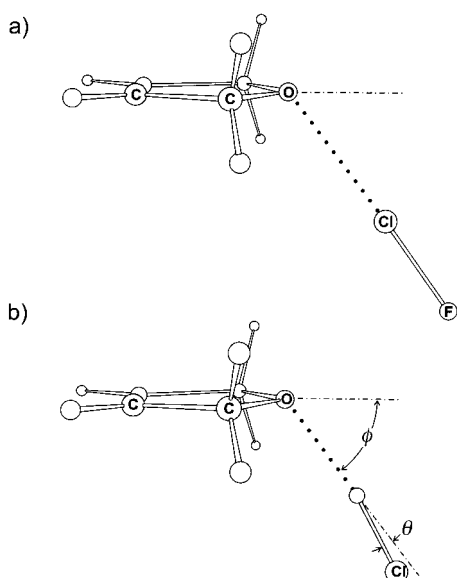


Figure 13. Observed geometries (C_s) of a) 2,5-dihydrofuran...ClF ($\phi = 53.0(3)^\circ$; $\theta = 2.0(2)^\circ$) and b) 2,5-dihydrofuran...HCl ($\phi = 54.3(3)^\circ$; $\theta = 9.5(1)^\circ$).

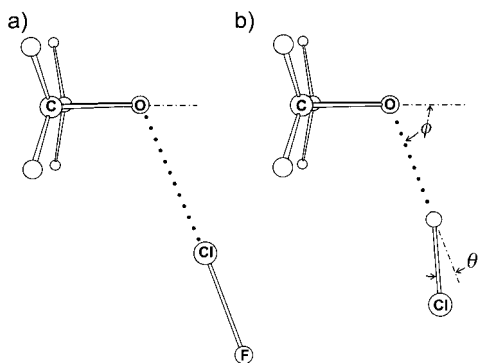


Figure 14. Observed geometries (C_s) of a) oxirane...ClF ($\phi = 67.3(1)^\circ$; $\theta = 2.9(1)^\circ$) and b) oxirane...HCl ($\phi = 69.1(1)^\circ$; $\theta = 16.5(1)^\circ$).

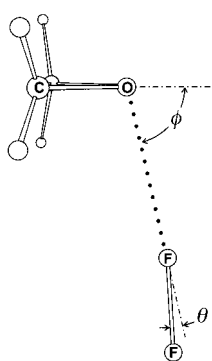


Figure 15. Observed geometry of oxirane... F_2 ($\phi = 76(4)^\circ$). Angle θ was assumed to take the value 10° . This leads to a value of $r(O \cdots F_i)$ similar to that of O-F in oxirane...HF. See Table 7 and text for discussion.

dihydrofuran. However, the hydrogen bond in $(CH_2)_2O \cdots HCl$ is significantly nonlinear ($\theta = 16.5^\circ$), while the $O \cdots Cl-F$ system in $(CH_2)_2O \cdots ClF$ deviates by only a few degrees from linearity.

The observation of complexes of oxirane with ClF and HCl is a testimony to the efficacy of the fast-mixing nozzle, given the reactivity of ClF and the facile opening of the oxirane ring by HCl. Perhaps even more remarkable is the detection and characterization of the complex of oxirane with F_2 .^[111] The resulting angular geometry of $(CH_2)_2O \cdots F_2$ is shown in Figure 15. Unfortunately, the absence of any nuclear quadrupole coupling associated with the F_2 subunit means that the angle α_{az} between the F_2 axis (z)

and the a axis cannot be determined in this case, and hence the extent of the nonlinearity of the $O \cdots F-F$ system could not be quantified. The geometry shown in Figure 15 is based on the assumption of $\theta = 10^\circ$ (minor nonlinearity), which leads to $\phi = 76(4)^\circ$, where the error arises from the assumption $\theta = 10 \pm 5^\circ$. Interestingly, even though the $O \cdots F$ interaction is weak ($k_o = 3.1 \text{ Nm}^{-1}$), there is no evidence of vibrational satellites or inversion doubling, as there was in $H_2S \cdots F_2$, for example.

The cyclic thioether thiirane forms isostructural complexes with ClF^[104] and HCl^[109] (Figure 16). The perpendicular structures with the angles $\phi \approx 90^\circ$ are readily understood on

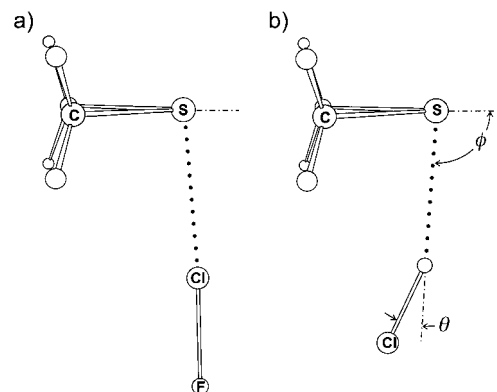


Figure 16. Observed geometries (C_s) of a) thiirane...ClF ($\phi = 85.0(2)^\circ$; $\theta = 3.5(2)^\circ$) and b) thiirane...HCl ($\phi = 94.5(20)^\circ$; $\theta = 21.0(5)^\circ$). There is some evidence for a significant contribution of the ionic structure $[(CH_2)_2S]^+ \cdots F^-$ to the valence-bond description of thiirane...ClF, which may account for the discrepancy between ϕ for these two complexes (see reference [104] for discussion).

the basis of an n-pair model of thiirane like that of H_2S (see Figure 9) and the rules for predicting angular geometries. They are also reminiscent of those of their acyclic analogues $H_2S \cdots ClF$ ^[57] and $H_2S \cdots HCl$ ^[96] (see Figure 9). Although it was shown that the $S \cdots Cl-F$ nuclei are nearly collinear in $H_2S \cdots ClF$, such a conclusion was not available for $H_2S \cdots HCl$. However, application of Equation (11) to the $(CH_2)_2S$ complexes shows that while the $S \cdots Cl-F$ nuclei in $(CH_2)_2S \cdots ClF$ deviate from collinearity by only $\theta = 3.5^\circ$, the hydrogen bond in $(CH_2)_2S \cdots HCl$ is highly nonlinear ($\theta = 21.0^\circ$).

For all complexes considered in this section so far, the electron-donor atom Z of B carries two equivalent non-bonding electron pairs. A prototype Lewis base that offers the possibility of a pair of inequivalent nonbonding electron pairs on the electron-donor atom is sulfur dioxide, the conventional n-pair model of which is shown in Figure 17. The complexes $SO_2 \cdots ClF$,^[112] $SO_2 \cdots HCl$,^[23, 113] and $SO_2 \cdots HF$ ^[114] have very similar angular geometries, the first two of which are included in Figure 17. In each case the ClF or HX molecule lies approximately along the axis of the n-pair that is *cis* to the S=O bond. The microwave spectrum of $SO_2 \cdots HCl$ provides evidence of considerable nonrigidity, so in the geometry displayed in Figure 17 the deviation of ϕ from the expected value may not be significant. The nuclei $O \cdots H-Cl$ in $SO_2 \cdots HCl$ ^[23] and $O \cdots Cl-F$ in $SO_2 \cdots ClF$ ^[112] are within a degree or so of collinearity, as indicated by precise determination of θ

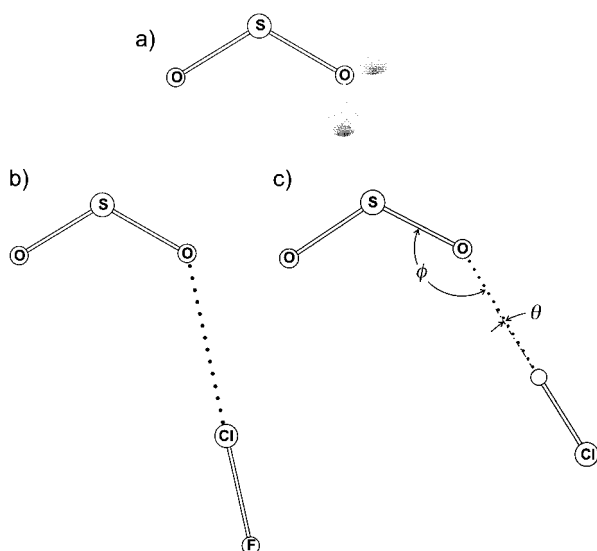


Figure 17. a) Nonbonding electron pair model of SO_2 and observed geometries of b) $\text{SO}_2 \cdots \text{ClF}$ ($\phi = 131.9(6)^\circ$; $\theta = -0.7(2)^\circ$) and c) $\text{SO}_2 \cdots \text{HCl}$ ($\phi = 143.0(1)^\circ$; $\theta = -2.5(7)^\circ$). The “floppiness” of the complex $\text{SO}_2 \cdots \text{HCl}$ may account for its larger angle ϕ .

from the off-diagonal element χ_{ab} of the Cl nuclear quadrupole coupling tensor. This fact is of importance in the simple model for describing deviations of hydrogen bonds and halogen bonds from linearity that is discussed in Section 3.5.2.

The discussions in this section reveal a parallel between the angular geometries of $\text{B} \cdots \text{ClF}$ and $\text{B} \cdots \text{HCl}$ complexes of C_s symmetry when B is an n-pair donor, but with the main difference that the hydrogen bond deviates significantly from linearity while the $\text{Z} \cdots \text{Cl}-\text{F}$ nuclei remain nearly collinear as B varies. A simple interpretation of this behavior is possible but will be postponed until after the angular geometries of complexes $\text{B} \cdots \text{XY}$ and $\text{B} \cdots \text{HX}$ in which B is a nonaromatic π donor or an aromatic π donor are considered in the following two sections.

3.3.4. π -Type Complexes in Which B is a Nonaromatic π -Electron Donor

Figures 18 and 19 show the experimentally determined angular geometries of the complexes of the two simplest π -electron donors ethene^[27] and ethyne,^[26] respectively, with Cl_2 , as well as those of ethene $\cdots\text{HCl}$ ^[115] and ethyne $\cdots\text{HCl}$,^[116] which are clearly isostructural with those of the corresponding chlorine complexes. Other complexes ethene $\cdots\text{XY}$ ($\text{XY} = \text{BrCl}$,^[46] ClF ,^[55] HF ,^[117] HBr ^[118]) also have the angular geometry shown in Figure 18 and, correspondingly, other complexes ethyne $\cdots\text{XY}$ ($\text{XY} = \text{BrCl}$,^[47] ClF ,^[54] and HF ^[119]) have been shown to have the planar T shape illustrated in Figure 19. In all cases, $\text{X}^{\delta+}$ of XY interacts with the π -electron density. All of these angular geometries are readily understood on the basis of rule (2) in Section 3.3.1, that is, the electrophile Cl_2 or HCl lies along the symmetry axis of a π orbital of the Lewis base. The familiar π bonding electron density distributions of ethene and ethyne are shown in Figures 18 and 19, respectively.

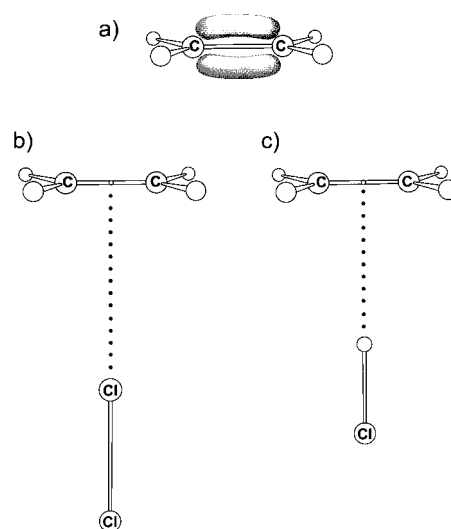


Figure 18. a) π -Bonding electron density model of ethene and observed geometries (perpendicular, C_{2v}) of b) ethene $\cdots\text{ClF}$ and c) ethene $\cdots\text{HCl}$. In this, and subsequent figures, the symbol \circ marks the center of the C–C multiple bond.

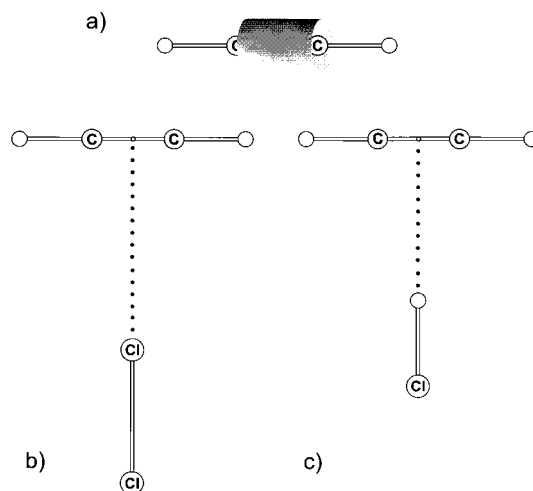


Figure 19. a) π -Bonding electron density model of ethyne (schematic; cylindrical symmetry) and observed geometries (planar, C_{2v}) of b) ethyne $\cdots\text{ClF}$ and c) ethyne $\cdots\text{HCl}$.

The similarity of cyclopropane in its chemical behavior to an olefin led to a description of the molecule (from Coulson and Moffitt)^[120] in which its unsaturated character was accounted for by a pseudo- π carbon–carbon bond formed by overlap of a pair of sp^3 hybrid orbitals on adjacent carbon atoms. A schematic electron-density distribution for one of the bonds of cyclopropane resulting from the Coulson–Moffitt model is displayed in Figure 20. Such bonds have often been referred to as “banana” bonds. The symmetry axis of the pseudo- π orbital coincides with a median of the cyclopropane equilateral triangle. Hence, according to rule (2), the angular geometry of complexes such as cyclopropane $\cdots\text{ClF}$ ^[121] and cyclopropane $\cdots\text{HCl}$ ^[122] should have C_{2v} symmetry with the ClF or HCl internuclear axis coincident with the median and with the electrophilic end $\text{Cl}^{\delta+}$ of ClF or $\text{H}^{\delta+}$ of HCl closer to the C–C bond than $\text{F}^{\delta-}$ or $\text{Cl}^{\delta-}$, respectively. The observed geometries of the two complexes (Figure 20b, c) reveal that this is indeed the case.

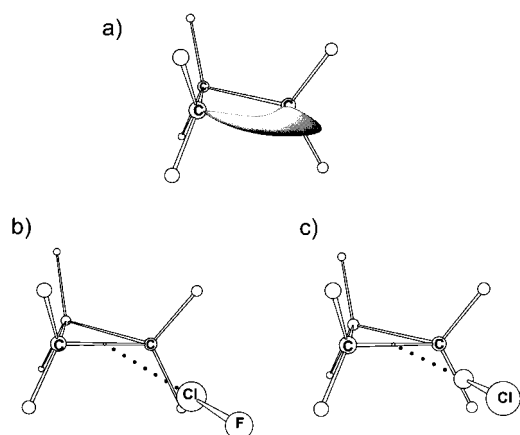


Figure 20. a) Pseudo- π electron density model (Coulson and Moffit^[120]) of cyclopropane and observed geometries of b) cyclopropane \cdots CIF and c) cyclopropane \cdots HCl.

The prototype Lewis base that carries a pair of conjugated, nonaromatic π bonds is 1,3-butadiene. According to rule (2), the axis of a CIF or HCl molecule, for example, will lie along the local symmetry axis of one of the π orbitals. Two possibilities then exist, however. Either the CIF/HCl interaction is localized and involves only one of the π bonds (if the potential energy barrier to tunneling between the four equivalent positions is sufficiently high), or tunneling occurs between the four positions for a low barrier. The geometry of the complex of CIF with 1,3-butadiene^[123] is drawn to scale in Figure 21. The ground-state rotational spectrum of this

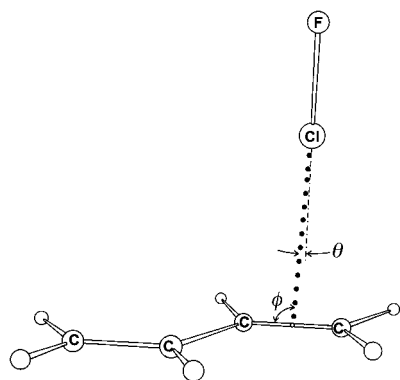


Figure 21. Observed geometry of 1,3-butadiene \cdots CIF. The CIF molecular axis is perpendicular to the plane of the nuclei of 1,3-butadiene, with $\phi = 95.0(2)^\circ$ and $\theta = 2.6(10)^\circ$. θ defines the angular deviation of the \cdots Cl-F system from linearity.

complex showed no evidence of quantum mechanical tunneling between the equivalent structures, and therefore, on the time scale of the microwave experiment, we conclude that the $\pi \cdots$ CIF interaction is localized at a single site. The geometry displayed in Figure 21 is consistent with rule (2) in that the CIF axis is perpendicular to the plane of the nuclei in 1,3-butadiene and the angle ϕ is 95° , where \circ indicates the center of the $C_1=C_2$ bond. A comparison with the corresponding HCl complex is not yet possible, because the rotational spectrum of 1,3-butadiene \cdots HCl exhibits the characteristics of nonrigid

rotor behavior, probably as a result of a low potential energy barrier between the four equivalent conformers.^[124]

Four equivalent centers of interaction between a π orbital and a Lewis acid such as CIF or HCl are also possible when the π donor is the prototype system carrying two cumulative π bonds, namely, allene. The π -electron density model of allene is displayed in Figure 22, together with the experimentally

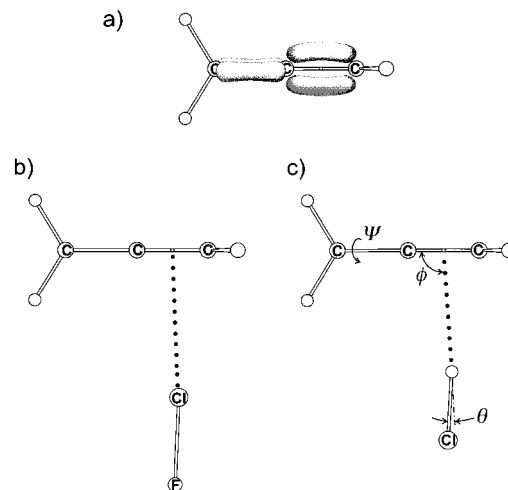


Figure 22. a) π -Bonding electron density model of allene and observed geometries (C_s) of b) allene \cdots CIF ($\phi = 92.5(7)^\circ$; $\theta = 4.9(15)^\circ$) and c) allene \cdots HCl ($\phi = 93(4)^\circ$; $\theta \approx 7^\circ$). ψ is the angle of rotation of the allene subunit with respect to its C_2 axis (the geometry with $\psi = 0$ is shown here).

determined angular geometries of allene \cdots HCl^[125] and allene \cdots CIF.^[126] Although all angles of rotation ψ about the $C=C=C$ axis are consistent with the spectroscopic constants observed in both investigations because allene is a symmetric-top molecule, the chemically reasonable choice $\psi = 0$ is shown in Figure 22. In that case, the electrophilic end $H^{\delta+}$ or $Cl^{\delta+}$ of HCl or CIF interacts with the maximum of π -electron density. The angle $\psi = 90^\circ$ would correspond to the interaction of these atoms with the nodal plane of a π orbital.

The C_s symmetry of allene \cdots HCl and allene \cdots CIF leads to nonzero elements χ_{ab} of the Cl nuclear quadrupole coupling tensor and hence, by the method described in Section 3.3.3, to the angles θ defining the nonlinearities of the $Z \cdots H-Cl$ and $Z \cdots Cl-F$ systems as well as the angles ϕ (see Figure 22 for definitions). We note again that the angle ϕ for each complex is close to the value of 90° required by rule (2). The value of $\theta \approx 7^\circ$ for allene \cdots HCl^[125] and $\theta = 4.9(15)^\circ$ ^[126] for allene \cdots CIF are both in a direction that suggests a secondary interaction of $Cl^{\delta-}$ and $F^{\delta-}$, respectively, with the nearest H atom on the C atom remote from the center of the π interaction. Recall that secondary interactions of this kind were observed for the $B \cdots HCl/B \cdots CIF$ complexes of C_s symmetry in which the primary interaction is with an n-pair donor.

The final example of a Lewis base that is a nonaromatic π donor is methylenecyclopropane. In the sense that methylenecyclopropane has two pseudo- π C-C bonds of a cyclopropane ring contiguous with the $C_1=C_2$ π bond, it may be taken as the prototype that carries cumulative π and pseudo- π bonds. The observed geometries of complexes of this Lewis base with CIF^[127] and HCl^[128] are shown in Figure 23. Clearly,

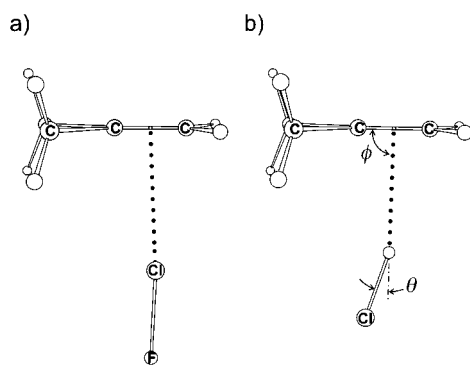


Figure 23. Observed geometries of a) methylenecyclopropane \cdots CIF ($\phi = 92.5(5)^\circ$; $\theta = 4.9(1)^\circ$) and b) methylenecyclopropane \cdots HCl ($\phi = 90.8^\circ$; $\theta = 17.5^\circ$). The similarity between the geometries of methylenecyclopropane \cdots CIF and allene \cdots CIF (Figure 22) is noteworthy.

the intermolecular interaction involves $\text{Cl}^{\delta+}$ or $\text{H}^{\delta+}$ and the π bond rather than the pseudo- π bond, and the fact that the angles ϕ are close to 90° in both complexes is consistent with rule (2). The $\text{Z} \cdots \text{H}-\text{Cl}$ system again shows considerable deviation from linearity, while that of $\text{Z} \cdots \text{Cl}-\text{F}$ system is small. If the values of $\theta \neq 0^\circ$ were an artefact of an unsymmetrical π bond, one would expect similar values for both the HCl and CIF complexes of methylenecyclopropane.

3.3.5. π -Type Complexes in Which B is an Aromatic π -Electron Donor

It is clear from the preceding section that rule (2) applies to all complexes $\text{B} \cdots \text{CIF}/\text{B} \cdots \text{HCl}$ so far investigated in which B is a nonaromatic π -electron donor. Thus, for those cases in which both $\text{B} \cdots \text{CIF}$ and $\text{B} \cdots \text{HCl}$ have been investigated, the pairs have isomorphous angular geometries that differ only in the extent of the nonlinearities of the $\text{Z} \cdots \text{Cl}-\text{F}$ and $\text{Z} \cdots \text{H}-\text{Cl}$ systems. In this section, we discuss the angular geometries of complexes in which B is potentially an aromatic π -electron donor. The molecules B considered are the prototype aromatic π -electron donor benzene and the two simple heteroaromatic molecules furan and thiophene. Although complexes $\text{B} \cdots \text{HX}$ have been investigated for $\text{X} = \text{F}, \text{Cl}$, and Br , the $\text{B} \cdots \text{XY}$ systems examined have so far been restricted to those with $\text{XY} = \text{CIF}$, since they are spectroscopically more tractable than other $\text{B} \cdots \text{XY}$.

When B is the prototype aromatic molecule benzene, rule (2) predicts that the electrophilic end $\text{Cl}^{\delta+}$ of CIF or $\text{H}^{\delta+}$ of HX will interact with the π -electron system, but the equivalence of the six maxima in the π -electron density that occur at the midpoints of the C–C bonds leads to an ambiguity. Two possibilities exist: $\text{Cl}^{\delta+}/\text{H}^{\delta+}$ is localized at the center of a C–C bond, as is the case for all of the nonaromatic π -electron donors (except for the interaction of allene with HCl), or internal motion of the CIF/HX subunit allows $\text{Cl}^{\delta+}/\text{H}^{\delta+}$ to sample the six equivalent positions.

The rotational spectra of benzene $\cdots \text{HX}$ ($\text{X} = \text{F},^{[129]} \text{Cl},^{[130]} \text{Br},^{[131]} \text{CN}^{[132]}$) and benzene $\cdots \text{CIF}^{[133]}$ are of the symmetric-top type in the vibrational ground state under supersonic-expansion conditions. However, benzene $\cdots \text{CIF}$ exhibits an additional rotational spectrum in such experiments and,

because of the low effective temperature of the gas, the satellite spectrum must be associated with a low-energy vibrationally excited state. The behavior of this vibrational satellite spectrum can be interpreted in terms of a Coriolis interaction between the ground state and the vibrationally excited state, which in turn leads to the conclusion that the observed geometry of benzene $\cdots \text{CIF}$ is as shown in Figure 24.

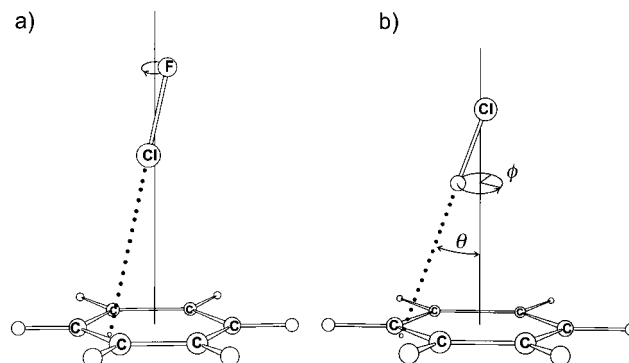


Figure 24. Observed geometries of a) benzene \cdots CIF and b) benzene \cdots HCl. The C_{6v} geometry ($\theta = 0^\circ$) represents a potential energy maximum in benzene \cdots CIF, and the $\text{Cl}^{\delta+}$ end of CIF samples the π -electron density in the zero-point state as a result of the angular motion ϕ as defined in (b). This motion is therefore governed by a “Mexican-hat” type of potential function. The point \circ represents the intersection of the extrapolated CIF internuclear axis with the benzene nuclear plane and lies 0.24 \AA from the center of the C–C bond, inside the ring. See text and reference [133] for discussion.

The C_{6v} structure corresponding to $\theta = 0$ occurs at a potential energy maximum, while in the zero-point state the CIF subunit executes the angular motion defined by ϕ in Figure 24. Thus, the electrophilic atom $\text{Cl}^{\delta+}$ samples the entire π -electron density, and the motion in the ϕ coordinate follows a nearly circular path along the potential energy minimum that encircles the maximum at $\theta = 0$ and encompasses the six carbon atoms. It is likely that the benzene $\cdots \text{HX}$ ($\text{X} = \text{F}, \text{Cl}, \text{Br}, \text{CN}$) complexes behave similarly, but no vibrational satellite spectra were observed. Unfortunately, it is not possible to distinguish on the basis of ground-state rotational spectra alone between a strictly C_{6v} equilibrium geometry and a geometry of the type observed for benzene $\cdots \text{CIF}$. However, in either case, the vibrational wavefunctions will have C_{6v} symmetry.

The heteroatoms of furan and thiophene formally carry a nonbonding electron pair in an orbital whose symmetry axis coincides with the C_2 axis of the molecule. It is of interest to examine whether rule (3) applies to complexes of furan and thiophene with CIF and HX, for the Lewis base carries an n-pair and aromatic π pairs in each case. The usual model of the n-pair and π -electron density in furan is shown in Figure 25a. The experimentally determined geometry of furan $\cdots \text{HCl}^{[134]}$ is depicted in Figure 25b. It has C_{2v} symmetry, and the HCl molecule lies along the C_2 axis of furan and forms a hydrogen bond to O. Evidently, rule (3) holds for furan $\cdots \text{HCl}$ because the n-pair on O, rather than the π electrons, defines the angular geometry. The result for furan $\cdots \text{HF}^{[135]}$ is similar.

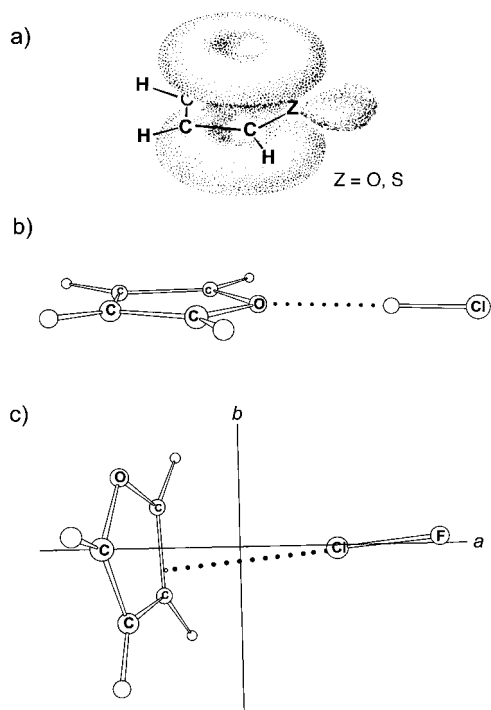


Figure 25. a) π -Bonding and nonbonding electron density model of furan ($Z = \text{O}$) or thiophene ($Z = \text{S}$) and the observed geometries of b) furan...HCl (planar, C_{2v}) and c) furan...ClF (C_1). Note that the point \circ of the intersection of the extrapolated ClF internuclear axis and the furan nuclear plane lies close to the center of the $\text{C}_2\text{--C}_3$ bond.

All of the results established so far for pairs of complexes B...ClF and B...HCl show that they are isostructural for a given B (see Sections 3.3.2–3.3.5). The case in which B is furan is the first for which this conclusion does not hold, and furan...ClF is the first in either series to contravene rule (3). The observed geometry^[136] (see Figure 25c) demonstrates unambiguously that the ClF subunit interacts with the electron density associated with the π system in the manner expected if rule (2) applies. An intriguing question then concerns the closely related molecule thiophene: Does it behave like furan with regard to its complexes with HCl and ClF, or is the pair thiophene...HCl/thiophene...ClF isostructural? If the latter, is the π system or the n-pair on S the center of the intermolecular interaction?

Some light may be shed on the electric charge distributions of furan and thiophene by considering their electric moments. Table 6 compares the electric dipole moments μ ^[137–140] and the three components Q_{aa} , Q_{bb} , Q_{cc} of the electric quadrupole

moments^[140, 141] of pyridine, furan, and thiophene. There is good agreement between the experimental values and those from ab initio calculations. All the electric dipole moments are negative, with the heteroatom at the negative end in each case. The component Q_{aa} of the electric quadrupole moment changes from a large negative value in pyridine, through zero for furan, and becomes positive in thiophene. The magnitudes of the electric dipole moments also decrease along this series. This behavior of the electric moments suggests a progressive withdrawal of negative charge along the C_2 axis from the n-pair on the heteroatom into the ring. However, Q_{cc} and hence the extension of the π cloud above and below the nuclear plane, is greatest for thiophene. The electric moments suggest that the aromatic π system of thiophene might be more nucleophilic than the n-pair on sulfur and, moreover, suggest that furan might represent a crossover point of the relative nucleophilicities of the two types of site.

The angular geometry of thiophene...HCl determined from analyses of the rotational spectra of several isotopomers is shown in Figure 26 in projection on the ab principal inertial

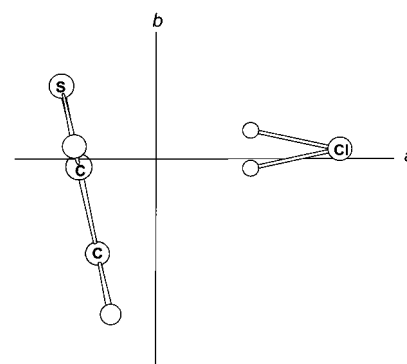


Figure 26. Observed geometry (C_s) of thiophene...HCl shown in projection in the ab principal inertial plane, which coincides with the molecular symmetry plane. Both orientations of the HCl subunit shown are consistent with the observed rotational constants and Cl nuclear quadrupole coupling constants of several isotopomers. See text for discussion.

plane.^[142] This plane is either a plane of symmetry (i.e., the complex has C_s symmetry) or there is a fairly low potential energy barrier at the C_s geometry, and the H atom oscillates backwards and forwards through the plane and samples electron density on each side of one face of the ring. It is not possible to distinguish between these possibilities on the basis of the rotational spectrum alone. Moreover, the angle α_{az} between the HCl axis (z) and the a axis is known in magnitude

Table 6. Molecular electric moments of pyridine, furan, and thiophene.

Molecular electric moment ^[a]	Pyridine		Furan		Thiophene	
	exptl.	theory	exptl.	theory	exptl.	theory
μ_a [10^{-30} Cm]	−7.17(15) ^[137]	−8.324	−2.285(3) ^[138]	−2.899	−1.83(3) ^[139]	−2.374
Q_{aa} [10^{-40} Cm ²]	−11.7(30)	−10.79	0.7(13)	0.06	5.7(53)	4.55
Q_{bb} [10^{-40} Cm ²]	32.4(30)	33.96	20.0(10)	22.72	22.0(50)	23.20
Q_{cc} [10^{-40} Cm ²]	−20.7(50)	−23.16	−20.0(10)	−22.78	−27.7(73)	−27.75

[a] The principal inertial axis a coincides with the C_2 symmetry axis of each molecule, while c is perpendicular to the plane of the nuclei in each case. The positive direction of a is towards the heteroatom. All theoretical values of the molecular electric moments are taken from reference [140]. [c] All experimental values of the electric quadrupole moments are due to Flygare et al.^[141]

(see Section 3.3.3) but not in sign, and hence both orientations of HCl with respect to the a axis shown in Figure 26 are possible. Whatever the detail, it is clear that thiophene \cdots HCl resembles benzene \cdots HCl (Figure 24) in its angular geometry and that the HCl molecule samples the π -electron density on one face of the ring. It is clearly not isostructural with furan \cdots HCl (see Figure 25). Thiophene \cdots HF^[143] is similar in geometry to thiophene \cdots HCl, with a similar ambiguity in the sign of α_{az} .

Analogous difficulties exist with the exact placement of the ClF unit in thiophene \cdots ClF^[144] and both structures implied in Figure 27 are consistent with all the observables from the

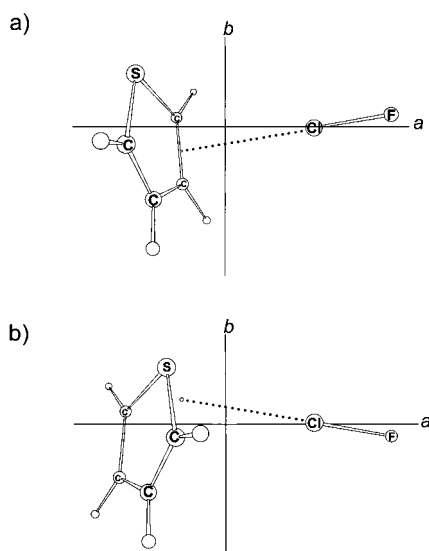


Figure 27. a), b) The two preferred geometries of thiophene \cdots ClF (C_1) that are consistent with the observed rotational constants and the complete Cl nuclear quadrupole coupling tensor of the ^{35}Cl and ^{37}Cl isotopomers. Note that geometry (a) is similar to that observed for furan \cdots ClF.

rotational spectrum, including the three angles α_{az} , α_{bz} , and α_{cz} . All three angles are available because the molecule has no symmetry and therefore all three off-diagonal elements χ_{ab} , χ_{ac} , and χ_{bc} of the Cl nuclear quadrupole coupling tensor are nonzero and experimentally determinable. It is clear from Figure 27 that the electrophilic end $\text{Cl}^{\delta+}$ of ClF interacts with the π -electron density on one face of the thiophene ring. We

note that one of the structures implied in Figure 27 is very similar to that established for furan \cdots ClF (see Figure 25) in that the extension of the ClF axis intersects the nuclear plane of thiophene near to the center of one of the $\text{C}_2=\text{C}_3$ bonds.

With reference to Table 6, a question of interest is now whether pyridine \cdots ClF and pyridine \cdots HCl are isostructural and if so whether the subunit ClF/HCl interacts with the n-pair as the nucleophilic center rather than the π -electron density. Certainly, the electric moments of Table 6 tend to suggest this. The observed geometry of pyridine \cdots HCl^[145] has C_{2v} symmetry, with a hydrogen bond between HCl and N (Figure 28). The complex pyridine \cdots ClF has yet to be investigated.

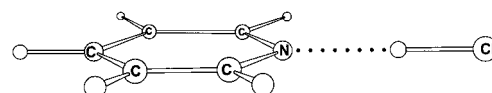



Figure 28. Observed geometry (C_{2v} , planar) of pyridine \cdots HCl.

3.4. Systematic Behavior among Radial Geometries of $\text{B} \cdots \text{XY}$

So far, in discussing complexes $\text{B} \cdots \text{XY}$ and comparing them with the corresponding hydrogen-bonded complexes $\text{B} \cdots \text{HX}$, we have focused on systematic relationships among angular geometries, the strength of binding (as measured by k_o), and the redistribution of electric charge within the XY subunit. It is also possible to identify systematic behavior in the radial geometries, that is, the distances $r(\text{Z} \cdots \text{X})$, where Z is the electron-donor atom in B for σ -type complexes or the electron-donor center in B for π -type complexes and X is the inner halogen atom of $\text{B} \cdots \text{XY}$.

We begin with the most weakly bound group of complexes, namely, those $\text{B} \cdots \text{X}_2$ in which the halogen is molecular fluorine. Table 7 compares the distances $r(\text{Z} \cdots \text{F}_i)$ in the two series $\text{B} \cdots \text{F}_2$ and $\text{B} \cdots \text{HF}$, where B is H_2S ,^[64, 95] HCN ,^[63, 87] CH_3CN ,^[146, 147] H_2O ,^[91, 92] $(\text{CH}_2)_2\text{O}$,^[111, 148] and NH_3 .^[65, 149] It is evident that $r(\text{Z} \cdots \text{F})$ is insignificantly different between the pair $\text{B} \cdots \text{F}_2$ and $\text{B} \cdots \text{HF}$ for a given B. Moreover, $r(\text{Z} \cdots \text{F})$ is identical to the sum of the van der Waals radii $\sigma(\text{Z}) + \sigma(\text{F})$ ^[150] of Z and F, given that the latter are not known better than to about 0.05 Å and hence that $\sigma(\text{Z}) + \sigma(\text{F})$ has an uncertainty of

Table 7. Comparison of angular geometries and distances $r(\text{Z} \cdots \text{F})$ in complexes $\text{B} \cdots \text{F}_2$ and $\text{B} \cdots \text{HF}$.

$\text{B} \cdots \text{XF}$	Angular geometry		$r(\text{Z} \cdots \text{F}_i/\text{F})$ [Å]		$\sigma(\text{Z}) + \sigma(\text{F})$ [Å] ^[a]
	symmetry	details	$\text{B} \cdots \text{F}_2$	$\text{B} \cdots \text{HF}$	
$\text{H}_2\text{S} \cdots \text{XF}$	C_s (Figure 10; $\text{X} = \text{F}$) C_s (Figure 9; $\text{X} = \text{H}$)	$\phi = 113(5)^\circ$ ^[64] $\phi = 91^\circ$ ^[95]	3.20(1) ^[64]	3.246 ^[95]	3.20
$\text{HCN} \cdots \text{XF}$	$C_{\infty v}$ ($\text{X} = \text{F}$ ^[63] and $\text{X} = \text{H}$ ^[87])		2.803(3) ^[63]	2.805(1) ^[87]	2.85
$\text{CH}_3\text{CN} \cdots \text{XF}$	C_{3v} ($\text{X} = \text{F}$ ^[146] and $\text{X} = \text{H}$ ^[147])		2.748(3) ^[146]	2.751(1) ^[147]	2.85
$\text{H}_2\text{O} \cdots \text{XF}$	C_{2v} (Figure 8; $\text{X} = \text{F}$ ^[91]) C_s (Figure 7; $\text{X} = \text{H}$ ^[92])		2.719(4) ^[91]	2.684(16) ^[b]	2.75
 $\cdots \text{XF}$	C_s (Figure 15; $\text{X} = \text{F}$) C_s (Figure 14; $\text{X} = \text{H}$)	$\phi = 76(4)^\circ$ ^[111] $\phi = 72.0(2)^\circ$ ^[148]	2.63(6) ^[111]	2.629(5) ^[148]	2.75
$\text{H}_3\text{N} \cdots \text{XF}$	C_{3v} ($\text{X} = \text{F}$ ^[65] and $\text{X} = \text{H}$ ^[149])		2.708(7) ^[65]	2.71 ^[149]	2.85

[a] Sum of van der Waals radii from reference [150]. [b] Fitted to rotational constants given by J. W. Bevan, Z. Kisiel, A. C. Legon, D. J. Millen, S. C. Rogers, *Proc. R. Soc. London A* **1980**, 372, 441–51 but with $\phi = 46^\circ$ as given in reference [92].

about 0.1 Å. This result is not unreasonable when the k_o for complexes $B \cdots F_2$ are considered.

In Section 3.2, it was noted that $B \cdots F_2$ interactions are extremely weak. The values of k_o recorded in Table 2 of Section 3.2 are in fact similar in magnitude to those of complexes of inert gas atoms with various partners. This similarity can be understood when it is recognized that not only does F_2 possess no electric dipole moment but also its electric quadrupole moment is close to zero.^[70] Consequently, F_2 appears to another molecule B as though it has a spherical electric charge distribution, that is, it behaves like an inert gas atom. It is then not unreasonable that the interaction distance $r(Z \cdots F)$ in the various $B \cdots F_2$ should be the sum of the van der Waals radii. Presumably, the dispersion interaction is relatively more important in $B \cdots F_2$ than other $B \cdots XY$. Nevertheless, the comparison of the angular geometries of $B \cdots F_2$ and $B \cdots HF$ for $B = H_2S, HCN, CH_3CN, H_2O, (CH_2)_2O$, and NH_3 in Table 7 indicates that electrostatic interaction involving δ^+F of $\delta^+F_{\delta^-}F^{\delta+}$ with B controls the shape of $B \cdots F_2$ in the same way that the B/δ^+H interaction does for $B \cdots HF$.

The fact that $r(Z \cdots F)$ is essentially identical in the two series $B \cdots HF$ and $B \cdots F_2$ suggests that, in modeling distances $r(Z \cdots F)$ in hydrogen-bonded complexes, the H atom of HF should be ignored. This procedure was used in the electrostatic model proposed by Buckingham and Fowler.^[68]

Molecular chlorine has no electric dipole moment, but its electric quadrupole moment is substantially larger than that of F_2 .^[70] This is reflected in the larger binding strengths of $B \cdots Cl_2$ complexes compared with those of $B \cdots F_2$ (see Section 3.2 and Table 2 for a discussion of k_o values). The distances $r(Z \cdots Cl)$ in various $B \cdots Cl_2$ ^[27, 32–38] are given in Table 8, where they are compared with those in the corresponding series $B \cdots HCl$ ^[76, 80, 84, 88, 96, 99, 115, 116] and with the sum $\sigma(Z) + \sigma(Cl)$ of

Table 8. Comparisons of distances $r(Z \cdots Cl)$ ^[a] in complexes $B \cdots Cl_2$ and $B \cdots HCl$.

B	$r(Z \cdots Cl_2/Cl) [\text{\AA}]$		$\Delta r [\text{\AA}]^{[b]}$		$\sigma(Z) + \sigma(Cl) [\text{\AA}]^{[c]}$	
	$B \cdots Cl_2$	ref.	$B \cdots HCl$	ref.		
H_3P	3.240	[34]	3.883	[80]	0.643	3.7
H_2S	3.249	[35]	3.809	[96]	0.560	3.65
OC	3.134	[32]	3.710	[84]	0.576	3.50
C_2H_4	3.128	[27]	3.724	[115]	0.596	3.50
C_2H_2	3.163	[36]	3.699	[116]	0.536	3.50
HF	2.96	[33]	3.367	[99]	0.41	3.15
HCN	2.915	[37]	3.405	[88]	0.490	3.30
NH_3	2.724	[38]	3.136	[76]	0.412	3.30

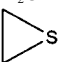
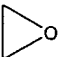
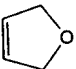
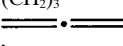
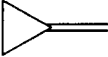
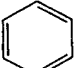
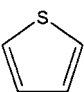
[a] Z is the electron-donor atom or electron-donor center in B. Values of $r(Z \cdots Cl)$ were taken from the indicated reference or calculated from data in the reference by the method of A. C. Legon, D. J. Millen, *Chem. Phys. Lett.* **1988**, *147*, 484–489. [b] $\Delta r = r(B \cdots HCl) - r(B \cdots Cl_2)$. [c] Sum of van der Waals radii taken from reference [150]. A radius of $\sigma(C) = 1.70$ Å was assumed for C in CO and for C–C multiple bonds.

the van der Waals radii^[150] of the atoms Z and Cl. Three conclusions are evident from Table 8. First, $r(Z \cdots Cl)$ contracts systematically by about 0.5 Å from $B \cdots HCl$ to $B \cdots Cl_2$. Secondly, the contraction Δr tends to decrease as the length $r(Z \cdots Cl)$ decreases. Thirdly, $r(Z \cdots Cl)$ for $B \cdots HCl$ is within about 0.1 Å of the sum of the van der Waals radii $\sigma(Z) + \sigma(Cl)$

of the acceptor center in B and Cl for all B, and $r(Z \cdots Cl)$ tends to become shorter than $\sigma(Z) + \sigma(Cl)$ for the more strongly bound species.

A similar pattern of contractions is observed (see Table 9) for the series $B \cdots ClF/B \cdots HCl$ for 17 different B (already referred to throughout this article), except that the contrac-

Table 9. Comparisons of distances $r(Z \cdots Cl)$ ^[a] in complexes in $B \cdots ClF$ and $B \cdots HCl$.

B	$r(Z \cdots Cl) [\text{\AA}]$		$\Delta r [\text{\AA}]^{[b]}$		$\sigma(Z) + \sigma(Cl) [\text{\AA}]^{[c]}$	
	$B \cdots ClF$	ref.	$B \cdots HCl$	ref.		
n-pair donors						
H_2S	2.857	[57]	3.809	[96]	0.952	3.65
OC	2.770	[53]	3.710	[84]	0.940	3.50
HF	2.77	[98]	3.367	[99]	0.60	3.15
SO_2	2.732	[112]	3.472	[23, 113]	0.740	3.20
HCN	2.639	[56]	3.405	[88]	0.766	3.30
H_2O	2.580	[58]	3.215	[93]	0.635	3.20
	2.472 ^[d]	[104]	3.62	[109]	1.15	3.65
	2.438	[103]	3.094	[23, 108]	0.656	3.20
	2.422	[101]	3.071	[105]	0.649	3.20
H_3N	2.376	[59]	3.136	[76]	0.760	3.30
π -pair donors						
C_2H_2	2.873	[54]	3.699	[116]	0.826	3.50
C_2H_4	2.766	[55]	3.724	[115]	0.958	3.50
$(CH_2)_3$	2.957	[121]	3.567	[122]	0.610	3.50
	2.774	[126]	3.55	[125]	0.78	3.50
	2.675	[127]	3.571	[128]	0.896	3.50
	3.313	[133]	3.903	[130]	0.590	3.50
	2.825	[144]	3.693	[142]	0.868	3.50

[a] See Table 8. [b] $\Delta r = r(B \cdots HCl) - r(B \cdots ClF)$. [c] Sum of van der Waals radii taken from reference [150]. A radius of $\sigma(C) = 1.70$ Å was assumed for C in CO and for C–C multiple bonds. [d] This $B \cdots ClF$ has a significant contribution from $[BCl]^+ \cdots F^-$ to the valence-bond description of the complex. See reference [104] and Section 4.2.

tions are systematically larger (mean value $\Delta r = 0.79$ Å compared with 0.53 Å). This is understandable, given that complexes $B \cdots ClF$ are systematically more strongly bound than those of $B \cdots Cl_2$, no doubt because ClF possesses an electric dipole moment while Cl_2 does not. The mean contraction of $r(Z \cdots Br)$ in complexes $B \cdots BrCl$ relative to the corresponding $B \cdots HBr$ —where B is CO ,^[45, 85] C_2H_4 ,^[46, 118] H_2S ,^[48, 97] HCN ,^[49, 89] and NH_3 ^[50, 77] (see Table 10)—of 0.83 Å is similar to that for the $B \cdots ClF/B \cdots HCl$ pairs. An insufficient number of $B \cdots Br_2$ have been investigated so far to allow any firm conclusions, except that there is again a substantial contraction of $r(Z \cdots Br)$ from $B \cdots HBr$ to $B \cdots Br_2$.^[39, 40, 77, 85]

Table 10. Comparisons of distances $r(\text{Z} \cdots \text{Br})^{[a]}$ in complexes $\text{B} \cdots \text{BrCl}$ or $\text{B} \cdots \text{Br}_2$ and $\text{B} \cdots \text{HBr}$.

B	$r(\text{Z} \cdots \text{Br}_1/\text{Br})$ [Å]				Δr [Å] ^[b]	$\sigma(\text{Z}) + \sigma(\text{Br})$ [Å] ^[c]
	$\text{B} \cdots \text{BrCl}/\text{Br}_2$	ref.	$\text{B} \cdots \text{HBr}$	ref.		
B \cdots BrCl						
H ₂ S	3.096	[48]	3.991	[97]	0.895	3.80
C ₂ H ₂	3.059	[47]	–	–	–	3.65
OC	3.004	[45]	3.917	[85]	0.913	3.65
C ₂ H ₄	2.979	[46]	3.917	[118]	0.938	3.65
HCN	2.834	[49]	3.610	[89]	0.776	3.45
NH ₃	2.628	[50]	3.255	[77]	0.627	3.45
B \cdots Br₂						
OC	3.050	[40]	3.917	[85]	0.867	3.65
NH ₃	2.72	[39]	3.255	[77]	0.535	3.45

[a] Z is the electron-donor atom or electron-donor center in B. Values of $r(\text{Z} \cdots \text{Br})$ were taken from the indicated reference or calculated from data in the reference by the method of A. C. Legon, D. J. Millen, *Chem. Phys. Lett.* **1988**, 147, 484–489.

[b] $\Delta r = r(\text{B} \cdots \text{HBr}) - r(\text{B} \cdots \text{BrCl})$ or $r(\text{B} \cdots \text{HBr}) - r(\text{B} \cdots \text{Br}_2)$. [c] See Table 8.

The systematic behavior in $r(\text{Z} \cdots \text{X})$ between $\text{B} \cdots \text{HX}$ and $\text{B} \cdots \text{XY}$ noted above can be explained in terms of the shape of halogen atoms in dihalogen molecules and anisotropic repulsion. The example of the $\text{B} \cdots \text{HCl}/\text{B} \cdots \text{Cl}_2$ pairs has been dealt with in detail and is discussed below. Similar considerations are likely to apply to $\text{B} \cdots \text{HBr}/\text{B} \cdots \text{BrCl}$.

Ab initio SCF calculations were carried out by using a helium atom to probe the repulsive potentials around the Cl_2 and HCl molecules.^[151] Two sets of energy calculations were carried out. Repulsive energy curves were calculated first for an end-on approach of He to Cl_2 and then for approach to each end of the HCl molecule, by obtaining the total energy and subtracting from it the induction contribution at a series of points. A repulsive wall was encountered about 0.6 Å earlier in the approach to the H end of HCl than to the Cl of Cl_2 or indeed to Cl in ClF. Moreover, a map of the repulsion-energy surface for approaches of He to Cl_2 shows that the Cl atom of Cl_2 is flattened by about 0.32 Å for head-on as opposed to perpendicular approach. The Cl_2 molecule therefore has the “snub-nosed” shape anticipated by Buckingham, as quoted in reference [26]. A similar conclusion was obtained for ClF. This snub-nosed character is evident when van der Waals spheres are placed on the atoms in $\text{H}_2\text{O} \cdots \text{ClF}$ and $\text{H}_2\text{O} \cdots \text{HCl}$, as shown by the spherical nets of appropriate radius drawn in Figure 29. It is clear that the van der Waals spheres of O and Cl just touch in $\text{H}_2\text{O} \cdots \text{HCl}$ but substantially interpenetrate in $\text{H}_2\text{O} \cdots \text{ClF}$, a situation that is highly unlikely in view of the repulsive energy involved. Presumably, the “sphere” on Cl in ClF should be drawn as “snub-nosed”, as suggested by the calculations of reference [151].

The situation in the related pair $\text{H}_2\text{O} \cdots \text{F}_2$ and $\text{H}_2\text{O} \cdots \text{HF}$, shown in a similar format in Figure 30, is quite different, however. The van der Waals spheres of oxygen and F just touch in both cases. This suggests that F_2 is not snub-nosed like Cl_2 and ClF. Ab initio calculations of the type carried out on Cl_2/HCl or ClF/HCl would be of interest for the F_2/HF pair. The conclusions of this section lead to the prediction that the F atom in F_2 is not anisotropic in the sense that Cl is in Cl_2 or ClF, or only slightly anisotropic.

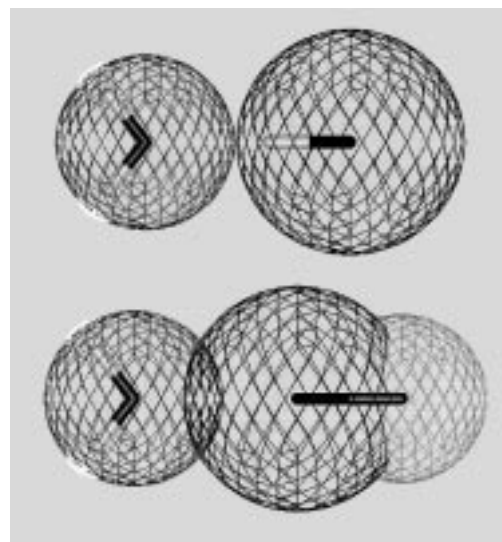


Figure 29. Stick models of $\text{H}_2\text{O} \cdots \text{HCl}$ (top) and $\text{H}_2\text{O} \cdots \text{ClF}$ (bottom) with spherical nets of the appropriate van der Waals radii centered on O, Cl, and F. Each model is drawn to scale at the experimental separation, with the configuration at O as planar for convenience. No van der Waals sphere is drawn on the H of HCl while (white) spheres of token radius are drawn on the H atoms of H_2O . Note that the O and Cl spheres just touch in $\text{H}_2\text{O} \cdots \text{HCl}$ but interpenetrate in $\text{H}_2\text{O} \cdots \text{ClF}$, leading to the hypothesis of a snub-nosed character for the Cl atom in ClF. See text for discussion.

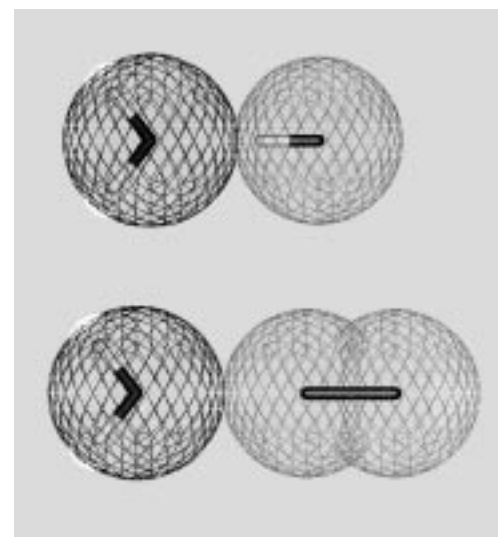


Figure 30. Stick models of $\text{H}_2\text{O} \cdots \text{HF}$ (top) and $\text{H}_2\text{O} \cdots \text{F}_2$ (bottom) with spherical nets of the appropriate van der Waals radii centered on O and F. Each model is drawn to scale at the experimental separation, with the configuration at O as planar for convenience. Note that the van der Waals spheres of O and F just touch in both complexes; hence that F_2 is not “snub-nosed” like Cl_2 and ClF. (Reproduced with permission from A. C. Legon, *Chem. Commun.* **1998**, 2737–2738.)

3.5. Conclusions about the Nature of $\text{B} \cdots \text{XY}$ from Systematic Behavior of Properties

3.5.1. Parallelisms among Properties of $\text{B} \cdots \text{XY}$ and $\text{B} \cdots \text{HX}$: A Model for the Halogen Bond

In Sections 3.1–3.4, the ways in which the properties of complexes $\text{B} \cdots \text{XY}$, where B is a Lewis base and XY is a homo- or heteronuclear dihalogen, change as B and XY are

systematically varied were considered. These properties include the electric charge redistribution in XY, the intermolecular stretching force constant k_{σ} , and the angular and radial geometries of the complex.

For most of the complexes considered so far, it was shown in Section 3.1 that the extent of the electric charge redistribution within the XY subunit is small. The intermolecular force constants k_{σ} , which were discussed in Section 3.2, indicate that these complexes are, for the most part, weakly bound. The combination of small electric charge redistribution and weak binding suggested that the simple electrostatic term (i.e., that involving interaction of the permanent, unperturbed electric charge distributions of the two molecules) is an important contribution to the interaction energy.

When in Section 3.3 the angular geometries of various series $B \cdots XY$ were discussed and compared with those in corresponding series of hydrogen-bonded complexes $B \cdots HX$, a strong parallelism was identified, and it became clear that the rules first enunciated^[67, 75] to rationalize angular geometries of $B \cdots HX$ also apply, after suitable modification, to $B \cdots XY$. The rules for the $B \cdots HX$ are implicitly electrostatic in origin, involving the identification of directions of greatest nucleophilicity (n-pair and π -pair directions) in the "electron donor" B. Subsequently, these rules were given a quantitative basis in the Buckingham–Fowler electrostatic model.^[68]

A further parallel between the $B \cdots XY$ and $B \cdots HX$ series was identified for the distances $r(Z \cdots X)$, where Z is the electron-donor atom/center in B. It was shown in Section 3.4 that this distance is systematically shorter in $B \cdots XY$ than in the corresponding $B \cdots HX$ for each of the series $B \cdots Cl_2/B \cdots HCl$, $B \cdots ClF/B \cdots HCl$, $B \cdots Br_2/B \cdots HBr$, and $B \cdots BrCl/B \cdots HBr$. This shortening can be attributed, in part at least, to an anisotropy of the X atom radius in molecules XY, and this effect was demonstrated by ab initio calculations^[151] in the case of Cl_2 and ClF . On the other hand, no such shortening is evident in the pair of series $B \cdots F_2/B \cdots HF$, a result which, when taken with the very weak intermolecular binding (as indicated by k_{σ}) in the $B \cdots F_2$ series, suggests that $B \cdots F_2$ complexes represent a limiting case. Evidently, F_2 is not snub nosed in the sense outlined for the other dihalogen molecules.

Given the remarkable parallelism of the $B \cdots XY$ and $B \cdots HX$ series summarized above and that (for the B and HX considered so far) the hydrogen bond in $B \cdots HX$ is accepted as being mainly electrostatic in origin, it seems reasonable to draw the conclusion that the interaction that predominates in defining the properties of the $B \cdots XY$ complexes is the electrostatic term (with the possible qualification in the case of $B \cdots F_2$ outlined in Section 3.4). Then, for example, the fact that the rules for angular geometries apply to both $B \cdots HX$ and $B \cdots XY$ is readily understood.

In view of the foregoing, it seems worthwhile to define a halogen bond^[152] that is an analogue of the hydrogen bond. Thus, the halogen bond is predominantly electrostatic in origin and involves the interaction of unperturbed electric charge distributions of B and XY. By analogy with the usual shorthand $B \cdots \delta^+H-X^{\delta-}$ for hydrogen-bonded complexes, we may likewise write $B \cdots \delta^+X-Y^{\delta-}$ for a halogen bond when XY is a heteronuclear dihalogen molecule. This shorthand

involves only the leading term (electric dipole moment) in the description of the electric charge distribution of XY. On the other hand, when XY is a homonuclear dihalogen, the halogen bond becomes $B \cdots \delta^+X^{\delta-}_2$, since the electric quadrupole moment of X_2 is the leading term in the description of its charge distribution.

With such an operational definition of the halogen bond, the fact that $B \cdots ClF$ and $B \cdots BrCl$ complexes are isomorphous with $B \cdots HX$ ($X = F, Cl, Br$) can be understood if the electrophilic end δ^+ of each XY or HX molecule seeks the axis of a nonbonding or π -bonding electron pair on B. It has been argued elsewhere^[153] that, in the absence of secondary interactions between the nucleophilic region $X^{\delta-}$ of HX and electrophilic regions of B, hydrogen bonds prefer a linear arrangement $Z \cdots H-X$, where Z is the electron-donor atom/region of B. Bending of the hydrogen bond tends to bring the two nucleophilic regions Z and X into contact, and this is energetically unfavorable. Presumably, similar considerations apply to halogen-bonded complexes $B \cdots XY$.

This last point raises an interesting question: Under what conditions do halogen bonds exhibit nonlinearity (i.e., non-collinear arrangements of the nuclei $Z \cdots X-Y$) and how do nonlinearities of hydrogen-bonded complexes $B \cdots HX$ compare with those of isomorphous halogen-bonded complexes $B \cdots XY$? These questions are addressed in the next section.

3.5.2. Nonlinearity in Hydrogen Bonds and "Halogen" Bonds

The angular geometries of a wide range of complexes $B \cdots XY$ and $B \cdots HX$ were considered in Section 3.3. For complexes $B \cdots ClF$ and $B \cdots HCl$ of C_s symmetry, it was also possible to determine the precise deviation of the $Z \cdots Cl-F$ or $Z \cdots H-Cl$ system from linearity by means of the off-diagonal element χ_{ab} or χ_{ac} (depending on whether the principal inertial plane ab or ac coincides with the molecular symmetry plane) of the Cl nuclear quadrupole coupling tensor. The method of establishing the angular deviation θ , as defined in the general case for the nuclei $Z \cdots X-Y$ in Figure 31, from the collinear ($\theta = 0^\circ$) arrangement was discussed in Section 3.3.3.

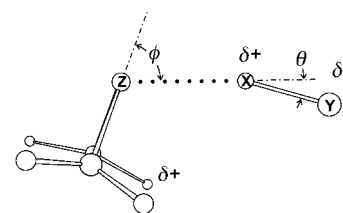
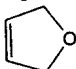
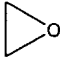
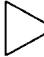

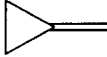


Figure 31. Definitions of the angles ϕ and θ in the general case of a complex $B \cdots XY$ of C_s symmetry, where B is, for example, H_2CO , oxirane, thiirane, 2,5-dihydrofuran, allene, or methylenecyclopropane. Z is the acceptor atom of B in n-pair complexes or the center of the π bond in π complexes.

The complexes $B \cdots ClF$ and $B \cdots HCl$ that were found to have C_s symmetry were those for which $B = H_2CO$,^[102, 107] 2,5-dihydrofuran,^[101, 105] oxirane,^[103, 108] thiirane,^[104, 109] allene,^[125, 126] and methylenecyclopropane.^[127, 128] Their angular geometries—which are displayed in Figures 12–14, 16, 22, and 23, respectively—were established to be isostructural in the pair

$B \cdots \text{ClF}/B \cdots \text{HCl}$ for a given B . As remarked in Sections 3.3.3 and 3.3.4, although the angles ϕ (see Figure 31) are virtually identical in $B \cdots \text{ClF}$ and $B \cdots \text{HCl}$ for a given B , the non-linearity θ is somewhat larger for the hydrogen-bonded complex. Table 11 summarizes the angles ϕ and θ for the two series of C_s complexes in question. It is evident that θ is very small in the $B \cdots \text{ClF}$. These observations about ϕ and θ will now be explained in terms of the simple electrostatic model

Table 11. Angles ϕ and θ determined for complexes $B \cdots \text{ClF}$ and $B \cdots \text{HCl}$ of C_s symmetry.^[a]

B	B \cdots ClF			B \cdots HCl		
	ϕ [°]	θ [°]	ref.	ϕ [°]	θ [°]	ref.
H ₂ CO	69.1(7)	3.2(7)	[102]	70.0(10)	20.5(8)	[107]
	53.0(3)	2.0(2)	[101]	54.3(3)	9.5(1)	[105]
	67.3(1)	2.9(1)	[103]	69.1(1)	16.5(1)	[23, 108]
	85.0(2)	3.5(2)	[104]	94.5(20)	21.0(5)	[109]
	92.5(7)	4.9(15)	[126]	94 (3)	≈ 7	[125]
	92.5(5)	4.9(1)	[127]	90.8(5)	17.5	[128]
SO ₂	131.9(6)	−0.7(2)	[112]	143.0(1)	−2.5(7)	[23, 113]

[a] The angles ϕ and θ are defined in Figures 12–14, 16, 17, 22, and 23 for the complexes $B \cdots \text{ClF}/B \cdots \text{HCl}$.

for the $B \cdots \text{ClF}$ and $B \cdots \text{HCl}$ interactions, the general outline of which was given in Section 3.5.1.

First, the subunit ClF or HCl is considered to form a halogen or hydrogen bond to the electron-donor atom or center in B according to the rules, that is, ClF or HCl lies along the axis of a nonbonding electron pair on Z or a π -bonding electron pair. When B is such that the rules predict a complex of C_s symmetry, as in the cases considered here, there is the possibility of a secondary interaction between the nucleophilic end $F^{\delta-}$ or $Cl^{\delta-}$ of ClF or HCl , respectively, and the more electrophilic region of B , as shown schematically in Figure 31. This secondary interaction can then be envisaged to cause $F^{\delta-}$ or $Cl^{\delta-}$ to move towards its electrophilic partner, whereby the pivot is the primary interaction site. At equilibrium, the force resisting the bending of the halogen or hydrogen bond, the secondary attractive force, and any repulsive force are balanced.

This model readily explains why the angles ϕ are identical for a given pair $B \cdots \text{ClF}/B \cdots \text{HCl}$, since whatever the strength of the secondary interaction, the pivot of the motion is $Cl^{\delta+}$ or $H^{\delta+}$ and ϕ does not change. On the other hand, it is clear why θ for $B \cdots \text{HCl}$ is larger than θ for $B \cdots \text{ClF}$. In general, the distance $r(Z \cdots \text{Cl})$ in $B \cdots \text{HCl}$ is smaller than the distance $r(Z \cdots \text{F})$ in $B \cdots \text{ClF}$, the $Z \cdots \text{ClF}$ primary interaction is stronger than that of $Z \cdots \text{HCl}$, and $F^{\delta-}$ is a poorer nucleophile than $Cl^{\delta-}$. All these factors operate in the same direction, that is, to make bending of the “chlorine” bond in $B \cdots \text{ClF}$ more difficult than bending of the hydrogen bond in $B \cdots \text{HCl}$ through the same angle θ . Data for $\text{SO}_2 \cdots \text{ClF}$ ^[112] and $\text{SO}_2 \cdots \text{HCl}$,^[113] both of which have planar C_s symmetry, are also included in Table 11. We note that in $\text{SO}_2 \cdots \text{HCl}$ ^[23, 113] and

$\text{SO}_2 \cdots \text{ClF}$ ^[112] the nucleophiles $Cl^{\delta-}$ and $F^{\delta-}$ are far removed from the electrophilic region of the molecule B , so that both the $O \cdots \text{H}-\text{Cl}$ and $O \cdots \text{Cl}-\text{F}$ systems are nearly linear (see Figure 17).

In view of the established very small deviation of θ from zero in the $B \cdots \text{ClF}$ complexes, a reasonable corollary to the rules for the prediction of angular geometries (Section 3.3.1) might be that the ClF molecule is a good probe of the directions of nonbonding electron pairs. Because of the significant nonlinearity of hydrogen bonds, HX is a less satisfactory indicator of nonbonding pair directions. This may be of relevance to VSEPR theory.

It will be of interest to examine the nonlinearities θ in complexes $B \cdots \text{Cl}_2$, $B \cdots \text{BrCl}$ and $B \cdots \text{Br}_2$ of appropriate symmetry. This will be a difficult task because of the considerable complications in the rotational spectra of such species that arise from multiple quadrupole coupling nuclei and a variety of naturally occurring isotopomers. Some values of θ were measured in a few $B \cdots \text{HBr}$ ^[23, 154–157] and $B \cdots \text{HF}$ ^[148, 158, 159] complexes, where B is oxirane, thiirane, methylenecyclopropane, 2,5-dihydrofuran, or formaldehyde. Unfortunately, the absence of quadrupolar nuclei in F_2 means that values of θ cannot be obtained for $B \cdots \text{F}_2$ by the method considered here.

4. The Existence of Mulliken Inner Complexes $[\text{BX}]^+ \cdots \text{Y}^-$ and $[\text{BH}]^+ \cdots \text{X}^-$ in the Gas Phase

This review is concerned with the properties of complexes of the type $B \cdots \text{XY}$, as determined for the ground state of the molecule from its rotational spectrum. It has also compared these properties with those of hydrogen-bonded complexes $B \cdots \text{HX}$ similarly determined. All the discussion so far has centered on complexes $B \cdots \text{XY}$ and $B \cdots \text{HX}$ that are of the Mulliken outer type, that is, those that are weakly bound and exhibit only minor electric charge redistribution. The $B \cdots \text{XY}$ were shown explicitly to be of the outer type by consideration of the changes in the halogen nuclear quadrupole coupling constants of XY on complex formation and the generally small values of k_a . The $B \cdots \text{HX}$ were also implicitly assumed to be of the same type. In fact, this conclusion can be established by a detailed consideration of molecular properties, as set out elsewhere.^[75]

The final question to be addressed here is: Are there circumstances in which Mulliken inner complexes $[\text{BX}]^+ \cdots \text{Y}^-$ or $[\text{BH}]^+ \cdots \text{X}^-$ can be detected in the ground state in the gas phase? This question was first formulated and answered in connection with the ammonium and methylammonium halides.

4.1. The Hydrogen Bond $B \cdots \text{HX}$ and How to Encourage Proton Transfer

Systematic investigations of members of the series $(\text{CH}_3)_{3-n}\text{H}_n\text{N} \cdots \text{HX}$ ($n=3, 2, 0$; Table 12) were made by means of their rotational spectra,^[76–78, 160–164] which were observed in a supersonically expanded jet produced in one of the two following ways. Either the vapor above the heated

Table 12. Series of complexes $(\text{CH}_3)_{3-n}\text{H}_n\text{N}\cdots\text{HX}$ investigated by rotational spectroscopy and the estimated percentage contributions of $[(\text{CH}_3)_{3-n}\text{H}_n\text{NH}]^+\cdots\text{X}^-$ to valence-bond descriptions of the molecules.

$\text{H}_3\text{N}\cdots\text{HCl}$ 0 %	$\text{CH}_3\text{NH}_2\cdots\text{HCl}$ 23 %	$(\text{CH}_3)_3\text{N}\cdots\text{HF}$ 5 %
$\text{H}_3\text{N}\cdots\text{HBr}$ 0 %		$(\text{CH}_3)_3\text{N}\cdots\text{HCl}$ 62 %
$\text{H}_3\text{N}\cdots\text{HI}$ 0 %		$(\text{CH}_3)_3\text{NH}^+\cdots\text{Br}^-$ 80 %
		$(\text{CH}_3)_3\text{NH}^+\cdots\text{I}^-$ 93 %

ionic solid $[(\text{CH}_3)_{3-n}\text{H}_n\text{NH}]^+\cdots\text{X}^-$ was entrained in argon and the resulting mixture expanded or $(\text{CH}_3)_{3-n}\text{H}_n\text{N}$ and HX were mixed in the fast-mixing nozzle and the resulting complexes observed as described above.

Analysis of the rotational spectra led to various properties of the complexes $(\text{CH}_3)_{3-n}\text{H}_n\text{N}\cdots\text{HX}$. Of particular importance in assessing the extent of proton transfer from HX to $(\text{CH}_3)_{3-n}\text{H}_n\text{N}$ were the halogen nuclear quadrupole coupling constants $\chi_{zz}(\text{X})$, where z is the HCl internuclear axis, and the intermolecular stretching force constant k_σ , as determined from the centrifugal distortion constant D_J or Δ_J . A detailed review of the arguments for the whole series $(\text{CH}_3)_{3-n}\text{H}_n\text{N}\cdots\text{HX}$ has been presented elsewhere.^[165] Only a summary is given here.

In a weakly bound complex such as $\text{HCN}\cdots\text{HX}$ ($\text{X} = \text{Cl}, \text{Br}, \text{I}$), for which k_σ values are close to 10 Nm^{-1} or less, the value of $\chi_{zz}(\text{X})$ can be modeled by allowing first for the modified electric field gradient at X resulting from the electric charge distribution of HCN and then for the zero-point motion of the complex. Details of how to do this are not important here and are discussed elsewhere.^[165, 166] No significant extension of the $\text{H}-\text{X}$ bond, and therefore no appreciable extent of proton transfer, needed to be invoked. $\text{HCN}\cdots\text{HX}$ are thus used as models for the weak limit. The values of $\chi_{zz}(\text{Cl})$ and k_σ for $\text{HC}^{14}\text{N}\cdots\text{H}^{35}\text{Cl}$ ^[88] are given in Table 13.

Table 13. Comparison of ^{35}Cl nuclear quadrupole coupling constants $\xi_{zz}(\text{Cl})$ and intermolecular stretching force constants k_σ of complexes $(\text{CH}_3)_{3-n}\text{H}_n\text{N}\cdots\text{HCl}$ with those of model systems.

Complex	$\xi_{zz}(\text{Cl})$ [MHz] ^[a]	$k_\sigma\text{ Nm}^{-1}$
$\text{HCN}\cdots\text{HCl}$ ^[88]	− 53.720	9.1
$\text{H}_3\text{N}\cdots\text{HCl}$ ^[76]	− 47.607(9)	17.6(3)
$\text{CH}_3\text{NH}_2\cdots\text{HCl}$ ^[160]	− 37.89(1)	—
$(\text{CH}_3)_3\text{N}\cdots\text{HCl}$ ^[162]	− 21.625(5)	84(3)
$\text{Na}^+\cdots\text{Cl}^-$	− 5.643(4) ^[167]	108.6 ^[168]

[a] z is the HCl internuclear axis.

The model molecules taken to represent the properties of the ion pair limit $[(\text{CH}_3)_{3-n}\text{H}_n\text{NH}]^+\cdots\text{X}^-$ were the sodium halides $\text{Na}^+\cdots\text{X}^-$, which are known to be ionic in the gas phase. These have force constants $k_\sigma \approx 100\text{ Nm}^{-1}$ and coupling constants $\chi_{zz}(\text{X}) \approx 0\text{ MHz}$, the latter being that expected for a spherically symmetric ion X^- , perturbed slightly by the nearby cation Na^+ . The values of $\chi_{zz}(\text{Cl})$ ^[167] and k_σ ^[168] for $\text{Na}^+\cdots\text{Cl}^-$ are included in Table 13.

The approach to the nature of $(\text{CH}_3)_{3-n}\text{H}_n\text{N}\cdots\text{HX}$ for a particular value of n can then be summarized by considering the measured $\chi_{zz}(\text{Cl})$ and k_σ values for $n = 3, 2$, and 0 , which are also given for the $(\text{CH}_3)_{3-n}\text{H}_n\text{N}\cdots\text{HCl}$ in Table 13.^[76, 160, 162] It is clear that $\text{H}_3\text{N}\cdots\text{HCl}$ lies close to the simple hydrogen bond limit, as exemplified by $\text{HCN}\cdots\text{HCl}$,

both in terms of $\chi_{zz}(\text{Cl})$ and k_σ . As NH_3 is progressively methylated, however, $\chi_{zz}(\text{Cl})$ decreases in magnitude while k_σ increases. Qualitatively, it is clear that the extent of proton transfer increases as n decreases from 3 to 2 to 0 . A quantitative interpretation of $\chi_{zz}(\text{Cl})$, with details as described in reference [165], shows that the percentage of proton transfer changes from approximately 0% when $n = 3$, to 23% when $n = 2$, to 62% when $n = 0$ (see Table 12). These results are in accord with chemical intuition, since the $+I$ effect of CH_3 groups increases the proton affinity of NH_3 as it is progressively methylated.^[165]

Chemical intuition also suggests that, as the HX molecule becomes easier to dissociate into ions H^+ and X^- along the series $\text{X} = \text{F}, \text{Cl}, \text{Br}$, or I , the extent of proton transfer should increase in this order for the $(\text{CH}_3)_3\text{N}\cdots\text{HX}$ series. Values of the percentage of proton transfer for $(\text{CH}_3)_3\text{N}\cdots\text{HX}$, $\text{X} = \text{Cl}$,^[162] Br ,^[163] or I ,^[164] as calculated from halogen nuclear hyperfine coupling constants (see reference [165]), are included in Table 12. We note again a monotonic increase in this quantity along the series $(\text{CH}_3)_3\text{N}\cdots\text{HX}$ ($\text{X} = \text{Cl}, \text{Br}$, or I). Indeed, even in the vapor phase, trimethylammonium iodide exists as the ion pair $[(\text{CH}_3)_3\text{NH}]^+\cdots\text{I}^-$, and the bromide is nearly so. Detailed energetic arguments, set out in reference [165], are in accord with these experimental results.

The conclusion from the preceding paragraphs is clear. The progressive methylation of ammonia and the progressive decrease of the dissociation energy for $\text{HX} \rightarrow \text{H}^+ + \text{X}^-$ along the series $\text{X} = \text{F}, \text{Cl}, \text{Br}$, and I lead eventually to a situation in which the Mulliken inner complex $[(\text{CH}_3)_{3-n}\text{H}_n\text{NH}]^+\cdots\text{X}^-$ becomes more stable than the Mulliken outer complex $(\text{CH}_3)_{3-n}\text{H}_n\text{N}\cdots\text{HX}$ (for $\text{X} = \text{Br}$ and I , $n = 0$). Interestingly, the percentage proton transfer in the right-hand vertical series and the horizontal series in Table 12 shows clearly that the proton is gradually being transferred, either as HX becomes progressively easier to dissociate or as n decreases from 3 to 0 . The extent of proton transfer for the $(\text{CH}_3)_3\text{N}\cdots\text{HX}$ complexes in low-temperature argon matrices is similar to that in the gas phase, while that for $\text{H}_3\text{N}\cdots\text{HX}$ complexes appears to be significantly greater in the matrix.^[9c] A detailed discussion^[165] of the complexes $\text{H}_3\text{P}\cdots\text{HX}$ and $(\text{CH}_3)_3\text{P}\cdots\text{HX}$ on the basis of similar criteria shows that even for $(\text{CH}_3)_3\text{P}\cdots\text{HBr}$ there is no evidence of proton transfer from HBr to $(\text{CH}_3)_3\text{P}$ in the gas phase. Energetic considerations reveal that this difference of behavior between the N and P series originates in the larger ionic radius of $(\text{CH}_3)_3\text{PH}^+$ relative to $(\text{CH}_3)_3\text{NH}^+$ and therefore a loss of Coulombic stabilization of the ion pair $(\text{CH}_3)_3\text{PH}^+\cdots\text{X}^-$ relative to the N analogue. It remains to discover whether any evidence exists for Mulliken inner complexes $[\text{BX}]^+\cdots\text{Y}^-$ involving dihalogen molecules XY .

4.2. The Halogen Bond $\text{B}\cdots\text{XY}$ and How to Encourage Charge Transfer

The first evidence that, in the valence bond description of a gas-phase complex $\text{B}\cdots\text{XY}$, it might be necessary to include a significant contribution from the ionic form $[\text{BX}]^+\cdots\text{Y}^-$ came from an analysis of the rotational spectrum of $\text{H}_3\text{N}\cdots\text{ClF}$ and, in particular, the magnitudes of the Cl nuclear quadru-

pole coupling constant and the intermolecular stretching force constant k_o .^[59] The latter is large (34.3 N m^{-1}) while the former is smaller than predicted from those of more weakly bound $\text{B} \cdots \text{ClF}$ and the considerations outlined in Section 3.1.2. In fact, the detailed arguments suggest a contribution of $\text{H}_3\text{NCl}^+ \cdots \text{F}^-$ of a few percent.

Given the enhancement of ion-pair character that accompanies complete methylation of $\text{H}_3\text{N} \cdots \text{HX}$ to give $(\text{CH}_3)_3\text{N} \cdots \text{HX}$, it seemed important to examine the corresponding system $(\text{CH}_3)_3\text{N} \cdots \text{ClF}$ by means of its rotational spectrum.^[169] The properties established in this way provided strong evidence of a nontrivial contribution of the form $[(\text{CH}_3)_3\text{NCl}]^+ \cdots \text{F}^-$ to the valence bond description.

First, the centrifugal distortion constant D_J is consistent with a large value of k_o . Second, the distance $r(\text{N} \cdots \text{Cl}) = 2.090 \text{ \AA}$, determined by isotopic substitution at both N and Cl, is short compared with the value of $2.639(3) \text{ \AA}$ in the weakly bound ($k_o = 12.3 \text{ N m}^{-1}$) $\text{HCN} \cdots \text{ClF}$.^[56] In fact, $r(\text{N} \cdots \text{Cl})$ in $(\text{CH}_3)_3\text{N} \cdots \text{ClF}$ is closer to the covalent distances $r(\text{N} - \text{Cl}) = 1.84 \text{ \AA}$ and $1.754(2) \text{ \AA}$ in O_2NCl ^[170] and NCl_3 ,^[171] respectively. Third, $\chi_{zz}(\text{Cl})$ in $(\text{CH}_3)_3\text{N} \cdots \text{ClF}$ can be interpreted in terms of about a 60 % contribution of the form $[(\text{CH}_3)_3\text{NCl}]^+ \cdots \text{F}^-$ by using arguments based on comparisons with values of $\chi_{zz}(\text{Cl})$ along the Cl bond direction z in molecules such as CH_3OCl , as discussed in detail in reference [169]. Fourth, the ^{14}N nuclear quadrupole coupling constant $\chi(^{14}\text{N})$ of $(\text{CH}_3)_3\text{N} \cdots \text{ClF}$ indicates a substantial ion pair contribution. Figure 32 shows the

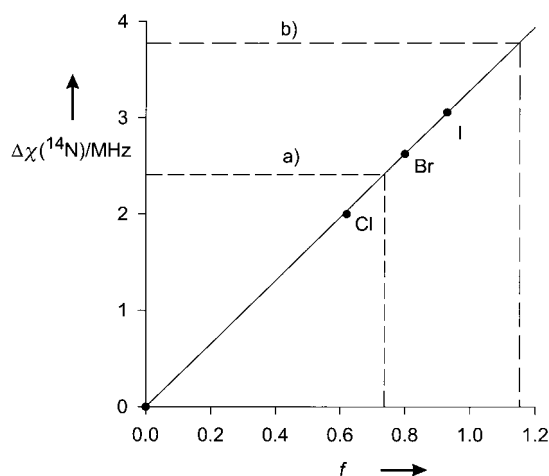


Figure 32. A plot of the change $\Delta\chi(^{14}\text{N})$ in the ^{14}N nuclear quadrupole coupling constant of $(\text{CH}_3)_3\text{N}$ on formation of $(\text{CH}_3)_3\text{N} \cdots \text{HX}$ against the fractional contribution f of the ionic structure $[(\text{CH}_3)_3\text{NH}]^+ \cdots \text{X}^-$ to the valence-bond description of the complex. Values of f were estimated from the nuclear quadrupole coupling constants of X (see text and reference [165] for discussion). The horizontal lines a) and b) mark the values of $\Delta\chi(^{14}\text{N})$ for $(\text{CH}_3)_3\text{N} \cdots \text{ClF}$ and $(\text{CH}_3)_3\text{N} \cdots \text{F}_2$, respectively, and indicate a significant contribution of $[(\text{CH}_3)_3\text{NX}]^+ \cdots \text{Y}^-$ to the valence-bond description of the complex in each case.

change $\Delta\chi(^{14}\text{N})$ of $\chi(^{14}\text{N})$ relative to free trimethylamine on formation of the trimethylammonium halides $(\text{CH}_3)_3\text{N} \cdots \text{HX}$ ($\text{X} = \text{Cl}, \text{Br}, \text{I}$)^[162–164] plotted against the fractional ionic character f , which was determined from the halogen nuclear quadrupole coupling constant. The result is a straight line through the origin (which is a proper point). Onto this line is

drawn $\Delta\chi(^{14}\text{N})$ for the formation of $(\text{CH}_3)_3\text{N} \cdots \text{ClF}$. The value implies that $f \approx 0.7$, although this result should not be taken literally since we are effectively assuming that the $\chi(^{14}\text{N})$ for the two ions $[(\text{CH}_3)_3\text{NCl}]^+$ and $[(\text{CH}_3)_3\text{NH}]^+$ are identical, and this is unlikely. Finally, there is evidence from the behavior of rotational transitions of $(\text{CH}_3)_3\text{N} \cdots \text{ClF}$ with increasing microwave power that the complex has a very large electric dipole moment.^[169]

The above evidence strongly supports a detectable contribution of the ion-pair structure $[(\text{CH}_3)_3\text{NCl}]^+ \cdots \text{F}^-$ to the valence-bond description of the complex $(\text{CH}_3)_3\text{N} \cdots \text{ClF}$. A contribution on the order of 50 % seems likely. Hence, a Mulliken complex of the inner type, with substantial charge transfer from the halogen molecule to the amine, appears to have been identified in the gas phase. Interestingly, IR matrix-isolation studies^[7c] on ClF complexes with both NH_3 and $(\text{CH}_3)_3\text{N}$ also suggest considerable ionic character in $\text{R}_3\text{N} \cdots \text{ClF}$ species. Are there other examples of this type? There is some evidence of ion-pair character in $(\text{CH}_3)_2\text{S} \cdots \text{ClF}$.^[104]

In view of the extreme weakness of $\text{B} \cdots \text{F}_2$ complexes referred to in Section 3.2, it was a surprise to find that $(\text{CH}_3)_3\text{N} \cdots \text{F}_2$ has a large electric dipole moment ($\approx 10 \text{ D}$) compared with that (ca. 1 D) expected from the weak binding model, a large intermolecular stretching force constant k_o , a short distance $r(\text{N} \cdots \text{F})$, and a small value of the ^{14}N - nuclear quadrupole coupling constant.^[172] If the value of $\Delta\chi(^{14}\text{N}) = \chi_{\text{complex}}(^{14}\text{N}) - \chi_0(^{14}\text{N})$, where $\chi_0(^{14}\text{N})$ refers to free trimethylamine, is placed on the straight line in Figure 32, it implies a substantial contribution from $[(\text{CH}_3)_3\text{NF}]^+ \cdots \text{F}^-$ to a valence-bond description of the complex (but with the same caveat raised in connection with $(\text{CH}_3)_3\text{N} \cdots \text{ClF}$), as do all the other properties mentioned. Evidently the $(\text{CH}_3)_3\text{N} \cdots \text{F}_2$ complex, unlike other $\text{B} \cdots \text{F}_2$, involves substantial charge transfer from F_2 to the base and may be described as a Mulliken inner complex. Recent ab initio calculations^[173, 174] indicate that the arguments concerning $\Delta\chi(^{14}\text{N})$ overestimate f and that the assumption of an unperturbed $(\text{CH}_3)_3\text{N}$ geometry, necessarily used to obtain $r(\text{N} \cdots \text{F}_i)$ in reference [172], leads to values of $r(\text{N} \cdots \text{F}_i)$ and $r(\text{F} \cdots \text{F})$ that are too small and too large, respectively.

In summary, there is evidence that the valence-bond description of complexes of trimethylamine with HCl , HBr , HI , ClF , and F_2 requires a significant contribution of the ionic structure $[(\text{CH}_3)_3\text{NH}]^+ \cdots \text{X}^-$ or $[(\text{CH}_3)_3\text{NX}]^+ \cdots \text{Y}^-$ to be invoked. In particular, proton transfer is effectively complete in $[(\text{CH}_3)_3\text{NH}]^+ \cdots \text{X}^-$ for $\text{X} = \text{Br}$ and I . This result means that although we begin with separate samples of trimethylamine and HX in the fast-mixing nozzle, about $10 \mu\text{s}$ after their first encounter, when collisionless expansion begins, the proton has been transferred. On the same time scale, there also appears to be a significant extension of the XY bond in $(\text{CH}_3)_3\text{N} \cdots \text{XY}$.

5. Summary and Outlook

Through the use of a fast-mixing nozzle in conjunction with a pulsed-jet, FT microwave spectrometer, the rotational

spectra of complexes $B \cdots XY$, formed from a wide range of simple Lewis bases B and homo- or heteronuclear dihalogen molecules XY , can be detected and analyzed to give several properties. The efficacy of the mixing nozzle is such that complexes can be observed in gas mixtures as reactive as H_2S/F_2 , NH_3/F_2 , and C_2H_2/ClF . It has been established in this article that the properties of the $B \cdots XY$ so observed exhibit a systematic behavior when B and XY are varied. In addition, a close relationship exists with properties in the corresponding series $B \cdots HX$. The properties in question are angular geometries (shapes), intermolecular separations $r(Z \cdots X)$, where Z is the electron-donor atom or center in B , the intermolecular binding strength (as indicated by the intermolecular stretching force constant k_0), and the fraction δ of an electronic charge redistributed from X to Y when $B \cdots XY$ is formed.

Except for the most strongly bound complexes, such as $(CH_3)_3N \cdots HX$ ($X = Cl, Br, \text{ or } I$) and $(CH_3)_3N \cdots XY$ ($XY = F_2$ or ClF), the complexes discussed are mostly of the Mulliken outer type. This conclusion is demonstrated by values of δ on the order of a few hundredths of an electronic charge and by values of k_0 on the order of 10 Nm^{-1} . In fact, there is an approximately linear relation between δ and k_0 for those series $B \cdots Cl_2$, $B \cdots Br_2$ and $B \cdots BrCl$ for which δ can be determined from the nuclear quadrupole coupling constants $\chi(X)$ and $\chi(Y)$ associated with both ends of XY . A similar relation may exist for the $B \cdots ClF$ series, but the absence of a quadrupolar probe of the electric charge distribution at F precludes an equivalent analysis.

A systematic relationship was also detected for k_0 values in the series $B \cdots XY$, where $XY = F_2, Cl_2, Br_2, BrCl$ and ClF . The k_0 for most of these complexes can be reproduced by the simple equation $k_0 = cE_{XY}N_B$, where c is constant and E_{XY} and N_B are the electrophilicity and nucleophilicity of the component molecules XY and B . Analogous behavior was noted previously in a wide range of hydrogen-bonded complexes $B \cdots HX$, for which the same equation applies. Moreover, when the same value of c was assumed for both the $B \cdots HX$ and the $B \cdots XY$ series, the nucleophilicities N_B of a given B generated from consideration of the two series are in good agreement. All members of the $B \cdots F_2$ series, except $(CH_3)_3N \cdots F_2$, are very weakly bound, a result understandable in terms of the electric charge distribution of F_2 , which is nearly spherical. Thus, F_2 behaves like a spherical inert gas atom as a first approximation when it interacts with B . The electrophilicities E_{XY} lie in the order $F_2 < Cl_2 < Br_2 < BrCl < ClF$, which is that of the dihalogen electric quadrupole and dipole moments. This suggests that electrostatic interactions are important in the description of the $B \cdots XY$ interaction, except perhaps when XY is F_2 .

The angular geometries of the $B \cdots XY$ show a remarkable pattern. For a given B , the complexes $B \cdots F_2$, $B \cdots Cl_2$, $B \cdots ClF$, and $B \cdots BrCl$ have isomorphous angular geometries. In addition, for the same B , the $B \cdots HX$ ($X = F, Cl, Br$) are also isostructural with $B \cdots XY$. It then follows that some simple rules, initially enunciated to rationalize the angular geometries of $B \cdots HX$, also apply, after appropriate reformulation, to the $B \cdots XY$. These rules are electrostatic in origin, since they require the electrophilic end $H^{\delta+}$ or $X^{\delta+}$ of HX or

XY , respectively, to seek the direction of greatest nucleophilicity in B , that is, the axis of a nonbonding or π -bonding electron pair. Evidently, the electrostatic component of the interaction energy is important in defining the angular geometry of $B \cdots XY$, as well as that of $B \cdots HX$. The main difference between $B \cdots XY$ and $B \cdots HX$ in this context is that, when symmetry allows, the deviation θ of the $Z \cdots H-X$ system from linearity is greater than that of the corresponding $Z \cdots X-Y$ arrangement.

Radial geometries of $B \cdots XY$ and $B \cdots HX$ are also systematically related. The difference $\Delta r = r_{HX}(Z \cdots X) - r_{XY}(Z \cdots X)$ is positive and nearly constant in each series $B \cdots HX/B \cdots XY$ ($XY = Cl_2, Br_2, BrCl, ClF$), and this leads to the conclusion that the van der Waals radius of the atom X in the dihalogen XY is shorter along the XY axis than perpendicular to it. Thus, the XY molecule can be described as snub-nosed. For the two series $B \cdots HF/B \cdots F_2$, however, Δr is very small; this indicates that the F atom in F_2 is nearly isotropic in its van der Waals radius.

The parallelism among the properties of $B \cdots XY$ and $B \cdots HX$ alluded to earlier in this section suggests that one might invoke the existence of a halogen bond that is an analogue of the hydrogen bond, that is, an interaction of electrostatic character involving largely unperturbed electric charge distributions of either B and XY or B and HX , respectively. The propensity of $B \cdots HCl$ to exhibit greater deviations of their $Z \cdots H-Cl$ nuclei from collinearity than those of $Z \cdots X-Y$ in $B \cdots XY$ may then be understood on the basis of a secondary interaction of $Cl^{\delta-}$ or $Y^{\delta-}$ with the nearest electrophilic region E of B in $B \cdots HCl$ or $B \cdots XY$, respectively. The distance $E \cdots \delta-F$ in $B \cdots ClF$ is larger than the corresponding distance $E \cdots \delta-Cl$ in $B \cdots HCl$ for a given B , and hence the force required to produce a given angular distortion of the stronger $Z \cdots Cl-F$ system is greater.

Finally, the existence of Mulliken inner complexes in the gas phase has been established. The proton affinity and X^+ affinity of NH_3 are both increased by progressive methylation. Examination of the properties of the series $(CH_3)_{3-n}H_nN \cdots HX$ as n is varied from 3 to 2 to 0 and X is varied from F through to I reveals that $(CH_3)_3N \cdots HBr$ and $(CH_3)_3N \cdots HI$ are more appropriately described in terms of the ion pairs $[(CH_3)_3NH]^+ \cdots X^-$, even in the gas phase. Yet again, there is evidence of parallel behavior in the corresponding series $(CH_3)_{3-n}H_nN \cdots XY$. For the two members of this series so far investigated ($n = 0$; $XY = F_2$ or ClF), it is necessary to invoke a contribution from $[(CH_3)_3NX]^+ \cdots Y^-$ in a valence-bond description of the complex.

In future, it will be desirable to investigate other dihalogen species XY and other Lewis bases, with the aim of establishing the limits of the generalizations established here. More quantitative models than those presented in this article will also be of interest, as will the systematic application of ab initio SCF calculations to selected series $B \cdots XY$.

Addendum

Since this review was submitted the rotational spectra of the series of complexes $B \cdots ICl$ ($B = Ar,^{[175]} CO,^{[176]} C_2H_2,^{[177]}$

C_2H_4 ,^[178] H_2O ,^[179] H_2S ,^[180] NH_3 ,^[181]) have been detected and analyzed. Table 14 displays the properties $r(\text{Z} \cdots \text{I})$, k_{σ} , δ_1 , and δ_2 , as determined from the spectroscopic constants (see Section 2.1). The definitions of Z and k_{σ} are given in Sections 3.3 and 3.2, respectively. The quantities δ_1 and δ_2 are the fractions of an electronic charge transferred from Z to I and from I to Cl, respectively, on complex formation—that is, inter- and intramolecular electron transfer—and were determined from modified versions of Equations (8) and (9), as described below.

The k_{σ} values of the $\text{B} \cdots \text{ICl}$ complexes given in Table 14 indicate, on comparison with those of other $\text{B} \cdots \text{X}_2$ and $\text{B} \cdots \text{XY}$ complexes (Table 2), that $\text{B} \cdots \text{ICl}$ is the most strongly bound of the series for a given base B. If $E_{\text{ICl}} = 9.9$ is chosen for the electrophilicity of ICl, the k_{σ} values for $\text{B} \cdots \text{ICl}$ (B = CO, C_2H_2 , C_2H_4 , H_2S , NH_3) are well reproduced by $k_{\sigma} = cN_{\text{B}}E_{\text{XY}}$ (see Section 3.2), as shown by the calculated values given in Table 14.

Table 14. Comparison of some properties of the complexes $\text{B} \cdots \text{ICl}$.

B	$r(\text{Z} \cdots \text{I})$ [Å] ^[a]	$\sigma(\text{Z}) + \sigma(\text{I})$ [Å]	k_{σ} [N m ⁻¹] ^[b]	δ_1 ^[c]	δ_2 ^[d]	Ref.
Ar	3.576(1)	4.05	3.20	0.0 ^[e]	0.0054	[175]
CO	3.011(1)	3.85	8.0 (8.3)	0.025	0.048	[176]
C_2H_2	3.115(1)	3.85	12.1 (12.4)	0.026	0.056	[177]
C_2H_4	3.033(2)	3.85	14.0 (14.0)	0.054	0.080	[178]
H_2O	2.807(1)	3.55	15.9	0.010	0.065	[179]
H_2S	3.155(1)	4.00	16.6 (16.0)	0.055	0.084	[180]
NH_3	2.711(2)	3.65	30.4 (29.5)	0.078	0.150	[181]

[a] Z is the electron-donor atom or electron-donor center in B. [b] Values of k_{σ} in italics and in parenthesis were calculated from the expression $k_{\sigma} = cN_{\text{B}}E_{\text{ICl}}$, with $E_{\text{ICl}} = 11.9$ and N_{B} values from Table 5. Values of N_{B} for Ar and H_2O are unavailable. [c] δ_1 is the fraction of an electronic charge transferred from Z to I on complex formation. See the text for the method of calculation from $\chi_{\text{zz}}(\text{I})$ and $\chi_{\text{zz}}(\text{Cl})$ values. [d] δ_2 is the fraction of an electronic charge transferred from I to Cl on complex formation. See the text for the method of calculation from $\chi_{\text{zz}}(\text{I})$ and $\chi_{\text{zz}}(\text{Cl})$ values. The net gain of electronic charge by I is $(\delta_1 - \delta_2)e$. [e] δ_1 is assumed to be negligible for $\text{Ar} \cdots \text{ICl}$.

The values of δ_1 and δ_2 in Table 14 were obtained by using the appropriate forms of Equation (8) and (9) (Section 3.1.2), that is, with δ in Equation (8) replaced by $(\delta_1 - \delta_2)$ and δ in Equation (9) replaced by δ_2 (see reference [176] for the detailed arguments). It was found that if the reasonable assumption $\delta_1 = 0.0$ is made for the weakly bound complex $\text{Ar} \cdots \text{ICl}$, the result is $\delta_2 = 5.4(1) \times 10^{-3}$ and $\phi_{\text{av}} = 5.45(1)^{\circ}$.^[175] The assumption $\delta_1 = 0.0$ proved unsatisfactory for the other $\text{B} \cdots \text{ICl}$ species because it led to ϕ_{av} values that become progressively larger along the series B = Ar, CO, C_2H_2 , C_2H_4 , H_2S , and NH_3 . This result is unreasonable in view of the increase in binding strength k_{σ} along the series (see Table 14). On the contrary, we expect ϕ_{av} to decrease as k_{σ} increases. Fortunately, ϕ_{av} is already small for $\text{Ar} \cdots \text{ICl}$, and if we assume $\phi_{\text{av}} = 4.5(5)^{\circ}$ for B = CO, C_2H_2 , and C_2H_4 and $4(1)^{\circ}$ for the more strongly bound cases B = H_2S , H_2O , and NH_3 we can be confident that the actual value of ϕ_{av} in each case is included in the range. The δ_1 and δ_2 values given in Table 14 were calculated from the modified versions of Equations (8) and (9) by using these values of ϕ_{av} . This procedure is tantamount to using $\text{Ar} \cdots \text{ICl}$ as the reference point $\delta_1 = 0$ for intermolecular electron transfer. It cannot be applied to the

other series ($\text{B} \cdots \text{Br}_2$ and $\text{B} \cdots \text{BrCl}$) in which δ_1 might be significant because the rotational spectra of $\text{Ar} \cdots \text{Br}_2$ and $\text{Ar} \cdots \text{BrCl}$, and hence the upper limits to the angles ϕ_{av} , are not known. It is interesting to note that the δ_1 values show a systematic decrease as the first ionization energy of the Lewis base B increases, with the exception of CO.^[182] This phenomenon will be discussed elsewhere.

Finally, the distances $r(\text{Z} \cdots \text{I})$ are systematically shorter than the sum $\sigma(\text{Z}) + \sigma(\text{I})$ of the van der Waals radii $\sigma(\text{Z})$ and $\sigma(\text{I})$ of Z and I (Table 14). This is consistent with the behavior noted for $\text{B} \cdots \text{Cl}_2$, $\text{B} \cdots \text{ClF}$, $\text{B} \cdots \text{Br}_2$, and $\text{B} \cdots \text{BrCl}$ (see Tables 8–10) and indicates that the ICl molecule is, like Cl_2 and ClF, snub-nosed (see Section 3.4).

I am grateful to my co-workers, whose experimental skills and tenacity made possible the work described in this article. Their names are evident in the literature cited here. In particular, the investigations of dihalogen complexes conducted by Joanna Thorn, David Lister, Hugh Warner, Hannelore Bloemink, Kelvin Hinds, Gina Cotti, Christopher Evans, Stephen Cooke, and Gary Corlett are mentioned. The earlier work on the hydrogen bond benefited especially from the efforts of Charles Willoughby, Zbigniew Kisiel, Annette Travis, Elizabeth Goodwin, Nigel Howard, Christopher Rego, Andrew Suckley, and Andrew Wallwork. I thank Professor John Holloway for providing ClF and F_2 and instructing us on their safe handling. I am grateful to the EPSRC for research grants and a Senior Fellowship. Finally, I am pleased to acknowledge the patience of Janet Jones and Robin Batten in preparing the typescript and the graphics, respectively.

Received: October 28, 1998 [A 309 IE]
German version: *Angew. Chem.* **1999**, *111*, 2850–2880

- [1] H. A. Benesi, J. H. Hildebrand, *J. Am. Chem. Soc.* **1949**, *71*, 2703–2727.
- [2] O. Hassel, C. Rømming, *Q. Rev. Chem. Soc.* **1962**, *16*, 1–18.
- [3] R. S. Mulliken, W. B. Person, *Molecular Complexes: A Lecture and Reprint Volume*, Wiley-Interscience, New York, **1969**, and references therein.
- [4] A. J. Downs, C. J. Adams in *Comprehensive Inorganic Chemistry* (Ed.: A. Trotman-Dickenson), Pergamon Press, Oxford, **1973**, chap. 26, pp. 1214–1220.
- [5] See, for example: a) C. K. Ingold, *Structure and Mechanism in Organic Chemistry* (Ed.: G. Bell), 2nd. ed., London, **1969**, pp. 964–988; b) J. E. Dubois, F. Garnier, *Spectrochim. Acta A* **1967**, *23*, 2279–2288; c) R. S. Brown, H. Slebocka-Tilk, A. J. Bennet, G. Bellucci, R. Bianchini, R. Ambrosetti, *J. Am. Chem. Soc.* **1990**, *112*, 6310–6316.
- [6] See, for example: a) H. Frei, G. C. Pimentel, *J. Chem. Phys.* **1983**, *78*, 3698–3712; b) A. K. Knudsen, G. C. Pimentel, *J. Chem. Phys.* **1983**, *78*, 6780–6792; c) S. N. Cesaro, H. Frei, G. C. Pimentel, *J. Phys. Chem.* **1983**, *87*, 2142–2147; d) K. A. Singmaster, G. C. Pimentel, *J. Phys. Chem.* **1990**, *94*, 5226–5229; e) S. A. Abrash, G. C. Pimentel, *J. Phys. Chem.* **1989**, *93*, 5828–5834.
- [7] See, for example: a) H. Bai, B. S. Ault, *J. Phys. Chem.* **1990**, *94*, 199–203; b) N. P. Machara, B. S. Ault, *Inorg. Chem.* **1988**, *27*, 2383–2385; c) N. P. Machara, B. S. Ault, *J. Phys. Chem.* **1988**, *92*, 2439–2442; d) N. P. Machara, B. S. Ault, *J. Phys. Chem.* **1988**, *92*, 73–77; e) B. S. Ault, *J. Phys. Chem.* **1987**, *91*, 4723–4727; f) C. E. Sass, B. S. Ault, *J. Phys. Chem.* **1987**, *91*, 3207–3211; g) N. P. Machara, B. S. Ault, *J. Phys. Chem.* **1987**, *91*, 2046–2050; h) B. S. Ault, *J. Phys. Chem.* **1986**, *90*, 2825–2829; i) N. P. Machara, B. S. Ault, *Inorg. Chem.* **1985**, *24*, 4251–4254.

- [8] See, for example: a) L. Andrews, T. C. McInnis, Y. Hannachi, *J. Phys. Chem.* **1992**, 96, 4248–4254; b) T. C. McInnis, L. Andrews, *J. Phys. Chem.* **1992**, 96, 2051–2059; c) P. Hassanzadeh, L. Andrews, *J. Phys. Chem.* **1992**, 96, 79–84; d) L. Andrews, T. C. McInnis, *Inorg. Chem.* **1991**, 30, 2990–2993; e) R. B. Bohn, R. D. Hunt, L. Andrews, *J. Phys. Chem.* **1989**, 93, 3979–3983; f) L. Andrews, R. Withnall, *Inorg. Chem.* **1989**, 28, 494–499; g) L. Andrews, R. D. Hunt, *J. Chem. Phys.* **1988**, 89, 3502–3504; h) R. D. Hunt, L. Andrews, *J. Phys. Chem.* **1988**, 92, 3769–3774; i) R. Lascola, R. Withnall, L. Andrews, *Inorg. Chem.* **1988**, 27, 642–648; j) L. Andrews, R. Lascola, *J. Am. Chem. Soc.* **1987**, 109, 6243–6247.
- [9] See, for example: a) A. J. Barnes, M. P. Wright, *THEOCHEM* **1986**, 28, 21–30; b) U. P. Agarwal, A. J. Barnes, W. J. Orville-Thomas, *Can. J. Chem.* **1985**, 63, 1705–1707; c) A. J. Barnes, T. R. Beech, Z. Mielke, *J. Chem. Soc. Faraday Trans. 2* **1984**, 80, 455–463; d) A. J. Barnes, J. N. S. Kuzniarski, Z. Mielke, *J. Chem. Soc. Faraday Trans. 2* **1984**, 80, 465–476; e) A. J. Barnes, A. C. Legon, *J. Mol. Struct.* **1998**, 448, 101–106.
- [10] B. S. Ault, *Rev. Chem. Intermed.* **1988**, 9, 233–269.
- [11] a) A. J. Barnes, *J. Mol. Struct.* **1983**, 100, 259–280; b) A. J. Barnes, *J. Mol. Struct.* **1988**, 177, 209–220.
- [12] L. Andrews, *J. Phys. Chem.* **1984**, 88, 2940–2949.
- [13] H. Frei, G. C. Pimentel, *Annu. Rev. Phys. Chem.* **1985**, 36, 491–524.
- [14] A. C. Legon, C. A. Rego, *J. Chem. Soc. Faraday Trans.* **1990**, 86, 1915–1921, and references therein.
- [15] A. C. Legon, *Chem. Soc. Rev.* **1990**, 19, 197–237.
- [16] A. C. Legon, D. J. Millen, *Chem. Rev.* **1986**, 86, 635–657.
- [17] T. R. Dyke, B. J. Howard, W. Klemperer, *J. Chem. Phys.* **1972**, 56, 2442–2454.
- [18] a) T. J. Balle, E. J. Campbell, M. R. Kennan, W. H. Flygare, *J. Chem. Phys.* **1980**, 72, 922–932; b) E. J. Campbell, L. W. Buxton, T. J. Balle, M. R. Keenan, W. H. Flygare, *J. Chem. Phys.* **1981**, 74, 829–840; c) E. J. Campbell, L. W. Buxton, T. J. Balle, W. H. Flygare, *J. Chem. Phys.* **1981**, 74, 813–829.
- [19] T. R. Dyke, *Top. Curr. Chem.* **1984**, 120, 85–113.
- [20] K. R. Leopold, G. T. Fraser, S. E. Novick, W. Klemperer, *Chem. Rev.* **1994**, 94, 1807–1827.
- [21] For a detailed description, see A. C. Legon in *Atomic and Molecular Beam Methods*, Vol. 2 (Ed.: G. Scoles), Oxford University Press, New York, **1992**, chap. 9, pp. 289–308.
- [22] D. J. Millen, *Can. J. Chem.* **1985**, 63, 1477–1479.
- [23] A. C. Legon, *Faraday Discuss. Chem. Soc.* **1994**, 97, 19–33.
- [24] *Gmelins Handbuch der Anorganischen Chemie, Fluorine Supplement*, Vol. 2, Springer, Berlin, **1980**, p. 169.
- [25] D. R. Miller in *Atomic and Molecular Beam Methods*, Vol. 1 (Ed.: G. Scoles), Oxford University Press, New York, **1988**, chap. 2, pp. 14–53.
- [26] H. I. Bloemink, K. Hinds, A. C. Legon, J. C. Thorn, *Chem. Phys. Lett.* **1994**, 223, 162–166.
- [27] H. I. Bloemink, K. Hinds, A. C. Legon, J. C. Thorn, *Chem. Eur. J.* **1995**, 1, 17–25.
- [28] A. C. Legon, *Chem. Phys. Lett.* **1995**, 237, 291–298.
- [29] A. C. Legon, P. W. Fowler, *Z. Naturforsch. A* **1992**, 47, 367–370.
- [30] P. W. Fowler, A. C. Legon, S. A. Peebles, *Mol. Phys.* **1996**, 88, 987–996.
- [31] For an account of the Townes–Dailey model see: C. H. Townes, A. L. Schawlow, *Microwave Spectroscopy*, McGraw-Hill, New York, **1955**, chap. 9.
- [32] W. Jäger, Y. Xu, M. C. L. Gerry, *J. Phys. Chem.* **1993**, 97, 3685–3689.
- [33] F. A. Biaoocchi, T. A. Dixon, W. Klemperer, *J. Chem. Phys.* **1982**, 77, 1632–1638.
- [34] A. C. Legon, H. E. Warner, *J. Chem. Phys.* **1993**, 98, 3827–3832.
- [35] H. I. Bloemink, S. J. Dolling, K. Hinds, A. C. Legon, *J. Chem. Soc. Faraday Trans.* **1995**, 91, 2059–2066.
- [36] H. I. Bloemink, S. A. Cooke, K. Hinds, A. C. Legon, J. C. Thorn, *J. Chem. Soc. Faraday Trans.* **1995**, 91, 1891–1900.
- [37] A. C. Legon, J. C. Thorn, *J. Chem. Soc. Faraday Trans.* **1993**, 89, 4157–4162.
- [38] A. C. Legon, D. G. Lister, J. C. Thorn, *J. Chem. Soc. Faraday Trans.* **1994**, 90, 3205–3212.
- [39] H. I. Bloemink, A. C. Legon, *J. Chem. Phys.* **1995**, 103, 876–882.
- [40] P. W. Fowler, A. C. Legon, J. M. A. Thumwood, E. R. Waclawik, *Mol. Phys.* **1999**, 97, 159–166.
- [41] M. Jaszunski, E. Kochanski, *J. Am. Chem. Soc.* **1977**, 99, 4624–4628.
- [42] P. W. Fowler, S. A. Peebles, A. C. Legon in *Advances in Quantum Chemistry*, Vol. 28 (Ed.: P. Löwdin), Academic Press, San Diego, **1997**, pp. 248–255.
- [43] “Microwave Molecular Spectra”: W. Gordy, R. L. Cook in *Techniques of Chemistry*, Vol. XVIII (Ed.: A. Weissberger), 3rd ed., Wiley, New York, **1984**, chap. XIV, pp. 725–802. Note that $\chi_A(X)$ and $\chi_A(Y)$ used in this review are identical with the $eQq_{n,1,0}$ described on p. 738 of this text.
- [44] A. C. Legon, *J. Chem. Soc. Faraday Trans.* **1995**, 91, 1881–1883.
- [45] S. Blanco, A. C. Legon, J. C. Thorn, *J. Chem. Soc. Faraday Trans.* **1994**, 90, 1365–1371.
- [46] H. I. Bloemink, K. Hinds, A. C. Legon, J. C. Thorn, *Angew. Chem.* **1994**, 106, 1577–1579; *Angew. Chem. Int. Ed. Engl.* **1994**, 33, 1512–1513.
- [47] H. I. Bloemink, K. Hinds, A. C. Legon, J. C. Thorn, *J. Chem. Soc. Chem. Commun.* **1994**, 1229–1230.
- [48] H. I. Bloemink, A. C. Legon, *Chem. Eur. J.* **1996**, 2, 265–270.
- [49] K. Hinds, A. C. Legon, *Chem. Phys. Lett.* **1995**, 240, 467–473.
- [50] H. I. Bloemink, A. C. Legon, J. C. Thorn, *J. Chem. Soc. Faraday Trans.* **1995**, 91, 781–787.
- [51] A. C. Legon, *Chem. Phys. Lett.* **1997**, 279, 55–64.
- [52] S. A. Cooke, G. Cotti, K. Hinds, J. H. Holloway, A. C. Legon, D. G. Lister, *J. Chem. Soc. Faraday Trans.* **1996**, 92, 2671–2676.
- [53] K. Hinds, J. H. Holloway, A. C. Legon, *Chem. Phys. Lett.* **1995**, 242, 407–414.
- [54] K. Hinds, J. H. Holloway, A. C. Legon, *J. Chem. Soc. Faraday Trans.* **1996**, 92, 1291–1296.
- [55] H. I. Bloemink, J. H. Holloway, A. C. Legon, *Chem. Phys. Lett.* **1996**, 250, 567–575.
- [56] K. Hinds, A. C. Legon, J. H. Holloway, *Mol. Phys.* **1996**, 88, 673–682.
- [57] H. I. Bloemink, K. Hinds, J. H. Holloway, A. C. Legon, *Chem. Phys. Lett.* **1995**, 242, 113–120.
- [58] S. A. Cooke, G. Cotti, C. M. Evans, J. H. Holloway, A. C. Legon, *Chem. Commun.* **1996**, 2327–2328.
- [59] H. I. Bloemink, C. M. Evans, J. H. Holloway, A. C. Legon, *Chem. Phys. Lett.* **1996**, 248, 260–268.
- [60] A. Maryott, F. Buckley, *NSRDS-NBS Circular 537*, US GPO, Washington, **1953**, quoted in: D. R. Lide, *CRC Handbook of Chemistry*, 75th ed., CRC Press, Raton, FL, **1994**.
- [61] A. C. Legon, D. J. Millen, *J. Am. Chem. Soc.* **1987**, 109, 356–358.
- [62] A. C. Legon, D. J. Millen, *J. Chem. Soc. Chem. Commun.* **1987**, 986–987.
- [63] S. A. Cooke, G. Cotti, C. M. Evans, J. H. Holloway, A. C. Legon, *Chem. Phys. Lett.* **1996**, 262, 308–314.
- [64] G. Cotti, C. M. Evans, J. H. Holloway, A. C. Legon, *Chem. Phys. Lett.* **1997**, 264, 513–521.
- [65] H. I. Bloemink, K. Hinds, J. H. Holloway, A. C. Legon, *Chem. Phys. Lett.* **1995**, 245, 598–604.
- [66] Convenient collections of k_a values for $B \cdots HF$, $B \cdots HCl$, $B \cdots HBr$ and $B \cdots HCN$ for a range of Lewis bases B are given in references [61] and [62]. The values in Table 3 are taken from these sources.
- [67] A. C. Legon, D. J. Millen, *Faraday Discuss. Chem. Soc.* **1982**, 73, 71–87.
- [68] A. D. Buckingham, P. W. Fowler, *Can. J. Chem.* **1985**, 63, 2018–2025.
- [69] A. D. Buckingham, C. Graham, J. H. Williams, *Mol. Phys.* **1983**, 49, 703–710.
- [70] S. A. Peebles, P. W. Fowler, A. C. Legon, unpublished results.
- [71] K. P. R. Nair, J. Hoeft, E. Tiemann, *Chem. Phys. Lett.* **1978**, 58, 153–156.
- [72] B. Fabricant, J. S. Muentner, *J. Chem. Phys.* **1977**, 66, 5274–5277.
- [73] R. Herges, *Angew. Chem.* **1995**, 107, 57–59; *Angew. Chem. Int. Ed. Engl.* **1995**, 34, 51–53, and references therein.
- [74] H. Matsuzawa, S. Iwata, *Chem. Phys.* **1992**, 163, 297–305.
- [75] A. C. Legon, D. J. Millen, *Chem. Soc. Rev.* **1987**, 16, 467–498.
- [76] N. W. Howard, A. C. Legon, *J. Chem. Phys.* **1988**, 88, 4694–4701.
- [77] N. W. Howard, A. C. Legon, *J. Chem. Phys.* **1987**, 86, 6722–6730.
- [78] A. C. Legon, D. Stephenson, *J. Chem. Soc. Faraday Trans.* **1992**, 88, 761–762.
- [79] A. C. Legon, L. C. Willoughby, *Chem. Phys.* **1983**, 74, 127–136.
- [80] A. C. Legon, L. C. Willoughby, *J. Chem. Soc. Chem. Commun.* **1982**, 997–998.
- [81] L. C. Willoughby, A. C. Legon, *J. Phys. Chem.* **1983**, 87, 2085–2090.

- [82] N. W. Howard, A. C. Legon, G. J. Luscombe, *J. Chem. Soc. Faraday Trans.* **1991**, 87, 507–512.
- [83] A. C. Legon, P. D. Soper, W. H. Flygare, *J. Chem. Phys.* **1981**, 74, 4944–4950.
- [84] P. D. Soper, A. C. Legon, W. H. Flygare, *J. Chem. Phys.* **1981**, 74, 2138–2142.
- [85] M. R. Keenan, T. K. Minton, A. C. Legon, T. J. Balle, W. H. Flygare, *Proc. Natl. Acad. Sci. USA* **1980**, 77, 5583–5587.
- [86] Z. Wang, R. R. Lucchese, J. W. Bevan, A. P. Suckley, C. A. Rego, A. C. Legon, *J. Chem. Phys.* **1993**, 98, 1761–1767.
- [87] A. C. Legon, D. J. Millen, L. C. Willoughby, *Proc. R. Soc. London A* **1985**, 401, 327–347.
- [88] A. C. Legon, E. J. Campbell, W. H. Flygare, *J. Chem. Phys.* **1982**, 76, 2267–2274.
- [89] E. J. Campbell, A. C. Legon, W. H. Flygare, *J. Chem. Phys.* **1982**, 76, 3494–3500.
- [90] P. W. Fowler, A. C. Legon, S. A. Peebles, *Chem. Phys. Lett.* **1994**, 226, 501–508.
- [91] S. A. Cooke, G. Cotti, J. H. Holloway, A. C. Legon, *Angew. Chem.* **1997**, 109, 81–83; *Angew. Chem. Int. Ed. Engl.* **1997**, 36, 129–130.
- [92] Z. Kisiel, A. C. Legon, D. J. Millen, *Proc. R. Soc. London A* **1982**, 381, 419–442.
- [93] A. C. Legon, L. C. Willoughby, *Chem. Phys. Lett.* **1983**, 95, 449–452.
- [94] A. C. Legon, A. P. Suckley, *Chem. Phys. Lett.* **1988**, 150, 153–158.
- [95] a) R. Viswanathan, T. R. Dyke, *J. Chem. Phys.* **1982**, 77, 1166–1174; b) L. C. Willoughby, A. J. Fillery-Travis, A. C. Legon, *J. Chem. Phys.* **1984**, 81, 20–26.
- [96] E. J. Goodwin, A. C. Legon, *J. Chem. Soc. Faraday Trans. 2* **1984**, 80, 51–65.
- [97] A. I. Jaman, A. C. Legon, *J. Mol. Struct.* **1986**, 145, 261–276.
- [98] S. E. Novick, K. C. Janda, W. Klemperer, *J. Chem. Phys.* **1976**, 65, 5115–5121.
- [99] K. C. Janda, J. M. Steed, S. E. Novick, W. Klemperer, *J. Chem. Phys.* **1977**, 67, 5162–5172.
- [100] G. T. Fraser, A. S. Pine, *J. Chem. Phys.* **1989**, 91, 637–645.
- [101] S. A. Cooke, G. K. Corlett, C. M. Evans, J. H. Holloway, A. C. Legon, *Chem. Phys. Lett.* **1997**, 275, 269–277.
- [102] S. A. Cooke, G. K. Corlett, C. M. Evans, A. C. Legon, J. H. Holloway, *J. Chem. Phys.* **1998**, 108, 39–45.
- [103] H. I. Bloemink, C. M. Evans, J. H. Holloway, A. C. Legon, *Chem. Phys. Lett.* **1996**, 251, 275–286.
- [104] C. M. Evans, J. H. Holloway, A. C. Legon, *Chem. Phys. Lett.* **1996**, 255, 119–128.
- [105] A. C. Legon, J. C. Thorn, *Chem. Phys. Lett.* **1994**, 227, 472–479.
- [106] G. T. Fraser, C. W. Gillies, J. Zozom, F. J. Lovas, R. D. Suenram, *J. Mol. Spectrosc.* **1987**, 126, 200–209.
- [107] A. C. Legon, *J. Chem. Soc. Faraday Trans.* **1996**, 92, 2677–2679.
- [108] A. C. Legon, C. A. Rego, A. L. Wallwork, *J. Chem. Phys.* **1992**, 97, 3050–3059.
- [109] C. M. Evans, A. C. Legon, *Chem. Phys.* **1995**, 198, 119–131.
- [110] G. G. Engerholm, Dissertation, University of California, Berkeley, **1965**; *Diss. Abstr. Inf.* **1966**, 26, 3580.
- [111] C. M. Evans, J. H. Holloway, A. C. Legon, *Chem. Phys. Lett.* **1997**, 267, 281–287.
- [112] G. Cotti, J. H. Holloway, A. C. Legon, *Chem. Phys. Lett.* **1996**, 255, 401–409.
- [113] A. J. Fillery-Travis, A. C. Legon, *Chem. Phys. Lett.* **1986**, 123, 4–8.
- [114] A. J. Fillery-Travis, A. C. Legon, *J. Chem. Phys.* **1986**, 85, 3180–3187.
- [115] P. D. Aldrich, A. C. Legon, W. H. Flygare, *J. Chem. Phys.* **1981**, 75, 2126–2134.
- [116] A. C. Legon, P. D. Aldrich, W. H. Flygare, *J. Chem. Phys.* **1981**, 75, 625–630.
- [117] J. A. Shea, W. H. Flygare, *J. Chem. Phys.* **1982**, 76, 4857–4864.
- [118] P. W. Fowler, A. C. Legon, J. M. A. Thumwood, E. R. Wacławik, *Coord. Chem. Rev.*, in press.
- [119] W. G. Read, W. H. Flygare, *J. Chem. Phys.* **1982**, 76, 292–300.
- [120] C. A. Coulson, W. E. Moffitt, *Philos. Mag.* **1949**, 40, 1–35.
- [121] K. Hinds, J. H. Holloway, A. C. Legon, *J. Chem. Soc. Faraday Trans.* **1997**, 93, 373–378.
- [122] A. C. Legon, P. D. Aldrich, W. H. Flygare, *J. Am. Chem. Soc.* **1982**, 104, 1486–1490.
- [123] S. A. Cooke, J. H. Holloway, A. C. Legon, *J. Chem. Soc. Faraday Trans.* **1997**, 93, 2361–2365.
- [124] Z. Kisiel, P. W. Fowler, A. C. Legon, unpublished results.
- [125] A. J. Fillery-Travis, A. C. Legon, unpublished results.
- [126] S. A. Cooke, J. H. Holloway, A. C. Legon, *Chem. Phys. Lett.* **1997**, 266, 61–69.
- [127] S. A. Cooke, J. H. Holloway, A. C. Legon, *J. Chem. Soc. Faraday Trans.* **1997**, 93, 4253–4258.
- [128] Z. Kisiel, P. W. Fowler, A. C. Legon, *J. Chem. Phys.* **1994**, 101, 4635–4643.
- [129] F. A. Baiocchi, J. H. Williams, W. Klemperer, *J. Phys. Chem.* **1983**, 87, 2079–2084.
- [130] W. G. Read, E. J. Campbell, G. Henderson, *J. Chem. Phys.* **1983**, 78, 3501–3508.
- [131] S. A. Cooke, G. K. Corlett, C. M. Evans, A. C. Legon, *Chem. Phys. Lett.* **1997**, 272, 61–68.
- [132] H. S. Gutowsky, E. Arunan, T. Emilsson, S. L. Tschopp, C. E. Dykstra, *J. Chem. Phys.* **1995**, 103, 3917–3927.
- [133] S. A. Cooke, C. M. Evans, J. H. Holloway, A. C. Legon, *J. Chem. Soc. Faraday Trans.* **1998**, 94, 2295–2302.
- [134] J. A. Shea, S. G. Kukolich, *J. Chem. Phys.* **1983**, 78, 3545–3551.
- [135] A. Lesarri, J. C. Lopez, J. L. Alonso, *J. Chem. Soc. Faraday Trans.* **1998**, 94, 729–733.
- [136] S. A. Cooke, G. K. Corlett, J. H. Holloway, A. C. Legon, *J. Chem. Soc. Faraday Trans.* **1998**, 94, 2675–2680.
- [137] B. B. De More, W. S. Wilcox, J. H. Goldstein, *J. Chem. Phys.* **1954**, 22, 876–877.
- [138] J. J. Oh, K. W. Hillig, R. L. Kuczkowski, R. K. Bohn, *J. Phys. Chem.* **1990**, 94, 4453–4455.
- [139] T. Ogata, K. Kozima, *J. Mol. Spectrosc.* **1972**, 42, 38–46.
- [140] A. Hinchliffe, *Ab Initio Determination of Molecular Properties*, Adam Hilger, Bristol, **1987**, chap. 5, pp. 68–99.
- [141] a) W. H. Flygare, R. C. Benson, *Mol. Phys.* **1971**, 20, 225–250; b) D. H. Sutter, W. H. Flygare, *Top. Curr. Chem.* **1976**, 63, 89–196, and references therein.
- [142] S. A. Cooke, G. K. Corlett, A. C. Legon, *J. Chem. Soc. Faraday Trans.* **1998**, 94, 1565–1570.
- [143] S. A. Cooke, G. K. Corlett, A. C. Legon, *Chem. Phys. Lett.* **1998**, 291, 269–276.
- [144] S. A. Cooke, J. H. Holloway, A. C. Legon, *Chem. Phys. Lett.* **1998**, 298, 151–160.
- [145] S. A. Cooke, G. K. Corlett, D. G. Lister, A. C. Legon, *J. Chem. Soc. Faraday Trans.* **1998**, 94, 837–841.
- [146] S. A. Cooke, G. Cotti, C. M. Evans, J. H. Holloway, A. C. Legon, *Chem. Phys. Lett.* **1996**, 260, 388–394.
- [147] P. Cope, D. J. Millen, L. C. Willoughby, A. C. Legon, *J. Chem. Soc. Faraday Trans. 2* **1986**, 82, 1197–1206.
- [148] A. C. Legon, A. L. Wallwork, D. J. Millen, *Chem. Phys. Lett.* **1991**, 178, 279–284.
- [149] Values in Table 7 for H₃N⋯HF were calculated from unpublished spectroscopic constants communicated to the author by P. R. R. Langridge-Smith and B. J. Howard.
- [150] L. Pauling, *The Nature of the Chemical Bond*, Cornell University Press, Ithaca, NY, **1960**, chap. 7, pp. 258–264.
- [151] S. A. Peebles, P. W. Fowler, A. C. Legon, *Chem. Phys. Lett.* **1995**, 240, 130–134.
- [152] A. C. Legon, *Chem. Eur. J.* **1998**, 4, 1890–1897.
- [153] A. C. Legon, D. J. Millen, S. C. Rogers, *J. Mol. Struct.* **1980**, 67, 29–34.
- [154] A. C. Legon, A. L. Wallwork, *J. Chem. Soc. Faraday Trans.* **1990**, 86, 3975–3982.
- [155] A. C. Legon, A. L. Wallwork, H. E. Warner, *J. Chem. Soc. Faraday Trans.* **1991**, 87, 3327–3334.
- [156] S. A. Cooke, G. K. Corlett, C. M. Evans, A. C. Legon, *J. Chem. Soc. Faraday Trans.* **1997**, 93, 2973–2976.
- [157] A. C. Legon, D. G. Lister, *J. Chem. Soc. Faraday Trans.* **1999**, in press.
- [158] M. J. Atkins, A. C. Legon, H. E. Warner, *Chem. Phys. Lett.* **1994**, 229, 267–272.
- [159] F. A. Baiocchi, W. Klemperer, *J. Chem. Phys.* **1983**, 78, 3509–3520.

- [160] A. C. Legon, C. A. Rego, *J. Chem. Soc. Faraday Trans.* **1993**, 89, 1173–1178.
- [161] a) A. C. Legon, C. A. Rego, *Chem. Phys. Lett.* **1989**, 154, 468–472;
b) A. C. Legon, C. A. Rego, *Chem. Phys. Lett.* **1989**, 157, 243–250.
- [162] A. C. Legon, C. A. Rego, *J. Chem. Phys.* **1989**, 90, 6867–6876.
- [163] A. C. Legon, A. L. Wallwork, C. A. Rego, *J. Chem. Phys.* **1990**, 92, 6397–6407.
- [164] A. C. Legon, C. A. Rego, *J. Chem. Phys.* **1993**, 99, 1463–1468.
- [165] A. C. Legon, *Chem. Soc. Rev.* **1993**, 22, 153–163.
- [166] A. C. Legon, D. J. Millen, *Proc. R. Soc. London A* **1988**, 417, 21–30.
- [167] F. H. de Leeuw, R. Van Wachem, A. Dymanus, *Abstr. Pap. Symposium on Molecular Structure and Spectroscopy* (Ohio, OH) **1969**, R5.
- [168] Calculated by using $\omega_e = (2\pi c)^{-1}(k_s/\mu)^{1/2}$ from ω_e given by: P. L. Clouser, W. Gordy, *Phys. Rev. A* **1964**, 134, 863.
- [169] H. I. Bloemink, J. H. Holloway, A. C. Legon, *Chem. Phys. Lett.* **1996**, 254, 59–68.
- [170] D. J. Millen, K. M. Sinnott, *J. Chem. Soc.* **1958**, 350–355.
- [171] G. Cazzoli, P. G. Favero, A. Del Borgo, *J. Mol. Spectrosc.* **1974**, 50, 82–92.
- [172] H. I. Bloemink, S. A. Cooke, J. H. Holloway, A. C. Legon, *Angew. Chem.* **1997**, 109, 1399–1401; *Angew. Chem. Int. Ed. Engl.* **1997**, 36, 1340–1342.
- [173] A. Karpfen, *Chem. Phys. Lett.* **1999**, 299, 493–502.
- [174] C. Domene, P. W. Fowler, A. C. Legon, *Chem. Phys. Lett.*, in press.
- [175] J. B. Davey, A. C. Legon, E. R. Waclawik, *Chem. Phys. Lett.* **1999**, 306, 133–144.
- [176] J. B. Davey, A. C. Legon, E. R. Waclawik, *Phys. Chem. Chem. Phys.* **1999**, 1, 3097–3102.
- [177] J. B. Davey, A. C. Legon, *Phys. Chem. Chem. Phys.* **1999**, 1, 3721–3726.
- [178] J. M. A. Thumwood, A. C. Legon, *Chem. Phys. Lett.* **1999**, 310, 88–96.
- [179] J. B. Davey, A. C. Legon, E. R. Waclawik, unpublished results.
- [180] A. C. Legon, E. R. Waclawik, unpublished results.
- [181] E. R. Waclawik, A. C. Legon, *Phys. Chem. Chem. Phys.* submitted.
- [182] A. C. Legon, unpublished results.